Dynamic Cooperative Communications in Wireless Ad-Hoc Networks

Haesoo Kim

Dissertation submitted to the Faculty of the

Virginia Polytechnic Institute and State University

in partial fulfillment of the requirements for the degree of

Doctor of Philosophy

in

Electrical Engineering

R. Michael Buehrer (Chair)

Jeffrey H. Reed

Aloysius A. Beex

Thomas Hou

Jong Kim

July 22, 2008

Blacksburg, Virginia

Dynamic Cooperative Communications in Wireless Ad-Hoc Networks

Haesoo Kim

(ABSTRACT)

This dissertation focuses on an efficient cooperative communication method for wireless ad hoc networks. Typically, performance enhancement via cooperative communications can be achieved at the cost of other system resources such as additional bandwidth, transmit power, or more complex synchronization methods between cooperating signals. However, the proposed cooperative transmission scheme in this research utilizes system resources more efficiently by reducing the redundant and wasteful cooperating signals typically required, while maintaining the desired performance improvement.

There are four main results in this dissertation. First, an efficient cooperative retransmission scheme is introduced to increase bandwidth efficiency by reducing wasteful cooperating signals. The proposed cooperative transmission method does not require any additional information for cooperation. Furthermore, we ensure good quality for the cooperating signals through a simple yet effective selection procedure. Multiple cooperating nodes can be involved in the cooperation without prior planning via distributed beamforming. The proposed cooperative retransmission scheme outperforms traditional retransmission by the source as well as other cooperative methods in terms of delay and packet error rate (PER).

Secondly, the outage probabilities of the cooperative retransmission scheme are analyzed for both the perfect synchronization case and when offset estimation is performed for distributed beamforming. The performance with offset estimation is close to the perfect synchronization case, especially for short data packets. A low-rate feedback channel is introduced to adjust the phase shift due to channel variation and the residual frequency offset. It is shown that substantial gain can be achieved with a low-rate feedback channel, even for long data packets.

Third, the throughput efficiency and average packet delay of the proposed cooperative retransmission scheme are analyzed using a two-state Markov model for both a simple automatic repeat request (ARQ) and a hybrid ARQ technique. The benefits of the cooperative ARQ approach are also verified in a multihop network with random configurations when there are concurrent packet transmissions. The average transmit power for the cooperating signals is also investigated in the proposed cooperative transmission scheme with various power control approaches. Finally, cooperative multiple input multiple output (MIMO) systems are examined, mainly focusing on power allocation methods to increase overall channel capacity. An efficient and simple power allocation method at the cooperating node is proposed which can be used for an arbitrary number of antennas without any additional information.

Acknowledgments

First of all, I would like to express my deepest gratitude to my advisor, Dr. R. Michael Buehrer, for his guidance and sustained support that make it possible for me to pursue a doctor's degree. I owe special thanks to him for advices and understanding that always helped me find the right path in difficult situations. Dr. Buehrer has been a wonderful mentor who encourages me to achieve my full potential.

I would like to state my sincere appreciation to my committee members, Dr. Jeffrey Reed, Dr. Aloysius Beex, Dr. Thomas Hou, and Dr. Jong Kim. They have been very helpful in improving my proposal and dissertation. I am grateful to them for sharing their time and expertise. I also thank my former advisor, Dr. Brian Woerner, who gave me the chance to work independently and be creative.

I thank all my colleagues at MPRG for many stimulating discussions on various research topics and industrial trends. I am also very thankful for the friendship of some members in MPRG: Dr. Kyung-Kyoon Bae, Dr. Jonghan Kim, Dr. Kyu-Woong Kim, Kye-Hun Lee, Jeongheon Lee, and Brian Choi. I also acknowledge fellow Korean students at ECE department for their friendship.

I can't imagine I can be here without my parents' support. I really thank them for their love, care and sacrifices they have made for their children. Their endless and unconditional love has been my biggest support throughout my life. I also thank my parents-in-law for their love and support. I can't forget my brother, sister-in-law, and sister for their love and encouragement.

Finally, my special thanks go to my wife, Jae Hee Hong, for being my side all the time and my son, Yong-Eun for giving me such a joy during the tough times as a Ph.D. student.

Contents

List of Figures

List of Tables

List of Acronyms

cdf	cumulative density function
i.i.d.	independent and identically distributed
pdf	probability density function
ACK	acknowledgment
AnF	amplify-and-forward
ARQ	automatic repeat request
AWGN	additive white Gaussian noise
BER	bit error rate
BPSK	binary phase shift keying
BS	base station
CDMA	code division multiple access
CP	cyclic prefix
CSI	channel state information
DFT	discrete Fourier transform
DnF	decode-and-forward
D-STC	distributed space time code
FDD	frequency division duplex
HARQ	hybrid ARQ
HSDPA	high-speed downlink packet access

ICI	inter-carrier interference
IDFT	inverse discrete Fourier transform
INR	incremental redundancy
ISI	inter-symbol interference
LAR	link adaptive regeneration
LOS	line of sight
MAC	multiple access control
MIMO	multiple input multiple output
ML	maximum likelihood
MMSE	minimum mean square error
M-PSK	M-ary phase shift keying
MRC	maximum ration combining
NACK	negative acknowledgment
OFDM	orthogonal frequency division multiplexing
PER	packet error rate
PN	pseudo noise
PR-INR	preferred relay INR
RF	radio frequency
SINR	signal to interference and noise ratio
SNR	signal to noise ratio
STBC	space time block code
STC	space time code
ST-OFDM	space time OFDM
SVD	singular value decomposition
SW ARQ	stop-and-wait ARQ

TDD	time division duplex
TDMA	time division multiple access
TR-STC	time-reverse STC
UMTS	universal mobile telecommunications system
WLAN	wireless local area networks
ZF	zero forcing
3G	third generation

Chapter 1

Introduction

To combat signal fading in a wireless environment, multiple antennas have been used extensively over the last few decades. As the demand for high data rate services over wireless links increases, the use of multiple antennas has become one of the fundamental techniques in the wireless communications area. There are three main categories that make use of multiple antennas: diversity, beamforming, and spatial multiplexing. Diversity and beamforming transmit the same signal and increase the received signal quality by using multiple transmit or receive antennas [1][2][3]. While they achieve high throughput by boosting signal quality, spatial multiplexing achieves it by transmitting different data streams on each transmit antenna and separating them at the receiver by exploiting channel information [4]. Typically these approaches are based on the assumption that multiple antennas are mounted on a single wireless device.

1.1 Motivation and Overview of Research

Almost every measure of the capabilities of digital electronic devices is linked to Moore's law[1] such as processing speed, memory capacity, and the resolution of digital cameras. However, it is still not easy to install multiple antennas in small mobile devices especially due to limitations of radio frequency (RF) components. Examples include most handsets or the nodes in a wireless sensor networks. Recently, cooperative communications (also called distributed or collaborative communications,) has been proposed to achieve the benefits of multiple antenna systems with single-antenna devices [6][7][8][9]. The basic idea is that multiple single antenna devices share their antennas to create a *virtual* multiple antenna system. Transmitting independent copies of the signal generates diversity and can mitigate the deleterious effects of fading. Cooperative communication generates this diversity, especially spatial diversity, via neighboring nodes. Beamforming with the proper coordination of neighboring nodes is another approach to create multiple antenna systems with multiple single-antenna nodes [10][11].

Cooperative communications provides many advantages in terms of capacity, link reliability, power consumption, and coverage in wireless ad-hoc networks. However, those benefits can be obtained at the cost of other system resources such as additional time slots, frequency bands, and transmit power. In this research, we focus on *efficient* cooperative communication techniques to minimize the use of other system resources. There are several challenges facing in cooperative communication methods including:

- Initiate user cooperation only when it is necessary

  Currently, most proposed cooperative communication schemes are initiated by the source or by the cooperating node based on the decoding result of the received sig-

---

[1]The number of transistors that can be inexpensively placed on an integrated circuit is increasing exponentially, doubling approximately every two years[5]

nal. When a direct link is good enough to recover the transmitted information at the destination, the signal from the cooperative node is a waste of system resources.

- Provide a good quality cooperating signal

The channel condition of the cooperating link is not considered in most of the previous cooperative approaches. This results in undesirable cooperation when the quality of cooperating signal is not good.

- Select the cooperating nodes flexibly

A similar scenario occurs when there are multiple neighboring nodes around the direct link. If the cooperative node is fixed a priori, alternate cooperative links cannot be used even though they have better quality than the current one. Therefore, it is preferable to select cooperative nodes dynamically based on the channel conditions of the possible cooperative links.

- Accommodate multiple cooperating nodes efficiently with minimal overhead

Distributed space time coding (D-STC) and distributed beamforming are common methods to use multiple cooperating nodes although distributed beamforming shows better spectral efficiency. However, it requires proper synchronization between cooperating signals to achieve beamforming gain.

- Achieve distributed beamforming in a time-varying channel

When distributed beamforming is used for cooperation and channel conditions of the cooperating links are not constant during a packet duration, an efficient offset adjustment method is required.

- Control transmit power of cooperating signals

The transmit power of cooperating signals should be controlled properly since it is a critical system resource and can increase interference to other communication links in wireless networks.

Considering these challenging issues in current cooperative communications, the main goals of this research are to

- Develop an *efficient* cooperative communication method

  Cooperative communication methods are investigated which use network resources efficiently. To eliminate the waste of system resources due to the unnecessary cooperating signals, an efficient cooperative communication is investigated where user cooperation is initiated for retransmission only when it is necessary. The quality of the cooperating signal is included in the selection of cooperating nodes to provide good cooperating signals. When multiple nodes can be involved in cooperation, an efficient cooperating method is proposed for cooperative diversity and distributed beamforming. The adaptability of the proposed cooperative method in a time-varying channel is examined. Power control for cooperating signals is also examined to save transmit power and to reduce interference to other communication links.

- Develop efficient synchronization methods for distributed beamforming

  Distributed beamforming is an attractive method in cooperative communications since it shows better performance than cooperative diversity and it can accommodate an arbitrary number of cooperating nodes. However, its performance depends strongly on synchronization errors. The performance degradation due to offset mismatches is analyzed and synchronization methods are investigated.

- Evaluate the performance of cooperative communications in multihop networks

Multihop links are typical in wireless ad-hoc networks to deliver data to the final destination. The network performance using cooperative techniques in multihop networks is investigated in terms of throughput efficiency, packet delay, and transmit power. The performance of cooperative communications in an interference environment is also investigated.

- Develop efficient power allocation methods for cooperative multiple input multiple output (MIMO) networks

Cooperative communication with multiple antennas at each node is considered as an extension of cooperative communication with single-antenna nodes where each node controls multiple cooperating signals. Using the fact that multiple cooperating signals can be managed at each node, an efficient cooperative method is investigated.

1.2   Outline of Dissertation

The main goal of this dissertation is to find efficient cooperative communication methods in wireless ad hoc networks. Chapter 2 presents an overview of cooperative communications. The previous works on cooperative communications will be categorized into two areas: cooperation with orthogonal channels and cooperation with the same channel. The orthogonal channel can be different time slots, frequency bands, and signature codes. Amplify-and-forward (AnF), decode-and-forward (DnF), and coded cooperation are included in this category. When the same channel is used for cooperation, space time code (STC) or distributed beamforming is used to obtain diversity or coherent signal combining at the destination. As an extended application, cooperative communications with multiple antennas at a node will also be introduced. From a network perspective, multihop and routing performance with cooperative communications will be summarized as another category.

Chapter 3 investigates an efficient cooperative incremental redundancy (INR) method for distributed networks. In the proposed retransmission scheme, the cooperative transmission is initiated only when it is necessary via cooperating nodes which are self-selected by listening to the message exchange between the source and the destination. When neighboring nodes are involved in the cooperation, good channels are obtained due to the fact that only those cooperative nodes that can decode the retransmission request message of the destination correctly participate. In the proposed INR method, multiple nodes can transmit the redundant code blocks at the same time using distributed beamforming to achieve additional gain. This cooperative retransmission scheme can be performed without any *a priori* knowledge of the neighboring nodes such as the number, position, or channel status.

The effect of synchronization in distributed beamforming is analyzed in Chapter 4. Distributed beamforming is a key part of the cooperative retransmission scheme proposed in Chapter 3. When multiple nodes are involved in cooperation, synchronization problems can be mitigated by assigning orthogonal signatures for each cooperating signal such as different time slots, frequency bands, or spreading codes. In distributed beamforming, where all cooperating signals are transmitted through one signal dimension, synchronization of the cooperating signals is achieved by proper processing at each cooperating node using available information. Even though synchronization is controlled at the transmitters, there is mismatch in carrier frequency, phase, and symbol time between the transmitter and the receiver due to hardware imperfections, wireless channel characteristics, and the random location of the transmitters. The effect of synchronization error in distributed beamforming is examined in this chapter.

Chapter 5 investigates the outage probability of the proposed cooperative retransmission scheme with both perfect synchronization and imperfect synchronization with offset estimation using a negative acknowledgment (NACK) message. The analytical results of the proposed retransmission scheme are compared with the simulated results. The residual

offsets of the cooperating signals can diminish the benefits of the cooperative retransmission scheme especially for long data packets. A low-rate feedback scheme is investigated to reduce the impact of the residual offsets. It is shown that outage probability and packet error rate (PER) performance are substantially improved at the cost of a small feedback bandwidth in the proposed cooperative retransmission scheme.

Chapter 6 presents the cooperative retransmission scheme in multihop networks. A two-state Markov model is used to investigate throughput efficiency and average packet delay of the proposed cooperative retransmission scheme for the simple automatic repeat request (ARQ) and chase combining. The analytical results are found to be in good agreement with the simulated results. Even with a small number of neighboring nodes, improved throughput efficiency and delay performance can be achieved by using the cooperative retransmission scheme in wireless ad hoc networks. The benefits of the cooperative ARQ are also verified in multihop networks with random configurations when there are concurrent packet transmissions. The transmit power of the retransmitting signal is examined and it can be significantly reduced by using a small feedback channel without sharing any information concerning other cooperating nodes.

Chapter 7 examines power allocation strategies in cooperative MIMO networks. It is found that waterfilling at the source and the relay does not achieve maximum capacity in cooperative MIMO networks. For the two antenna case, the optimal power allocation method at the relay is presented when waterfilling is used at the source. An inverse-waterfilling power allocation at the relay is proposed to increase the overall channel capacity which is found to be close to the performance of optimal power allocation at the relay. To increase the probability that the relay can work cooperatively, waterfilling to the relay is also examined. Chapter 8 summarizes the main points of the dissertation.

1.3   Contributions

The main contributions of this research are:

- An efficient cooperative ARQ technique to increase spectral efficiency by reducing wasteful cooperation and providing good quality cooperating signals;

- Evaluation of the effect of synchronization errors in distributed beamforming;

- A feedback approach to adjust phase offset in time-varying channels when distributed beamforming is used for cooperation;

- Analysis of throughput efficiency and average packet delay of the cooperative retransmission scheme by using a two-state Markov model;

- Evaluation of the performance of the cooperative retransmission scheme in multihop networks when there are concurrent packet transmissions.

- An efficient power allocation method for cooperative communications when nodes have multiple antennas.

Paper submissions and publications:

- Haesoo Kim and R. M. Buehrer, "A Technique to Exploit Cooperation for Packet Retransmission in Wireless Ad Hoc Networks," Journal of Communications and Networks, vol. 10, no. 2, pp. 148-155, June 2008.

- Haesoo Kim and R. M. Buehrer, "Throughput and Delay Analysis of A Cooperative Retransmission Scheme using Distributed Beamforming," to be submitted to IEEE Transactions on Wireless Communications.

- Haesoo Kim and R. M. Buehrer, "Power Allocation Strategies in Cooperative MIMO Networks," IEEE Wireless Communications and Networking Conference (WCNC), vol. 3, pp. 1675-1680, 2006.

Chapter 2

Review of Cooperative Communications

Transmit diversity and beamforming generally require multiple antennas at the transmitter. However, it is still not easy to install multiple antennas in small wireless devices due to size, cost, and hardware limitations. Recently, cooperative communication has been proposed to create a *virtual* multiple antenna system using multiple single-antenna devices and coordinated transmission.

The initial work in the area of distributed communication was done by Cover and El Gamal in the presence of additive white Gaussian noise (AWGN) [12], which is called the "relay channel". The performance of cooperative diversity in a fading wireless environment was subsequently investigated with different cooperative methods [6][7][8][9]. The possibility of distributed beamforming was also examined by using a master node to achieve synchronization between the cooperating signals [10][11].

A common categorization of cooperative communications is cooperative diversity and distributed beamforming. However, a different categorization will be used in this research to emphasize bandwidth efficiency. When multiple nodes are involved in cooperation, two types
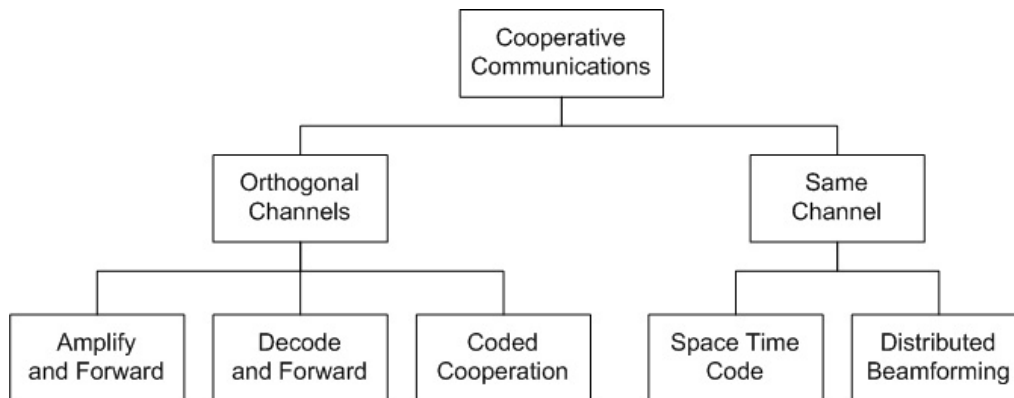
Figure 2.1: Category of cooperative communication based on channel usage

of cooperative protocol can be considered for the cooperating signals. The first approach is that cooperative nodes use orthogonal signal dimensions to avoid interference among the cooperating signals. Orthogonal signal dimensions can be different time slots, different frequency bands, or different spreading codes for each cooperating node. There are three basic cooperating methods in this category depending on the forwarding form of the cooperating signal; amplify-and-forward, decode-and-forward, and coded cooperation. Another approach is that all cooperating nodes transmit the same or different signals at the same time through the same signal dimension. When cooperating nodes transmit their corresponding code blocks which are pre-assigned to form STC, diversity gain can be achieved by using cooperating signals. Distributed beamforming is another method using the same signal dimension where cooperating nodes adjust their frequency, phase, and timing offsets to achieve the coherent signal summation at the destination. Note that there is an initial broadcasting stage in both categories where the source transmits the signal to the neighboring nodes and/or the destination.

The approaches of cooperative communications in wireless ad-hoc networks are categorized as shown in Figure 2.1. More details for each method will be summarized in this chapter.

2.1   Cooperation via Orthogonal Channels

The performance of cooperative diversity in a wireless fading environment was investigated with amplify-and-forward, decode-and-forward, and selective cooperation in [6][7]. Coded cooperation is a method that combines cooperation with channel coding [8][9][13]. All methods mentioned above are initially proposed with a single cooperating node and can be extended to multiple cooperating signals by assigning additional orthogonal channels.

2.1.1   Amplify and Forward

One simple cooperative method is the amplify-and-forward method shown in Figure 2.2. At the first time slot, the cooperating node receives the signal when it is delivered to the destination from the source. At the next time interval, the cooperating node amplifies and retransmits the received noisy version of the signal to the destination. The destination combines both signals sent by the source and the relay to achieve diversity from two independent channels.

The symbol error probability with multiple amplify-and-forward cooperating signals was analyzed in [14] where each cooperating node uses a different channel to deliver the signal. The destination combines all received signal using a maximum ratio combiner (MRC) to achieve maximum performance. In this analysis, there is no information exchange among relays. When the cooperative relay has channel information for the direct link, a power allocation method for amplify-and-forward is described in [15].

The applicability of the amplify-and-forward method in the downlink of a time division multiple access (TDMA) cellular system was investigated in [16]. The base station (BS) transmits the signal to each destination and its assigned cooperating node in separate time slots, and the cooperating nodes transmit the received signals to the corresponding destinations simultaneously in the same time slot to improve the spectral efficiency. The

Figure 2.2: Cooperative communications using amplify-and-forward method (A. Nosratinia, T. E. Hunter, and A. Hedayet, "Cooperative communication in wireless networks," *IEEE Communications Magazine*, ©2004 IEEE)

tradeoff between spectral efficiency by using a common relay slot and an increased interference was analyzed. The cooperating node was assumed to be the nearest idle mobile to the destination. However, node selection procedure was not specified and BS required perfect knowledge of relay-to-destination channel to maximize the throughput.

Several relay allocation schemes were proposed for cooperative diversity in multi-carrier systems when the amplify-and-forward method is used [17]. All or partial subcarriers are assigned for each cooperating node depending on allocation schemes. Theoretical bounds of the outage probability were derived at high SNR and good performance gain can be achieved at the cost of the knowledge of the channel state information (CSI) for all relays.

2.1.2   Decode and Forward

In this method, the cooperating node decodes the received signal from the source during the first time interval and retransmits the decoded signal to the destination in the next time interval as shown in Figure 2.3. An example of the decode-and-forward method was proposed by Sendonaris *et al* in [18]. This work presents a simple decode-and-forward method for code division multiple access (CDMA) systems. In the first and second time intervals, two users transmit their own signals, *i.e.*, $\{s_1^{(1)}, s_2^{(1)}\}$ from user 1 and $\{s_1^{(2)}, s_2^{(2)}\}$ from user 2. Each user

detects the other user's second bit while its own bits are transmitting. In the third time interval, both users transmit a linear combination of their own second bit and the partner's second bit with the appropriate spreading code. Cooperative diversity gain can be achieved by combining the multiple received bits.

The use of differential encoding at the relays was proposed in [19] where the decoded bits are re-encoded and differential maximum likelihood (ML) demodulation is used at the destination. When erroneous bits are delivered via the cooperating link, the BER performance with ML receiver at the destination was investigated in [20]. The weighted combiner of the cooperating signal at the destination was proposed in [21][22], where the cooperating node requires the average received SNR of the destination to adjust its transmit power which is referred to link adaptive regeneration (LAR). Diversity order of the decode-and-forward cooperation was analyzed when LAR is combining with the *relay selection* [23]. The basic idea of the *relay selection* is to let the neighboring node with the best channel condition be the cooperating node, which selection procedure is performed at the beginning of transmission by using some pilot signals to obtain all the necessary channel information around the direct link [24][25].

The decode-and-forward method has the advantage of simplicity and adaptability to channel conditions. However, it is possible that detection of the partner's bit is unsuccessful and that can be detrimental to the final decision at the destination.

2.1.3   Selective Cooperation

In amplify-and-forward and decode-and-forward methods, a problem arises when the channel from the source to the cooperative node is not of sufficient quality to retransmit the received signal. In the amplify-and-forward method, a low quality signal at the cooperating node does not help much at the destination even though it is forwarded after amplification. A
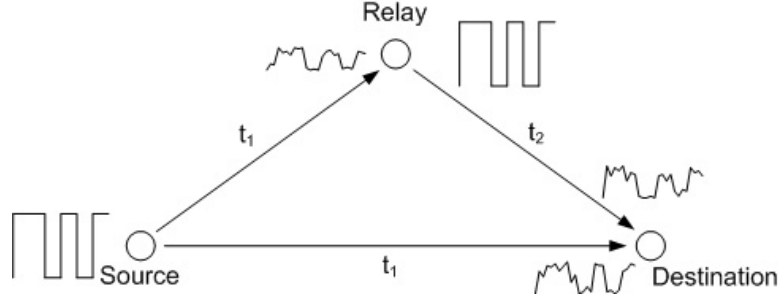
Figure 2.3: Cooperative communications using decode-and-forward method (A. Nosratinia, T. E. Hunter, and A. Hedayet, "Cooperative communication in wireless networks," *IEEE Communications Magazine*, ©2004 IEEE)

similar situation exists in the decode-and-forward method when the regenerated signal is erroneous. If it is assumed that the cooperating node retransmits the received signal only when it is decoded correctly, there is the possibility of losing of a time slot due to the error at the relay.

Selective cooperation is proposed to overcome this problem. If the received SNR at the cooperating node is less than the predefined threshold SNR, the source repeats its transmission during the second time interval instead of the cooperating node [6]. The waste of an additional time slot due to the bad signal quality at the cooperating node can be avoided using this scheme. However, the scheme requires sharing channel information between the source and the cooperating node.

2.1.4   Coded Cooperation

The basic idea behind coded cooperation is that some parts of each user's codewords are received via a different fading path from its partner [8]. The cooperative users divide their information data into two successive frames. In the first frame, each user transmits the first frame which is a valid codeword to decode the original data. If the user successfully decodes the cooperative user's data, the user generates the second frame of partner's data

and transmits it at the next time frame. This additional data frame is combined with the first frame data to achieve a more powerful code word. If the user cannot decode the partner's data, the user's own second frame data is transmitted at the next time frame. Figure 2.4 shows an example of coded cooperation when the relay has no information data to transmit. Similar coded cooperation methods were proposed in [26][27] where both users transmit their data by dividing the first frame and work cooperatively via different frequency bands or different time slots depending on the decoding result.

Coded cooperation can be combined with incremental redundancy (INR) which is a hybrid automatic repeat request (ARQ) method [28]. In [28], the source broadcasts the first codeword to neighboring nodes inside a cluster and user cooperation is initiated depending on their decoding results. The total received code block at the destination is undergone block fading channel and cooperative diversity can be achieved. This approach requires the initial stage to select possible cooperating nodes and their corresponding codeword. It has to note that the cooperating signals are delivered to the destination without taking into account of channel condition between cooperating nodes and the destination. Also, the whole code blocks are transmitted without the response from the destination and it cannot fully use the benefit of the INR ARQ scheme.

Another application of the INR scheme in cooperative communications was proposed in [29] where energy efficiency was examined in a multihop configuration. The intermediate node combines the previously overheard hop transmissions which form a codeword for reliable decoding. The significant energy saving can be obtained by assigning the proper number of punctured bits at each hop node. However, the amount of the received energy at the next node is required information at the current node for the proper power assignment.

The general performance analysis for block fading channels in a single transmission link was performed in [30][31][32]. In their analysis, it is assumed that redundant code blocks are undergone different fading channels to the destination. When the wireless channel is static
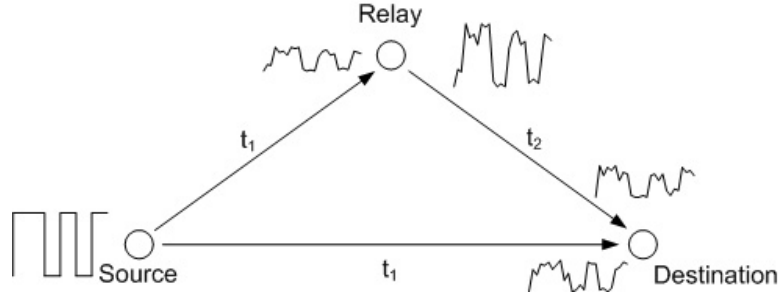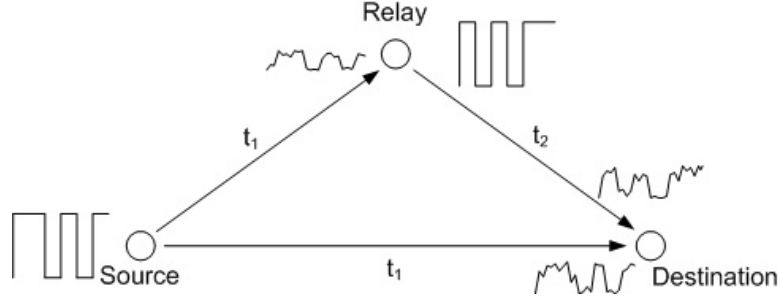
Figure 2.4: Cooperative communications using coded cooperation (A. Nosratinia, T. E. Hunter, and A. Hedayet, "Cooperative communication in wireless networks," *IEEE Communications Magazine*, ©2004 IEEE)

or varying slowly during the entire code block transmission, however, the advantage of block fading channels is decreased.

2.2 Cooperation via Same Channel

The cooperative communications methods considered in the previous section require orthogonal signal dimension for each cooperating signal such as different time slots, frequency bands, or spreading codes to avoid interference between the cooperating signals. The increased orthogonal dimension reduces the advantage of cooperative communications by using more system resources. In other words, the cooperative diversity can be achieved at the cost of decreasing bandwidth efficiency. In this section, we summarize the cooperative communication approaches where all cooperating signals are transmitted through the same channel to improve bandwidth efficiency.

2.2.1 Distributed Space Time Code

Many works have investigated on distributed space time code (D-STC) after it was proposed in [7] where the outage capacity of cooperative STC at high SNR was analyzed. The basic
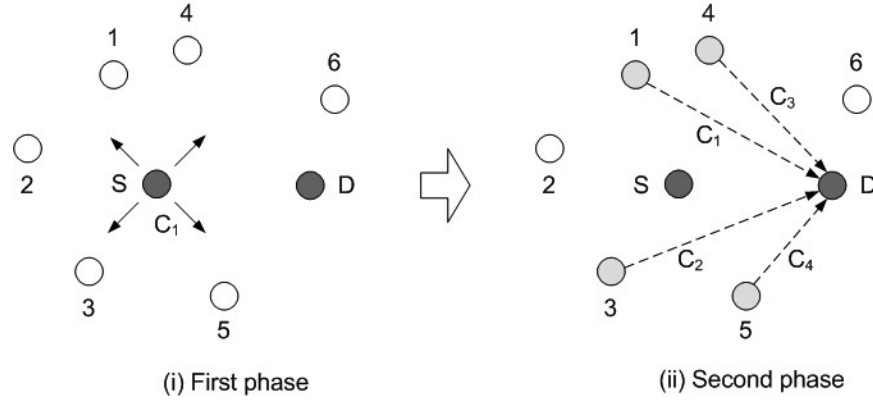
Figure 2.5: Cooperative communications with distributed STC

idea of distributed STC is that the source broadcasts the signal during the first time slot and STC transmission is performed during the second time slot through cooperative nodes. An example of distributed STC is shown in Figure 2.5.

The effect of decision errors in distributed STC was analyzed where the cooperating nodes might make decision errors and retransmit erroneous symbols to the destination during the second time interval [33]. The authors derived the optimal maximum likelihood (ML) detector in case of binary phase shift keying (BPSK) transmission. Orthogonal frequency division multiplexing (OFDM) was considered with cyclic prefix (CP) to reduce the effect of timing synchronization error between the cooperating signals.

Distributed STC with amplify-and-forward method at the cooperating node was investigated in [34]. In this method, two frequency bands are used for signal transmission. The cooperating node receives the signal from the source through one frequency band and forwards it to the destination through another frequency band. The optimum power allocation at the relay was found with full channel information.

As the number of cooperative nodes increases, the design of orthogonal space time block code (STBC) is difficult and a rate loss is unavoidable. If quasi-orthogonal STBC is used to maintain full rate, the decoding complexity increases rapidly as the number of

cooperative nodes increases. A new type of distributed STBC was proposed in [35], where each node is assigned a unique signature vector and it provides diversity gain. The method for the optimization of signature vectors was also investigated.

The bit error probability and optimum power allocation strategy between cooperating nodes were investigated in distributed STBC in [36]. While the source transmits the signal during the first time interval, the cooperating nodes are selected based on their decoding results among the neighboring nodes. The cooperating nodes including the source transmit distributed STBC with the proper power allocation during the second time interval. However, the design of STBC for a large number of cooperating nodes was not considered and the stored table was required at the destination to assign the cooperating signal power according to its channel condition.

Energy efficiency of cooperative MIMO using Alamouti diversity schemes was investigated in [37]. They considered cooperative transmission and reception by grouping the nodes. Each node in the transmit cluster broadcasts its information to its neighboring nodes using different time slots. After each node receives all the required information of other nodes, they encode the transmit sequence with Alamouti code with the proper power allocation. On the receiving side, multiple nodes receive the signal and forward it to the final destination to do the joint detection. The result shows that total energy consumption and delay can be reduced over certain distance ranges at the cost of additional information exchange and decoding complexity.

2.2.2 Distributed Beamforming

The basic idea of distributed beamforming is that the received signals from multiple nodes are summed coherently at the destination by multiplying a proper weight at each cooperating node. The main issues in distributed beamforming are synchronization problems: phase,
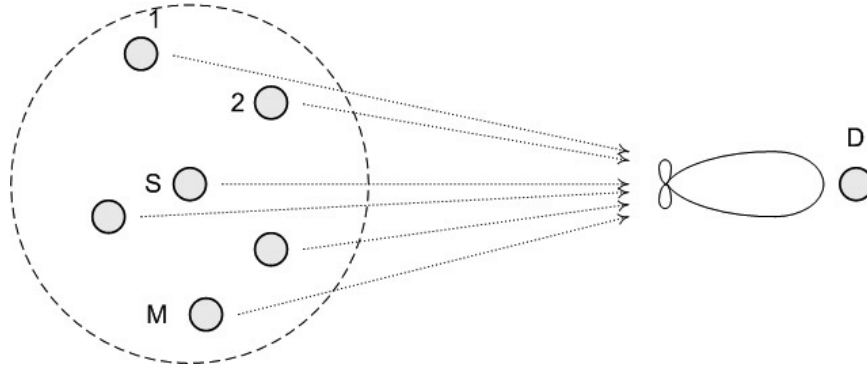
Figure 2.6: Cooperative communications with distributed beamforming

symbol time, and carrier frequency synchronization. In [10], a master-slave method is used to achieve synchronization. At the initial stage, a master which may be the destination sends the reference signal to neighboring nodes. All nodes involving in cooperation lock their carrier frequencies on the reference signal and extract channel information. After receiving the trigger signal, each cooperating node transmits the signal with the proper weight and delay. The weight and the delay at each cooperating node can be obtained by the reference signal and the distance information between a master and each cooperating node. Figure 2.6 shows an example of distributed beamforming. All synchronization processing are done at the transmitters with the obtained information from the reference signal. This method is very simple and does not require the complex signal processing at the destination. However, the finding of distance between cooperating nods and the destination is another challenging issue in distributed networks.

When distributed beamforming was initially proposed, cooperating nodes adjusted their phase to the designated master node. In [11], phase synchronization was achieved by feedback information. Each cooperating node transmits the signal with random phase offset and the destination compares the received SNR with the previous one. If the new received SNR is greater than the previous one, new phase offset at each cooperating node is updated

via message exchange. This process continues for the given time interval. The required overhead for phase adjustment will increases as the number of cooperating nodes increases and this approach might not be good enough in time-varying channel.

The power allocation method in distributed beamforming was investigated in [38], where amplify-and-forward cooperation was used in cooperating nodes. However, it does not consider the synchronization issues between the cooperating signals and the destination requires channel information of all cooperating nodes and broadcasts it for power adjustment between the cooperating signals.

Distributed beamforming with multiple nodes was investigated in [39]. They focused on the beam pattern with perfect and imperfect phase information at multiple nodes.

2.2.3 Synchronization Issues

As mentioned earlier, there are synchronization issues in the cooperative communication methods when the same channel is used for cooperating signals. Phase offsets among the cooperating signals come from the independent cooperating channels which need to be adjusted to achieve distributed beamforming gain. Symbol timing mismatch occurs due to the differences of propagation delay and signal processing time between cooperating nodes. Carrier frequency offsets among the cooperating signals occur since cooperating nodes use their own local oscillator.

The effect of phase synchronization error was analyzed in [10], where symbol timing error was ignored based on the assumption that it is small enough as compared to the symbol duration. In analysis, carrier frequency synchronization is assumed to be achieved by using the reference signal broadcasted from the master node.

To reduce the effect of synchronization error, time-reverse space time code (TR-STC) and space time OFDM (ST-OFDM) methods were investigated in [40] where the robustness

to symbol synchronization error was achieved. However, frequency synchronization error was not considered which is more important in OFDM systems. The effect of symbol synchronization error was investigated in terms of inter-symbol interference (ISI) [41]. It was shown that 10% symbol timing error does not have much effect on the BER performance of the cooperative transmission. However, there is no benefit in cooperative transmission for large timing error. Time synchronization is an important issue in distributed networks and many methods for time synchronization in sensor networks can be found in [42][43][44][45].

The effect of frequency offset among cooperative nodes in distributed STC was investigated in [46]. It was shown that the performance of distributed STC is significantly degraded by frequency offset between the cooperating signals. Two frequency estimation methods, training based method and blind method, have been discussed.

2.3   Cooperation in Network Perspective

The use of cooperative communications in a multihop configuration and routing schemes also has an interest to improve network performance. Incremental redundancy was considered to improve the energy efficiency in multihop networks [29]. The intermediate nodes combine the overheard hop transmissions and assign the proper number of punctured bits for the successful decoding at next hop. In this approach, the current transmit node requires perfect knowledge of the received energy at next node. The use of overheard signal of the previous hops to increase the detection probability was also considered and the performances with the conventional and the cooperative multihop transmission were compared in [47][48].

The tradeoff between energy and delay was analyzed in multihop networks [49]. For the cooperative signal transmission and reception, multiple nodes are grouped as a cluster in each hop and Alamouti codes are used for diversity gain. Multihop transmission through the cluster of cooperative nodes was investigated in [50]. Alamouti codes are used between

the nodes in clusters with regenerative and non-regenerative methods. However, additional information exchange is required in each cluster to form Alamouti codes.

The cooperative multiple access control (MAC) and routing protocols were proposed to reduce the energy consumption in the network [51]. At the initial stage, the cooperative nodes are formed by exchanging control messages with neighboring nodes and optimal transmit power is determined. At the second stage, cooperative nodes transmit the signal at the same time using different pseudo noise (PN) sequences which are assigned at the initial stage. The routing protocol to maximize the advantage of cooperative transmission was established by exchanging local information among the cooperating nodes. In [52], authors proposed route searching algorithms with cooperation of other nodes to minimize overall power consumption. However, it requires all channel information of networks.

The cooperative communication can help connectivity in wireless ad hoc networks by increasing the radio range [53]. It is shown that the cooperative network can be fully connected with high probability.

Cooperation through the best neighboring node was proposed in [54]. The source and the destination exchange the control message before the actual data transmission and the neighboring node which has best channel condition to both links sends a message for cooperation. The generation of response message at the neighboring nodes is controlled by the timer which depends on the channel condition to the source and the destination. This method requires no *a priori* information of nodes' position and channel condition. A number of protocols have been proposed to use opportunistic cooperating channels in wireless ad hoc networks [55][56]. In those protocols, however, only one relay will be selected to forward the data packet to the destination and additional information is required for the node selection procedure such as inter-node loss rates and geographic distance. Furthermore, those approaches limit the potential performance gain by restricting the number of the forwarding nodes to one even when multiple neighboring nodes can be involved in cooperation.

2.4   Cooperative Communications with Multiple Antennas

The basic methods of cooperative communications have been introduced in the previous sections. However, the initial work of cooperative communications was focused on the single antenna systems. In this section, the cooperative communication systems with multiple antennas at the node will be introduced.

The capacity of MIMO relay channels has been investigated for the Gaussian and the Rayleigh fading cases [57]. In [57], the authors assumed that the cooperating node operates with a full duplex mode. A more realistic scenario was investigated in [58], where the cooperative protocol was divided into three traffic patterns depending on the usage of time slots. In this analysis, however, only the source and the destination were assumed to have multiple antennas, while cooperating nodes had one antenna. When channel state information is available at the cooperating node, the power allocation method at the cooperating node to maximize the capacity of cooperative transmission was investigated for the amplify-and-forward cooperation [59]. When cooperative nodes share their channel information, power allocation strategies to maximize channel capacity were shown in [60] where singular value decomposition (SVD) is applied to achieve orthogonal channel between the source and cooperating nodes.

The performance with multiple antennas in cooperating nodes was investigated with zero forcing (ZF) and QR decomposition methods [61]. They claim that the cooperative transmission has worse capacity than the direct transmission due to the use of multiple time slots when the direct path is in line-of-sight (LOS) and has high SNR. It is also shown that cooperating nodes need to be close to the source to achieve capacity improvement.

For the multiple antennas at the source and the destination, the upper bound of coherent MIMO relay network capacity was shown in [62]. They proposed the relay protocol to

eliminate the multistream interference by assigning each relay to one of data streams with known channel information. When the relays have no channel information, decoding method at the destination is important to achieve capacity gain.

2.5   Chapter Summary

Cooperative communication is an attractive technique for distributed networks, where closely located single antenna nodes transmit and receive the signal cooperatively to create virtual antenna arrays.

In this overview, the cooperative methods were categorized into two areas: cooperation via orthogonal channels and cooperation via the same channel. The orthogonal channels can be different time slots, frequency bands, and signature codes. Amplify-and-forward, decode-and-forward, and coded cooperation are included in this category. When the same channel is used for cooperation, distributed STC or distributed beamforming is used to obtain diversity or coherent combining at the destination. The synchronization issues were also discussed when the same channel is used by all cooperating nodes at the same time. As an extended application, cooperation with multiple antennas at a node was also summarized. From a network perspective, multihop and routing performance with cooperative communications were also summarized.

Chapter 3

INR Scheme for Cooperative Diversity and Distributed Beamforming

Cooperative communications can provide many advantages in terms of capacity, link reliability, power consumption, and coverage range. Most importantly, cooperative communications provides a means for low-power nodes to achieve the performance of larger, high-power nodes. However, the main disadvantage of cooperative communications is bandwidth efficiency. Furthermore, even when the same channel is used for cooperation to increase bandwidth efficiency, the cooperating signal will be redundant if the received signal from the source is of sufficient quality to decode the original information data. A third drawback is that when the cooperating signal is of poor quality, it may hurt performance. This is because in most of the previous work the quality of cooperative signals is not considered when cooperating nodes are selected.

In wireless communication systems, erroneous packet reception is inevitable due to the harsh communication environment. Incremental redundancy is an ARQ scheme which

achieves both reliable transmission and efficient channel usage by providing additional information only when it is necessary [63]. In [28], cooperative diversity was achieved by transmitting redundant code blocks via different cooperative relays. However, the technique should be considered as a method to obtain block fading channels, *i.e.*, temporal diversity, not an ARQ method since decoding at the destination is performed after receiving all coded blocks. In coded cooperation [8], channel resources are used more efficiently by transmitting the partner's or the node's own information depending on the decoding result of the partner's received code block. However, the technique does not account for channel conditions from the transmitter to the destination.

In this chapter we will propose and analyze an efficient cooperative retransmission scheme which addresses the drawbacks listed above. The approach is (a) bandwidth efficient since it does not require additional channels, (b) it only uses cooperation when needed, (c) does not allow nodes with poor channel conditions to cooperate, and (d) most importantly it accomplishes this with very little overhead.

3.1   Cooperative INR Scheme

Incremental Redundancy is an ARQ method for reducing delay and improving the throughput of data transmission which is also referred to hybrid ARQ II. In a traditional INR scheme, information data is coded with a special type of encoder and divided into N blocks at the source, $\mathbf{C} = \{\mathbf{C_1}, \mathbf{C_2}, ..., \mathbf{C_N}\}$. During the first time slot, the source transmits the first code block, $\mathbf{C_1}$, to the destination. If the destination decodes the received code block successfully, it responds with an acknowledgment (ACK) message and the source transmits the next data information block. If the destination cannot decode the received code block, it responds with a NACK message to request the next code block, $\mathbf{C_2}$. Upon receiving the next code block, the destination performs the decoding process again after appending it

to the previous received data. This procedure continues until the received data is decoded successfully at the destination or the final code block is reached. An example of incremental redundancy hybrid ARQ is high speed downlink packet access (HSDPA) [64][65]. HSDPA is adopted in universal mobile telecommunications system (UMTS) to provide higher data transfer speeds and capacity.

In the *cooperative* INR scheme developed here, the first code block is transmitted from the source to the destination during the first time slot, just as in the conventional INR scheme. While the destination receives and decodes the first code block, the neighboring nodes also decode the overheard code block. If an ACK message is replied by the destination, the next information block is encoded and transmitted from the source. When the destination cannot decode the received data and requests an additional code block with a NACK message, a subset of the neighboring nodes also overhear this request. Those neighboring nodes which decode both the information data and the NACK message successfully will be cooperative nodes and they will send the next code block to the destination after receiving the NACK message. The quality of the next code block will likely be good since the selected cooperative nodes have good channels as demonstrated by their ability to decode the NACK message correctly.

Each neighboring node decides independently to send the next code block based on the overheard messages which are exchanged between the source and the destination. In other words, there is no separate node selection process, thus eliminating any associated overhead. However, it is thus possible for multiple nodes to transmit the next code block at the same time. To achieve the coherent sum of multiple signals at the destination, channel phase and carrier frequency from cooperative nodes to the destination must be synchronized when the next code block is transmitted. Channel state information (CSI) for each cooperating link can be obtained from the NACK message and will be used for phase offset compensation. It is assumed that carrier frequency synchronization can also be obtained from the NACK

message or from a busy tone signal if a busy tone multiple access scheme is used [66]. It is also assumed that the symbol duration is long enough to ignore the propagation difference from cooperative nodes to the destination. This assumption is reasonable for short-range sensor networks. Symbol delay differences can also be mitigated through OFDM using a cyclic prefix. This INR method will be referred to as INR with preferred relays (PR-INR). Table 3.1 shows the procedure of PR-INR in distributed networks.

Figure 3.1 shows an example of the PR-INR scheme in distributed networks with two code blocks. During the first exchange of data and ACK/NACK packets, R_4 and R_5 can decode both packets correctly and will be cooperating nodes. When $\mathbf{C_2}$ is requested by the destination, these nodes transmit the next code block to the destination by using distributed beamforming as shown in Figure 3.1(b). There are several advantages of the PR-INR method. This method does not require any *a priori* information of the neighboring nodes or an initial stage to form the cooperative cluster, which reduces the required overhead time. Also user cooperation will be initiated only when an additional code block is requested by the destination. Cooperative nodes are self-selected based on channel conditions from the source as well as from the destination, which results in good signal quality for the redundant code blocks. Furthermore, distributed beamforming gain can be achieved when multiple relays are involved in the cooperation.

3.2   Goodput and Outage Probability

In this section, the performance of the PR-INR scheme will be compared with coded cooperation [8] and the clustering INR method [28]. Also, the outage probability of cooperative retransmission scheme will be analyzed and compared with the retransmission scheme by the source.

Table 3.1: Algorithm of a PR-INR scheme in distributed networks

---

Generate whole code blocks at the source, $\mathbf{C} = \{\mathbf{C_1}, \mathbf{C_2}, ..., \mathbf{C_N}\}$
Transmit $\mathbf{C_1}$ *to the destination*
  Decode $\mathbf{C_1}$ *at the destination and the neighboring nodes*
  Send ACK or NACK to the source
If ACK is received, go to next information data
If NACK is received, do n=2 to N
  Send $\mathbf{C_n}$ *after channel compensation at nodes which can transmit* $\mathbf{C_n}$
      and receive NACK from the destination
  If no relays can send $\mathbf{C_n}$*, send* $\mathbf{C_n}$ *at the source*
  If ACK is received, go to next information data
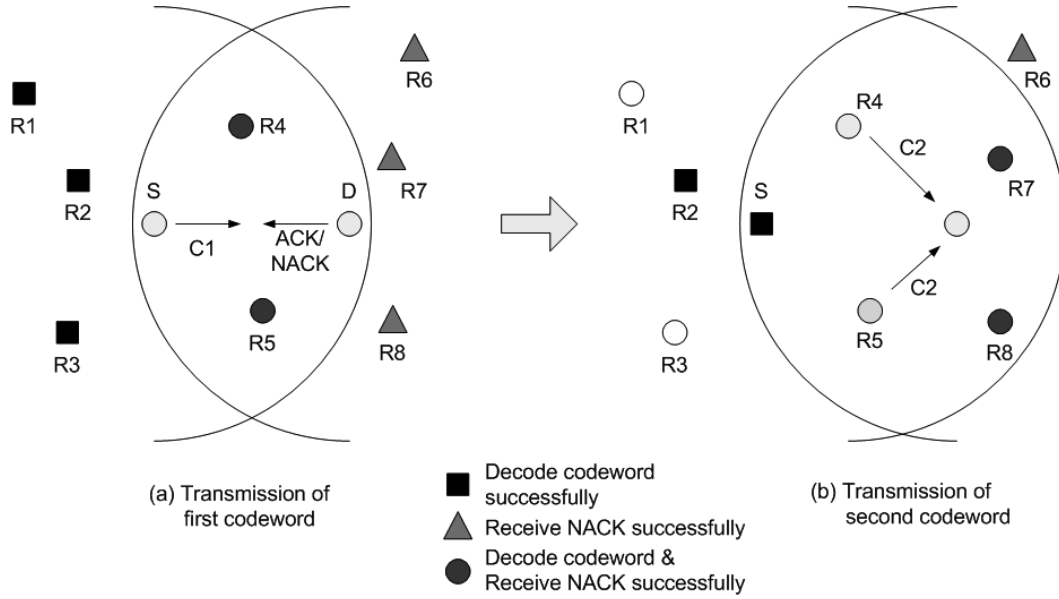
Figure 3.1: Example of PR-INR in distributed networks

3.2.1   Goodput of Cooperative Retransmission

In coded cooperation, only one redundant code block is delivered to the destination through the cooperative node. To meet this constraint, a convolutional code with one redundant code block will be used for performance comparison. A $R = 1/3$ convolutional code with $K = 4$ is considered. The polynomial generators are $g_1 = 15_{(8)}$, $g_2 = 17_{(8)}$ and $g_3 = 13_{(8)}$. The first code block, $\mathbf{C_1}$, is a $R = 1/2$ convolutional code which is obtained by puncturing of the whole code block. The punctured bits will be the redundant code block, $\mathbf{C_2}$. The length of the information is fixed to 128 bytes and BPSK modulation is used. Let N_b be the number of information bits in the coded packet. The goodput will be used as the comparison metric which is defined as

$$G = \frac{\text{\# of successful packets}}{\text{\# of transmitted packets}} \cdot \frac{\text{\# of information bits / received packet}}{\text{\# of bits / received packet}}. \tag{3.1}$$

In the initial proposal of coded cooperation, the cooperative signal is transmitted over different frequency bands at the same time [8]. For a fair comparison, a time division protocol is used for coded cooperation in this work.

In coded cooperation with a time division protocol, the first code block transmits to the destination and the cooperative node in the first time slot. If the cooperative node decodes the received signal correctly, the second code block will be transmitted through the cooperative node. If the cooperative node cannot decode it, the source will transmit the second code block in the next time slot. As a result, a total $3N_b$ bits ($2N_b$ bits in $\mathbf{C_1}$ and N_b bits in $\mathbf{C_2}$) are delivered to the destination. Coded cooperation considered here is shown in Figure 3.2.

In the cooperative INR with clustering technique [28], the source broadcasts the first code block during the first time slot and waits for ACK or NACK messages from neighboring nodes. If cooperative nodes decode the received code block successfully, they transmit the
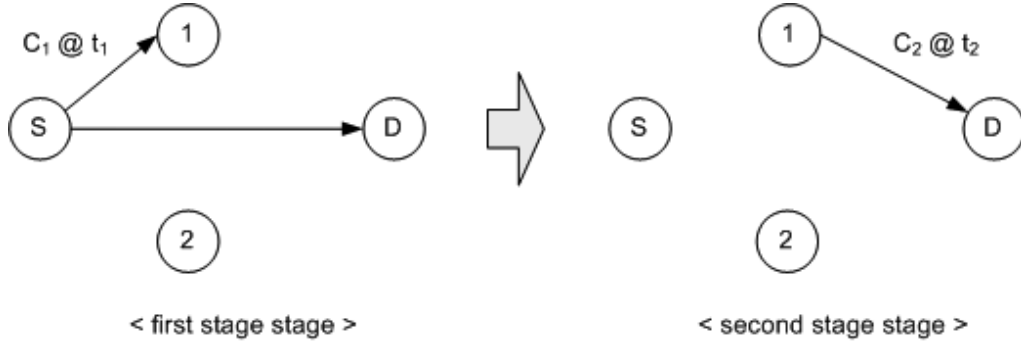
Figure 3.2: Example of coded cooperation

corresponding code blocks in the appropriate time slots. If the source receives a NACK message from the node, the source transmits the corresponding code block in the given time slot. Therefore, a total $5N_b$ bits including the initial stage is transmitted by the clustering method. An example of the clustering INR method with two neighboring nodes is shown in Figure 3.3.

In the PR-INR scheme, the use of the second time slot is decided by the feedback message from the destination. If the decoding of the first code block fails, the second code block will be transmitted by any possible neighboring nodes. The number of the total transmitted bits in the PR-INR method depends on the $\mathbf{C_2}$ transmission. If $\mathbf{C_2}$ is requested by the destination, the total number of transmitted bits is $3N_b$. Otherwise, it is $2N_b$. It is assumed that feedback messages, ACK and NACK packets, are short enough to be ignored as compared to data packets in the clustering and PR-INR methods.

Figure 3.4 shows the goodput of the three cooperative methods. There are two neighboring nodes which can be independently located close or far from the destination. We assume that the distance between the neighboring nodes and the source is $d_{sr} = 0.3$ and the distance between the neighboring nodes and the destination is $d_{rd} = 0.76$ or $d_{rd} = 1.27$. It is assumed that 3 dB SNR is required to decode a NACK message correctly in the PR-INR method. For fair comparison, total transmit power of the redundant code block in the pro-
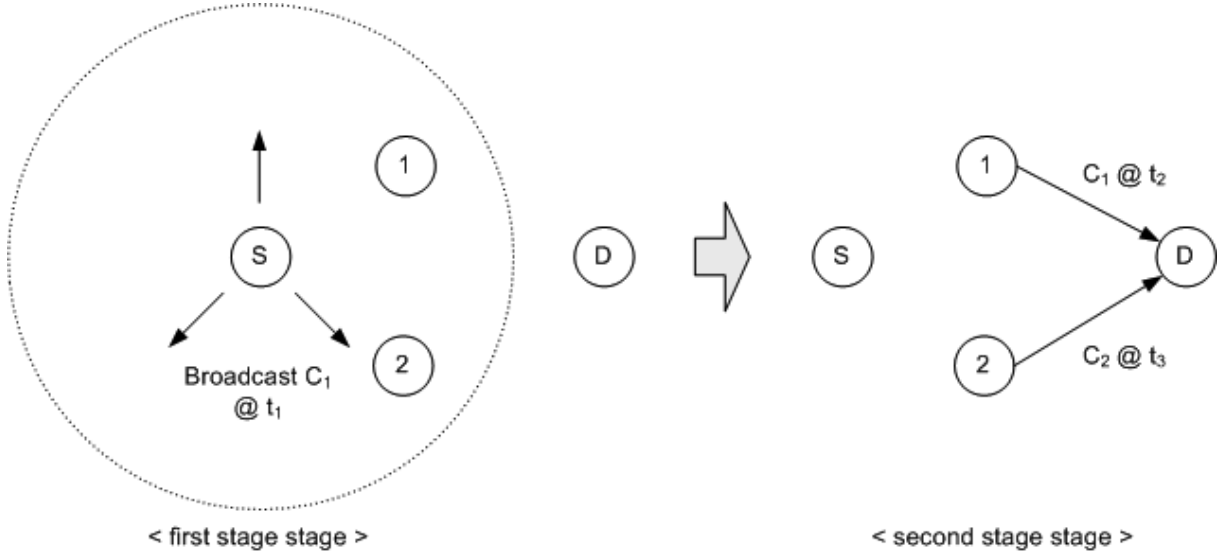
Figure 3.3: Example of clustering INR (R. Liu, P. Spasojević, and E. Soljanin, "Cooperative diversity with incremental redundancy turbo coding for quasi-static wireless networks," *IEEE SPAWC*, ©IEEE 2005)

posed method is normalized with the number of cooperating nodes. The PR-INR method provides the best performance except in the low SNR region where the whole code blocks are transmitted through the shorter path links in the clustering INR method. When the position of the two neighboring nodes is switched, the PR-INR method shows the same performance whereas the other two methods are affected by their positions. This result comes from the fact that cooperative nodes are not fixed in the PR-INR method. In coded cooperation and the clustering method, even though other nodes have better channel conditions to the destination than cooperative nodes, they cannot be involved in cooperation since cooperative nodes are already fixed before data transmission.

Another advantage of the PR-INR method as compared to the other two methods is that there is no limitation in the number of cooperative nodes. When there are multiple relays around the source and the destination, additional gain can be obtained by distributed beamforming in the PR-INR method. Figure 3.5 shows the goodput when two cooperative
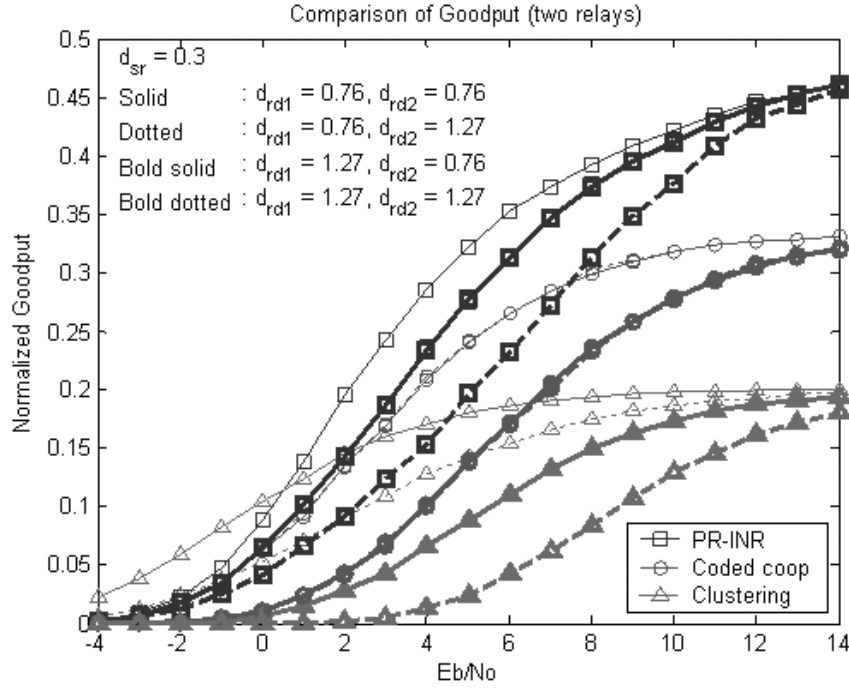
Figure 3.4: Comparison of goodput with PR-INR, coded cooperation, and the clustering INR methods (# of neighboring nodes = 2, $d_{sr} = 0.3$, $d_{rd} = 0.76$ or 1.27)
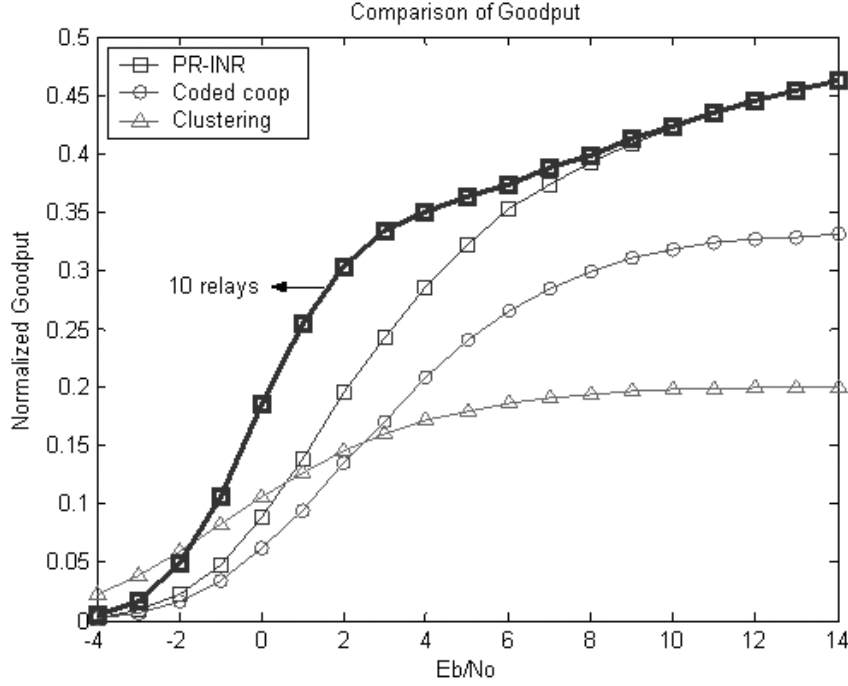
Figure 3.5: Comparison of goodput with PR-INR, coded cooperation, and the clustering INR methods (# of neighboring nodes = 10, $d_{sr1} = d_{sr2} = 0.3$, $d_{rd1} = d_{rd2} = 0.76$)

nodes are located between the source and the destination and an additional eight relays are uniformly distributed around the source within a circle of 0.5. The goodput gain with multiple nodes in the PR-INR scheme can be seen in the moderate SNR range. The advantage with multiple nodes is more clear in the PER performance as shown in Figure 3.6 where it decreases very sharply as compared to other cooperative methods. Note that perfect synchronization was assumed by using a NACK message in the PR-INR scheme when distributed beamforming is used. The offset estimation method using a NACK message for cooperating signals will be investigated in Chapter 5.
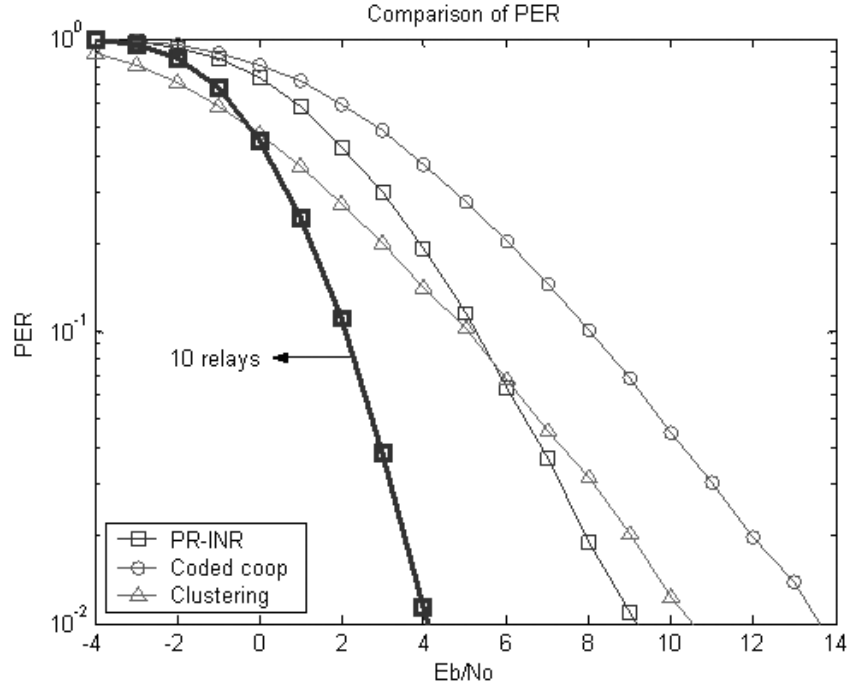
Figure 3.6: Comparison of PER with PR-INR, coded cooperation, and the clustering INR methods (# of neighboring nodes = 10, $d_{sr1} = d_{sr2} = 0.3$, $d_{rd1} = d_{rd2} = 0.76$)

3.2.2   Outage Probability of Cooperative Retransmission

The outage probability of the PR-INR scheme will now be examined and compared with the typical retransmission scheme by the source. When different code blocks are delivered to the destination, the performance of retransmission scheme depends not only diversity but also coding gain. In this analysis, therefore, it is assumed that same data is retransmitted and all received signals are combined with MRC.

First, let's consider the outage probability of retransmission from the source. The received signals during two time slots are given by

$$
\begin{aligned}
\mathbf{r}_1 &= \sqrt{\alpha_{sd}} h_{sd,1}\mathbf{s} + \mathbf{n}_1 \\
\mathbf{r}_2 &= \sqrt{\alpha_{sd}} h_{sd,2}\mathbf{s} + \mathbf{n}_2
\end{aligned}
\tag{3.2}
$$

where α_{sd} is the large scale path loss of the direct link and $h_{sd,i}$ is the small scale channel coefficient of ith transmission of the direct link which is assumed to be i.i.d. complex Gaussian random variable with zero mean and 0.5 variance per dimension. It is assumed that channel coefficients of the first and the second transmission are independent and identically distributed (i.i.d.) by considering random backoff time before retransmission. $\mathbf{s}$ is the transmit signal and $\mathbf{n}_i$ is complex Gaussian noise of the ith received signal which is zero mean with variance σ_n^2. The mutual information of the first received signal and the combined signal with the second received signal are given by

$$
\begin{aligned}
I_{sd}^1 &= \log_2\left(1 + \eta|h_{sd,1}|^2\right) \\
I_{sd}^2 &= \frac{1}{2}\log_2\left(1 + \eta[|h_{sd,1}|^2 + |h_{sd,2}|^2]\right)
\end{aligned}
\tag{3.3}
$$

where $\eta = \alpha_{sd}/\sigma_n^2$ is the average SNR of the direct link. The $1/2$ in I_{sd}^2 results from the use of additional time slot for retransmission. $|h_{sd,1}|^2$ is an exponentially distributed random variable, U_1, and $|h_{sd,1}|^2 + |h_{sd,2}|^2$ is the sum of exponentially distributed random variables,

U_2. The probability density function (pdf) and cumulative density function (cdf) of the sum of k exponential random variables can be easily evaluated by multiple convolution and its integration which are given by

$$
\begin{aligned}
f_{U_k}(u) &= \frac{1}{(k-1)!} u^{k-1} e^{-u} \\
F_{U_k}(u) &= \frac{1}{(k-1)!} \gamma(k, u)
\end{aligned}
\tag{3.4}
$$

where $\gamma(a, x)$ is incomplete gamma function given by

$$
\gamma(a, x) = \int_0^x t^{a-1} e^{-t} dt.
\tag{3.5}
$$

The outage probability of k transmitted and combined signals from the source can be obtained by

$$
\begin{aligned}
P_{o,k}^{sd} &= \Pr\{I_{sd}^k < R_{th}\} \\
&= F_{U_k}\left(\frac{2^{kR_{th}} - 1}{\eta}\right) = \frac{1}{(k-1)!} \gamma\left(k, \frac{2^{kR_{th}} - 1}{\eta}\right)
\end{aligned}
\tag{3.6}
$$

where R_{th} is a threshold data rate which will be the transmit data rate at the source. When L cooperating nodes are involved in cooperation, the received signal during the second time slot is given by

$$
\mathbf{r}_2 = \frac{1}{\sqrt{L}} \sum_{l=1}^{L} \sqrt{\alpha_{rd,l}} h_{rd,l} \mathbf{s} + \mathbf{n}_2
\tag{3.7}
$$

where $\alpha_{rd,l}$ and $h_{rd,l}$ represent the large scale path loss and channel coefficient of cooperating link l, respectively. Note that again the total transmit power of the retransmitted signal is normalized by the number of cooperating nodes. When perfect synchronization is assumed among the cooperating signals, the mutual information of combined signal is given by

$$I_{co}^L = \frac{1}{2} \log_2 \left(1 + \eta |h_{sd,1}|^2 + \frac{1}{L\sigma_n^2} \left[\sum_{l=1}^{L} \sqrt{\alpha_{rd,l}} |h_{rd,l}| \right]^2 \right).$$ (3.8)

The distribution of the combined signal is not easy to obtain for the general case. For simplicity, let's consider the case when the long term path loss of all cooperating nodes is same, $\alpha_{sr,l} = \alpha_{sr}$ and $\alpha_{rd,l} = \alpha_{rd}$ for $l = 1, 2, \cdots, L$. Then, (3.8) can be rewritten as

$$I_{co}^L = \frac{1}{2} \log_2 \left(1 + \eta \left[|h_{sd,1}|^2 + \frac{\delta}{L} W_L^2 \right] \right)$$ (3.9)

where $\delta = (d_{rd}/d_{sd})^{-\kappa}$ with propagation coefficient κ and $W_L = \sum_{l=1}^{L} |h_{rd,l}|$. The approximated pdf of W_L is given by [67]

$$f_{W_L}(w) = \frac{w^{2L-1} e^{-w^2/2b(L)}}{2^{L-1} b(L)^L (L-1)!}$$ (3.10)

where $b(L) = \frac{1}{2L}[(2L-1)!!]^{1/L}$ and $(2L-1)!! = (2L-1) \cdot (2L-3) \cdots 3 \cdot 1$. The pdf of $X_L = W_L^2$ is given by

$$f_{X_L}(x) = \frac{x^{L-1} e^{-x/2b(L)}}{2^L b(L)^L (L-1)!}.$$ (3.11)

The distribution of combined signal is given by the weighted sum of the exponential random variable and X_L, $Y_L = U_1 + \frac{\delta}{L} X_L$, where the pdf of U_1 is given in (3.4). The pdf of Y_L can be obtained by

$$f_{Y_L}(y) = \frac{1}{(1 - \xi(L))^L (L-1)!} e^{-y} \gamma \left(L, \frac{1 - \xi(L)}{\xi(L)} y \right)$$ (3.12)

where $\xi(L) = 2\delta b(L)/L$ and its cdf is given by

$$F_{Y_L}(y) = \frac{1 - e^{-y}}{(1 - \xi(L))^L} - \frac{\xi(L)}{(1 - \xi(L))^L} \sum_{l=0}^{L-1} \frac{(1 - \xi(L))^l}{l!} \gamma \left(l + 1, \frac{y}{\xi(L)} \right).$$ (3.13)

The outage probability of cooperative retransmission using the PR-INR scheme depends on the probability of cooperation from the neighboring nodes. To be involved in cooperation, the mutual information of the neighboring node must be greater than the threshold data rate, R_{th}, and the channel condition to the destination should be good enough to receive the NACK message correctly. The mutual information of the received signal at the neighboring node is given by

$$I_{sr} = \log_2 \left(1 + \eta_{sr}|h_{sr}|^2\right) \tag{3.14}$$

where $\eta_{sr} = \alpha_{sr}/\sigma_n^2$ and α_{sr} is the large scale path loss between the source and the neighboring node. h_{sr} is channel coefficient between the source and the neighboring node which is given by $\mathcal{CN}(0,0.5)$. The probability of cooperation of the neighboring nodes is given by

$$
\begin{aligned}
p_{co} &= \Pr\{I_{sr} > R_{th}\} \Pr\{\eta_{rd}|h_{rd}|^2 > \eta_{NACK}\} \\
&= \exp\left(-\frac{2^{R_{th}} - 1}{\eta_{sr}}\right) \exp\left(-\frac{\eta_{NACK}}{\eta_{rd}}\right)
\end{aligned}
\tag{3.15}
$$

where η_{rd} are average SNR of the cooperating node to destination link and η_{NACK} is the required SNR to receive the NACK message correctly.

The outage probability of cooperative retransmission with M neighboring nodes is given by

$$
\begin{aligned}
P_{o,M}^{co} &= (1 - p_{co})^M P_{o,2}^{sd} \\
&+ \sum_{m=1}^{M} \binom{M}{m} p_{co}^m (1 - p_{co})^{M-m} F_{Y_m}\left(\frac{2^{2R_{th}-1}}{\eta}\right)
\end{aligned}
\tag{3.16}
$$

The first term represents the outage probability when there is no cooperating node out of M neighboring nodes and the second term represents the outage probability when there are m

cooperating nodes. Finally, the outage probability with M neighboring nodes can be formed

using (3.6) and (3.13) and is given by

$$
P_{o,M}^{co} = (1 - p_{co})^M \gamma\left(2, \frac{2^{2R_{th}} - 1}{\eta}\right) + \sum_{m=1}^{M} \binom{M}{m} p_{co}^m (1 - p_{co})^{M-m}
$$

$$
\cdot \left\{ \frac{1 - e^{-\frac{2^{2R_{th}} - 1}{\eta}}}{[1 - \xi(m)]^m} - \frac{\xi(m)}{[1 - \xi(m)]^m} \cdot \sum_{l=0}^{m-1} \frac{(1 - \xi(m))^l}{l!} \gamma\left(l + 1, \frac{2^{2R_{th}} - 1}{\xi(m)\eta}\right) \right\}
$$

(3.17)

Figure 3.7 shows the outage probability of retransmission by the source and cooperating

nodes. The number of neighboring nodes varies from one to four, $M = \{1,2,3,4\}$. It is

assumed that all neighboring nodes have same average SNR to the source and the destination,

$d_{sr} = 0.3d_{sd}$ and $d_{rd} = 0.76d_{sd}$. The required SNR for successful reception of the NACK

message is assumed to be 3 dB SNR and the threshold data rate is 1 bps/Hz, $R_{th} = 1$ bps/Hz.

The dotted line shows the outage probability of the single transmission of direct link. The

retransmission by the source shows better outage probability than the single transmission

due to diversity gain except low values of SNR where diversity gain cannot overcome the

use of an additional time slot for retransmission. For the cooperative retransmission with

$M = 1$ which can be considered as a form of decode-and-forward cooperation, the outage

performance is better than the retransmission by the source due to the gain from the shorter

path link. When there is retransmission through multiple neighboring nodes, better outage

performance can be obtained as the number of neighboring nodes increases due to distributed

beamforming gain.

Figure 3.8 shows the outage probability as the threshold data rate varies with the SNR

of direct link fixed at $\eta = 8$ dB. The proposed cooperative retransmission shows better outage

performance as compared to decode-and-forward cooperation and simple retransmission by

the source by using all possible neighboring nodes for retransmission. Note that perfect
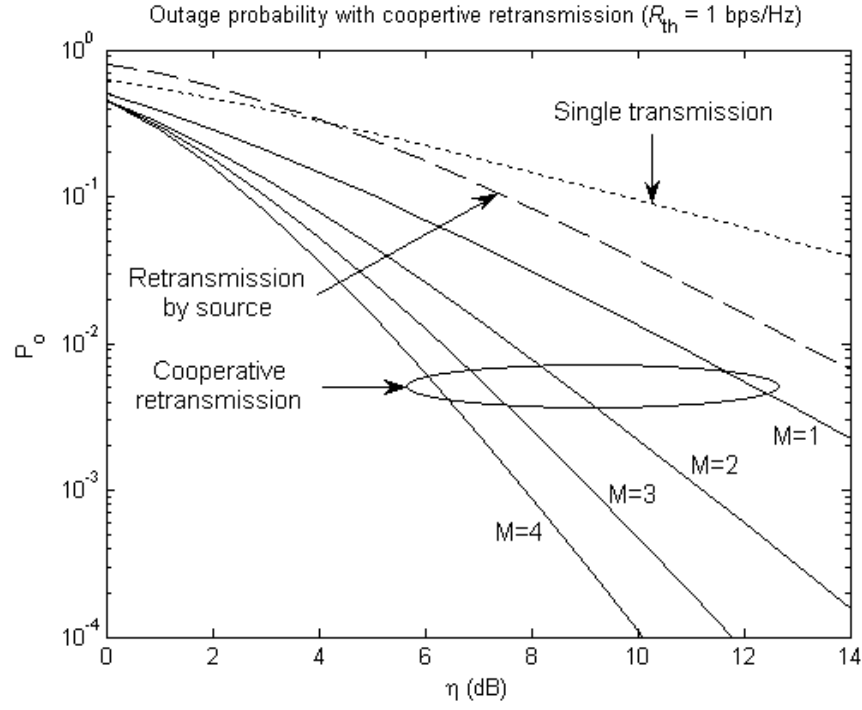
Figure 3.7: Outage probability of retransmission via the source and cooperative nodes (fixed $R_{th} = 1$ bps/Hz, $\eta_{NACK} = 3$ dB, $d_{sr} = 0.3d_{sd}$, $d_{rd} = 0.76d_{sd}$, M={1,2,3,4})
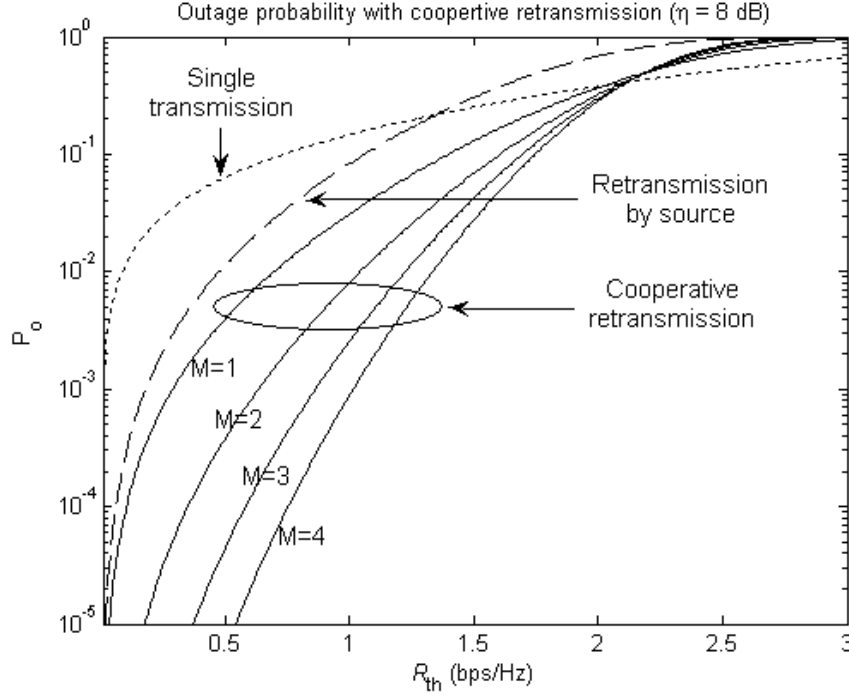
Figure 3.8: Outage probability of retransmission via the source and cooperative nodes (fixed $\eta = 8$ dB, $\eta_{NACK} = 3$ dB, $d_{sr} = 0.3d_{sd}$, $d_{rd} = 0.76d_{sd}$, $M=\{1,2,3,4\}$)

phase and frequency synchronization have been assumed in this analysis. If there is an error in phase and frequency estimation, full distributed beamforming gain cannot be achieved. The performance degradation due to synchronization errors will be examined in Chapter 4.

3.3 Chapter Summary

In this chapter, an efficient cooperative INR method was investigated for distributed networks. In the proposed retransmission scheme, cooperative nodes are self-selecting by listening to the message exchange between the source and the destination. When neighboring nodes are involved in the cooperation, good channels are obtained due to the fact that only those cooperative nodes that can decode the NACK message of the destination correctly

participate. In the PR-INR method, multiple nodes can transmit the redundant code blocks at the same time using distributed beamforming to achieve additional gain. This cooperative retransmission scheme can be performed without any *a priori* knowledge of the neighboring nodes such as the number, position, or channel status.

The proposed PR-INR scheme shows better goodput and PER performance in nearly every SNR range as compared to coded cooperation and the clustering INR method. The closed form expression of outage probability of the proposed retransmission scheme was evaluated when cooperating signals have the same average SNR. It was shown that the proposed cooperative retransmission scheme outperforms retransmission by the source and decode-and-forward cooperation.

In the proposed retransmission scheme, perfect synchronization was assumed for cooperating signals. However, this assumption might not be valid for real wireless communication links. In Chapter 4, the effect of synchronization errors will be examined.

Chapter 4

Synchronization Errors in Distributed Beamforming

In conventional transmit beamforming systems, only phase synchronization of the transmitted signals is considered due to the facts that a single local oscillator is used and the distance difference of the multiple signal paths is small enough to be ignored. In distributed beamforming (which is used in the proposed retransmission scheme in the previous chapter), however, multiple copies of the transmit signal are generated from different locations with different local oscillators. Therefore, all three synchronization issues, *i.e.*, phase, frequency, and symbol time, have to be properly controlled to achieve beamforming gain. We will investigate the impact of synchronization errors in distributed beamforming in this chapter.

4.1   System Model

We will consider distributed beamforming with M cooperating nodes. In this chapter, we focus on the effects of synchronization errors instead of synchronization methods which will be investigated in Chapter 5. Assuming that M cooperating nodes adjust their offsets using

the NACK message as shown in Figure 2.6, the received signal at the destination can be expressed by

$$r(t) = \frac{1}{\sqrt{M}} \sum_{m=1}^{M} \sqrt{\alpha_m} |h_m| x(t - \tau_m) e^{j2\pi f_m t} e^{j\theta_m} + n(t) \tag{4.1}$$

where α_m and h_m represent the long term signal loss and channel coefficient of the cooperating signal m, respectively. $x(t)$ is the transmit signal. τ_m, f_m, and θ_m are residual symbol timing offset, frequency offset, and phase offset between the destination and the cooperating node m, respectively. $n(t)$ is noise at the destination. It is assumed that τ_m is uniformly distributed in $-\tau_{\max} \leq \tau_m \leq \tau_{\max}$. It is also assumed that f_m and θ_m are uniformly distributed in $-f_{\max} \leq f_m \leq f_{\max}$ and $-\theta_{\max} \leq \theta_m \leq \theta_{\max}$, respectively. Note that the total transmit power is normalized by the number of cooperating nodes. The amount of SNR degradation due to synchronization errors will be investigated for single-carrier and multi-carrier, especially OFDM, systems. We will analyze the effect of the three offsets separately since they are generally independent of each other.

4.2   Single-carrier Systems

4.2.1   Symbol Time Offset

When only symbol time offset is considered in single-carrier systems, the received signal in (4.1) can be rewritten as

$$r(t) = \frac{1}{\sqrt{M}} \sum_{m=1}^{M} \sqrt{\alpha_m} |h_m| x(t - \tau_m) + n(t) \tag{4.2}$$

When there are symbol time offsets between the cooperating signals, adjacent symbols will affect the output of the matched filter at the destination. Without loss of generality, symbol

timing of M cooperating signals can be modeled as shown in Figure 4.1, where T is the symbol duration. The output of the matched filter for symbol i can be expressed by

$$r(i) = \frac{1}{T} \int_{iT}^{(i+1)T} r(t)x^*(t)dt. \tag{4.3}$$

Let $s_i(t)$ be the ith transmit symbol which is given by

$$s_i(t) = x(iT + t) \qquad 0 < t < T \quad \text{for} \quad i = 1, 2, \cdots, K_s \tag{4.4}$$

where K_s is the number of symbols in the transmitted signal. Then, (4.3) can be rewritten as

$$
\begin{aligned}
r(i) &= \frac{1}{T} \int_0^T r(iT + t)s_i^*(t)dt \\
&= \frac{1}{T\sqrt{M}} \sum_{m=1}^{M_l} \int_0^T \sqrt{\alpha_m}|h_m|\tau_m s_{i+1}(t)s_i^*(t)dt \\
&+ \frac{1}{T\sqrt{M}} \sum_{m=1}^{M} \int_0^T \sqrt{\alpha_m}|h_m|(T - \tau_m)s_i(t)s_i^*(t)dt \\
&+ \frac{1}{T\sqrt{M}} \sum_{m=M_l+1}^{M} \int_0^T \sqrt{\alpha_m}|h_m|\tau_m s_{i-1}(t)s_i^*(t)dt \\
&+ \frac{1}{T} \int_0^T n(iT + t)s_i^*(t)dt
\end{aligned} \tag{4.5}
$$

where M_l is the number of cooperating signals whose symbols start earlier than the timing of the matched filter. In that case, there is ISI with the next symbol as shown in the first term in (4.5). Also, ISI with the previous symbol occurs for the remaining cooperating signals which is given in the third term. When square pulse shape is assumed, (4.5) can be expressed by
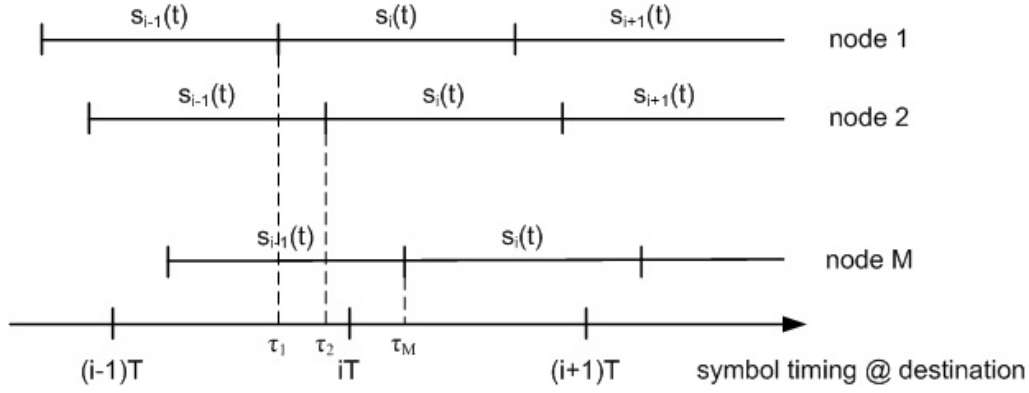
Figure 4.1: Symbol timing diagram in distributed beamforming

$$
\begin{aligned}
r(i) &= \frac{1}{\sqrt{M}} \sum_{m=1}^{M_l} \sqrt{\alpha_m} |h_m| \frac{\tau_m}{T} \rho(1) + \frac{1}{\sqrt{M}} \sum_{m=1}^{M} \sqrt{\alpha_m} |h_m| \frac{\tau_m}{T} \rho(0) \\
&\quad + \frac{1}{\sqrt{M}} \sum_{m=M_l+1}^{M} \sqrt{\alpha_m} |h_m| \frac{\tau_m}{T} \rho(-1) + n(i) \\
&= \frac{1}{\sqrt{M}} \sum_{m=1}^{M_l} \sqrt{\alpha_m} |h_m| \frac{\tau_m}{T} \rho(1) + \sqrt{M} \left\{ \frac{1}{M} \sum_{m=1}^{M} \sqrt{\alpha_m} |h_m| \frac{\tau_m}{T} \rho(0) \right\} \\
&\quad + \frac{1}{\sqrt{M}} \sum_{m=M_l+1}^{M} \sqrt{\alpha_m} |h_m| \frac{\tau_m}{T} \rho(-1) + n(i)
\end{aligned}
\tag{4.6}
$$

where

$$
\rho(k - l) = \int_0^T s_k(t) s_l^*(t) dt
\tag{4.7}
$$

and

$$
n(i) = \frac{1}{T} \int_0^T n(iT + t) s_i^*(t) dt.
\tag{4.8}
$$

If M is large enough to use the law of large numbers, (4.6) can be approximated as

$$r(i) \approx \sqrt{M} E\left[\sqrt{\alpha_m}|h_m|\frac{T - \tau_m}{T}\rho(0)\right] + \frac{1}{\sqrt{M}}\sum_{m=1}^{M_l}\sqrt{\alpha_m}|h_m|\frac{\tau_m}{T}\rho(1)$$
$$+ \frac{1}{\sqrt{M}}\sum_{m=M_l+1}^{M}\sqrt{\alpha_m}|h_m|\frac{\tau_m}{T}\rho(-1) + n(i) \tag{4.9}$$

where $E[x]$ is the expectation of x. If transmit symbols are independent and equally probable, symbol power is satisfied with

$$E[\rho(i)] = \begin{cases} 1, & i = 0 \\ 0, & otherwise. \end{cases} \tag{4.10}$$

Finally, the average received symbol magnitude with symbol timing offset is given by

$$r_{so} = E[r_s(i)] = \sqrt{M} E\left[\sqrt{\alpha_m}|h_m|\frac{T - \tau_m}{T}\rho(0)\right]$$
$$= \sqrt{M} E[\sqrt{\alpha_m}]E[|h_m|]E\left[\frac{T - \tau_m}{T}\right] \tag{4.11}$$

where $r_s(i)$ is the signal part of the received symbol i. $E[\sqrt{\alpha_m}]$ and $E[|h_m|]$ depend on the wireless channel characteristic and are not related with synchronization errors. When there is symbol timing offset of the cooperating signals in distributed beamforming, the average SNR of the received signal is given by

$$SNR = \frac{M E[\sqrt{\alpha_m}]^2 E[|h_m|]^2}{\sigma_n^2} E\left[\frac{T - \tau_m}{T}\right]^2$$
$$= SNR_{perf} \cdot L_{so} \tag{4.12}$$

where σ_n^2 is noise variance and SNR_{perf} is the achievable SNR including distributed beamforming gain with perfect synchronization given by

$$SNR_{perf} = \frac{ME[\sqrt{\alpha_m}]^2 E[|h_m|]^2}{\sigma_n^2}. \tag{4.13}$$

Note that distributed beamforming gain increases linearly as the number of cooperating signals increases. L_{so} is average SNR loss due to symbol timing offset which is given by

$$\begin{aligned} L_{so} &= E\left[\frac{T - \tau_m}{T}\right]^2 \\ &= 20\log\left(\frac{T - \tau_{\max}/2}{T}\right) (dB) \end{aligned} \tag{4.14}$$

4.2.2 Phase Offset

When there is only phase offset among the cooperating signals, the received signal in (4.1) can be rewritten as

$$r(t) = \frac{1}{\sqrt{M}} \sum_{m=1}^{M} \sqrt{\alpha_m} |h_m| x(t) e^{j\theta_m} + n(t) \tag{4.15}$$

and the output of the matched filter is given by

$$\begin{aligned} r(i) &= \frac{1}{T} \int_0^T r(iT + t) s_i^*(t) dt \\ &= \frac{1}{T\sqrt{M}} \sum_{m=1}^{M} \int_0^T \sqrt{\alpha_m} |h_m| e^{j\theta_m} s_i(t) s_i^*(t) dt + n(i) \\ &\approx \sqrt{M} E[\sqrt{\alpha_m}] E[|h_m|] E\left[e^{j\theta_m}\right] + n(i). \end{aligned} \tag{4.16}$$

Note that phase offset is assumed to be constant over the packet duration and the final approximation is obtained by using the law of large numbers. The average received symbol magnitude with phase offset is given by

$$r_{po} = \sqrt{M} E[\sqrt{\alpha_m}] E[|h_m|] E[e^{j\theta_m}] \tag{4.17}$$

When there is phase offset among the cooperating signals in distributed beamforming, the average SNR of the received signal is given by

$$\begin{aligned} SNR &= \frac{M E[\sqrt{\alpha_m}]^2 E[|h_m|]^2}{\sigma_n^2} E\left[e^{j\theta_m}\right]^2 \\ &= SNR_{perf} \cdot L_{po} \end{aligned} \tag{4.18}$$

where L_{po} is average SNR loss due to phase offset among the cooperating signals given by

$$\begin{aligned} L_{po} &= E\left[e^{j\theta_m}\right]^2 \\ &= 20 \log\left[\frac{\sin(\theta_{\max})}{\theta_{\max}}\right] (dB) \end{aligned} \tag{4.19}$$

4.2.3 Frequency Offset

With only frequency offset between the cooperating signals, the received signal in (4.1) can be rewritten as

$$r(t) = \frac{1}{\sqrt{M}} \sum_{m=1}^{M} \sqrt{\alpha_m} |h_m| x(t) e^{j2\pi f_m t} + n(t) \tag{4.20}$$

and the output of matched filter is given by

$$
\begin{aligned}
r(i) &= \frac{1}{T}\int_0^T r(iT+t)s_i^*(t)dt \\
&= \frac{1}{T\sqrt{M}}\sum_{m=1}^M \int_0^T \sqrt{\alpha_m}|h_m|e^{j2\pi f_m iT}e^{j2\pi f_m t}s_i(t)s_i^*(t)dt + n(i) \\
&= \frac{1}{\sqrt{M}}\sum_{m=1}^M \sqrt{\alpha_m}|h_m|e^{j2\pi f_m iT}\frac{e^{j2\pi f_m T}-1}{j2\pi f_m T} + n(i) \\
&\approx \sqrt{M}E[\sqrt{\alpha_m}]E[|h_m|]E\left[e^{j2\pi f_m iT}\frac{e^{j2\pi f_m T}-1}{j2\pi f_m T}\right] + n(i).
\end{aligned}
\tag{4.21}
$$

Again the law of large numbers is used for the final approximation. The average received symbol magnitude with frequency offset is given by

$$
\begin{aligned}
r_{fo} &= \sqrt{M}E[\sqrt{\alpha_m}]E[|h_m|]E\left[E_i[e^{j2\pi f_m iT}]\frac{e^{j2\pi f_m T}-1}{j2\pi f_m T}\right] \\
&= \sqrt{M}E[\sqrt{\alpha_m}]E[|h_m|]E\left[\frac{e^{j2\pi f_m K_s T}-1}{j2\pi f_m K_s T}\cdot\frac{e^{j2\pi f_m T}-1}{j2\pi f_m T}\right].
\end{aligned}
\tag{4.22}
$$

The average SNR of the received signal with frequency offset is given by

$$
\begin{aligned}
SNR &= \frac{ME[\sqrt{\alpha_m}]^2 E[|h_m|]^2}{\sigma_n^2}E\left[\left|\frac{e^{j2\pi f_m K_s T}-1}{j2\pi f_m K_s T}\cdot\frac{e^{j2\pi f_m T}-1}{j2\pi f_m T}\right|\right]^2 \\
&= SNR_{perf}\cdot L_{fo}
\end{aligned}
\tag{4.23}
$$

where L_{fo} is average SNR loss due to frequency offset between the cooperating signals given by

$$
\begin{aligned}
L_{fo} &= E\left[\left|\frac{e^{j2\pi f_m K_s T}-1}{j2\pi f_m K_s T}\cdot\frac{e^{j2\pi f_m T}-1}{j2\pi f_m T}\right|\right]^2 \\
&= 20\log\left(\frac{-\sin(\pi f_{max}T)\sin(\pi f_{max}K_s T)}{\pi^2 f_{max}^2 K_s T^2}-\frac{(K_s-1)Si(\pi f_{max}(K_s-1)T)}{2\pi f_{max}K_s T}\right. \\
&\quad \left.+\frac{(K_s+1)Si(\pi f_{max}(K_s+1)T)}{2\pi f_{max}K_s T}\right)(dB).
\end{aligned}
\tag{4.24}
$$

$Si(x)$ is sine integral defined as

$$Si(x) = \int_0^x \frac{\sin u}{u} du. \tag{4.25}$$

By combining the three offsets, the distributed beamforming gain with M cooperating signals in single-carrier systems is given by

$$SNR = SNR_{perf} L_{so} L_{po} L_{fo} \tag{4.26}$$

The first term represents the achievable distributed beamforming gain with perfect synchronization which is reduced by the latter terms when there are synchronization errors.

4.3 Multi-carrier Systems

We will consider OFDM systems as multi-carrier systems. In OFDM systems, the information symbols are mapped onto the subcarrier of the inverse discrete Fourier transform (IDFT) and creating an OFDM symbol. The output of the IDFT is converted to a serial sequence and a guard interval is added using cyclic prefix. After the CP has been removed, the receiver performs the inverse operation of the transmitter, *i.e.*, discrete Fourier transform (DFT), to extract the transmitted symbols. When there are N subcarriers, the OFDM symbols can be expressed by

$$x(t) = \frac{1}{N} \sum_{n=0}^{N-1} s(n) e^{j2\pi \frac{n}{T_{mc}} t} \tag{4.27}$$

where $s(n)$ is the information symbol on subcarrier n and T_{mc} is the OFDM symbol duration which is N times longer than single-carrier systems, $T_{mc} = NT$.

When the cyclic prefix is assumed to be long enough to avoid ISI between OFDM symbols, the received signal of M cooperating signals after removing the cyclic prefix is given by

$$r(t) = \frac{1}{\sqrt{M}} \sum_{m=1}^{M} \sqrt{\alpha_m} |h_m| x(t - \tau_m) e^{j2\pi f_m t} e^{j\theta_m} + n(t). \tag{4.28}$$

Note that again the total transmit power is normalized with the number of cooperating

signals.

4.3.1   Symbol Time Offset

As we did in single-carrier systems, we will consider the effect of each offset separately. When

there is only symbol time offset, the received signal in (4.28) is given by

$$r(t) = \frac{1}{\sqrt{M}} \sum_{m=1}^{M} \sqrt{\alpha_m} |h_m| x(t - \tau_m) + n(t). \tag{4.29}$$

The received data on subcarrier k can be obtained by

$$r(k) = \frac{1}{T_{mc}} \int_{0}^{T_{mc}} r(t) e^{-j2\pi \frac{k}{T_{mc}} t} dt + n(k) \qquad \text{for} \quad k = 1, 2, \cdots, N \tag{4.30}$$

where $n(k)$ is noise on subcarrier k given by

$$n(k) = \frac{1}{T_{mc}} \int_{0}^{T_{mc}} n(t) e^{-j2\pi \frac{k}{T_{mc}} t} dt. \tag{4.31}$$

By substituting (4.27) and (4.29) into (4.30), the received data can be rewritten as

$$\begin{aligned}
r(k) &= \frac{1}{\sqrt{M} T_{mc}} \int_{0}^{T_{mc}} \sum_{m=1}^{M} \frac{1}{N} \sum_{n=0}^{N-1} \sqrt{\alpha_m} |h_m| s(n) e^{-j2\pi \frac{n}{T_{mc}} \tau_m} e^{j2\pi \frac{n-k}{T_{mc}} t} dt + n(k) \\
&= \frac{1}{\sqrt{M} T_{mc}} \int_{0}^{T_{mc}} \sum_{m=1}^{M} \sqrt{\alpha_m} |h_m| s(k) e^{-j2\pi \frac{k}{T_{mc}} \tau_m} dt + n(k) \\
&= s(k) \frac{1}{\sqrt{M}} \sum_{m=1}^{M} \sqrt{\alpha_m} |h_m| e^{-j2\pi \frac{k}{T_{mc}} \tau_m} + n(k)
\end{aligned} \tag{4.32}$$

When the number of cooperating nodes is large enough, (4.32) can be approximated

as

$$r(k) \approx s(k)\sqrt{M}E[\sqrt{\alpha_m}]E[|h_m|]E\left[e^{-j2\pi\frac{k}{T_{mc}}\tau_m}\right] + n(k). \tag{4.33}$$

The average SNR of subcarrier k with symbol timing offset is given by

$$
\begin{aligned}
SNR &= \frac{ME[\sqrt{\alpha_m}]^2 E[|h_m|]^2}{\sigma_n^2}E\left[e^{-j2\pi\frac{k}{T_{mc}}\tau_m}\right]^2 \\
&= SNR_{perf} \cdot L_{so,k}
\end{aligned}
\tag{4.34}
$$

where SNR_{perf} is the achievable distributed beamforming gain which is same as single-carrier systems. $L_{so,k}$ is average SNR loss of subcarrier k when there is symbol timing offset between the cooperating signals and given by

$$
\begin{aligned}
L_{so,k} &= E\left[e^{-j2\pi\frac{k}{T_{mc}}\tau_m}\right]^2 = \left[\frac{\sin(\pi k\tau_{\max}/T_{mc})}{\pi k\tau_{\max}/T_{mc}}\right]^2 \\
&= 20\log\left[\text{sinc}\left(\frac{k\tau_{\max}}{T_{mc}}\right)\right] (dB).
\end{aligned}
\tag{4.35}
$$

In OFDM systems, high frequency subcarriers are more susceptible to symbol timing offset as compared to low frequency ones as shown in (4.35). When symbol timing error is less than the cyclic prefix, however, OFDM systems are more robust to symbol timing error than single-carrier systems due to the increased symbol duration.

4.3.2   Phase Offset

With only phase offset between cooperating signals, the received OFDM signal is given by

$$r(t) = \frac{1}{\sqrt{M}}\sum_{m=1}^{M}\sqrt{\alpha_m}|h_m|x(t)e^{j\theta_m} + n(t). \tag{4.36}$$

The received signal on subcarrier k can be obtained by using the same procedure as before

and given by

$$
\begin{aligned}
r(k) &= \frac{1}{\sqrt{M}T_{mc}} \int_0^{T_{mc}} \sum_{m=1}^{M} \frac{1}{N} \sum_{n=0}^{N-1} \sqrt{\alpha_m} |h_m| s(n) e^{j2\pi \frac{n-k}{T_{mc}}t} e^{j\theta_m} dt + n(k) \\
&= \frac{1}{\sqrt{M}} \sum_{m=1}^{M} \sqrt{\alpha_m} |h_m| s(k) e^{j\theta_m} + n(k) \\
&\approx s(k)\sqrt{M} E[\sqrt{\alpha_m}] E[|h_m|] E[e^{j\theta_m}] + n(k)
\end{aligned}
\tag{4.37}
$$

The average SNR of subcarrier k with phase offset is given by

$$
\begin{aligned}
SNR &= \frac{M E[\sqrt{\alpha_m}]^2 E[|h_m|]^2}{\sigma_n^2} E\left[e^{j\theta_m}\right]^2 \\
&= SNR_{perf} \cdot L_{po,k}
\end{aligned}
\tag{4.38}
$$

$L_{po,k}$ is average SNR loss of subcarrier k due to phase offset between the cooperating signals. Note that it does not depend on the subcarrier number and is found to be same as in single-carrier systems. $L_{po,k}$ is given by

$$
\begin{aligned}
L_{po,k} &= E\left[e^{j\theta_m}\right]^2 \\
&= 20 \log \left[\frac{\sin(\theta_{\max})}{\theta_{\max}}\right] (dB)
\end{aligned}
\tag{4.39}
$$

4.3.3   Frequency Offset

When there is frequency offset between the cooperating signals, the received signal is given by

$$
r(t) = \frac{1}{\sqrt{M}} \sum_{m=1}^{M} \sqrt{\alpha_m} |h_m| x(t) e^{j2\pi f_m t} + n(t).
\tag{4.40}
$$

and the signal on subcarrier k is obtained by

$$r(k) = \frac{1}{\sqrt{M}T_{mc}} \int_0^{T_{mc}} \sum_{m=1}^{M} \frac{1}{N} \sum_{n=0}^{N-1} \sqrt{\alpha_m}|h_m|s(n)e^{j2\pi\frac{n-k}{T_{mc}}t}e^{j2\pi f_m t}dt + n(k)$$

$$= s(k)\frac{1}{\sqrt{M}} \sum_{m=1}^{M} \sqrt{\alpha_m}|h_m|\left\{\frac{1}{T_{mc}} \int_0^{T_{mc}} e^{j2\pi f_m t}dt \right.$$

$$\left. + \frac{1}{N} \sum_{\substack{n=0 \\ n\neq k}}^{N-1} \frac{1}{T_{mc}} \int_0^{T_{mc}} e^{j2\pi\frac{n-k}{T_{mc}}t}e^{j2\pi f_m t}dt\right\} + n(k) \tag{4.41}$$

where the first term of the final expression represents the loss of the desired signal on sub-carrier k and the second term represents inter-carrier interference (ICI) due to the residual frequency offset between the cooperating signals. Figure 4.2 shows an example of effect of frequency offset in OFDM systems. When there is no frequency offset in the received OFDM signal, the full signal power on each subcarrier can be obtained without interference from the other subcarriers since the subcarrier frequencies are chosen to be orthogonal to each other. If there is frequency offset in the received signal, the orthogonality cannot be satisfied as shown in the figure and there is signal loss of the desired subcarrier as well as ICI from the other subcarriers.

Using the law of large numbers, (4.41) can be approximated as

$$r(k) \approx s(k)\sqrt{M}E[\sqrt{\alpha_m}]E[h_m]\left\{E\left[\frac{1}{T_{mc}} \int_0^{T_{mc}} e^{j2\pi f_m t}dt\right]\right.$$

$$\left. + \frac{1}{N} \sum_{\substack{n=0 \\ n\neq k}}^{N-1} E\left[\frac{1}{T_{mc}} \int_0^{T_{mc}} e^{j2\pi f_m t}e^{j2\pi\frac{n-k}{T_{mc}}t}dt\right]\right\} + n(k) \tag{4.42}$$

$$= s(k)\sqrt{M}E[\sqrt{\alpha_m}]E[h_m]\left(D_{fo,k} + ICI(k)\right) + n(k)$$

where $D_{fo,k}$ is the signal loss of subcarrier k due to frequency offset and given by

$$D_{fo,k} = E\left[\frac{1}{T_{mc}} \int_0^{T_{mc}} e^{j2\pi f_m t}dt\right] = \frac{Si(2\pi f_{\max}T_{mc})}{2\pi f_{\max}T_{mc}}. \tag{4.43}$$
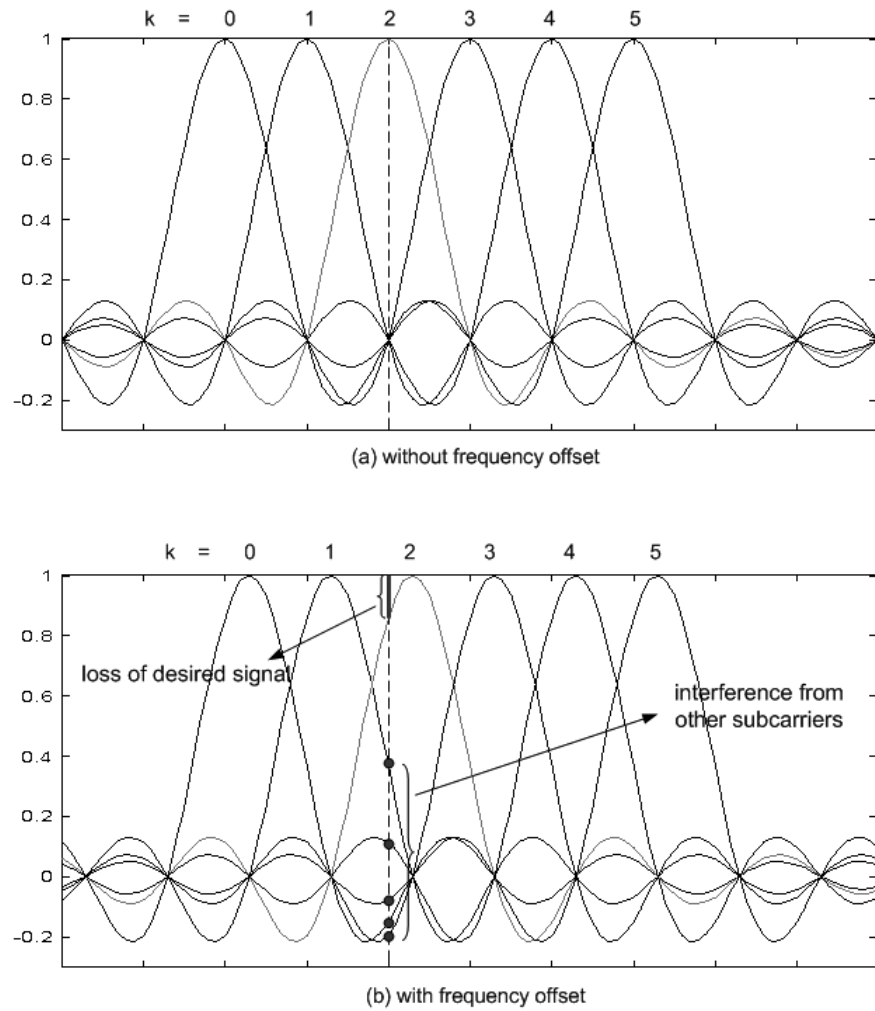
Figure 4.2: Effect of frequency offset in OFDM systems; (a) No frequency offset (b) With frequency offset

$L_{fo,k}$ is average SNR loss of subcarrier k due to frequency offset between the cooperating signals and given by

$$L_{fo,k} = 20\log D_{fo,k} \quad (dB) \tag{4.44}$$

$ICI(k)$ is interference due to frequency offset on subcarrier k which is given by

$$ICI(k) = \frac{1}{N}\sum_{\substack{n=0 \\ n\neq k}}^{N-1} E\left[\frac{1}{T_{mc}}\int_0^{T_{mc}} e^{j2\pi f_m t}e^{j2\pi\frac{n-k}{T_{mc}}t}dt\right]. \tag{4.45}$$

and it can be rewritten as

$$\begin{aligned}ICI(k) &= \frac{1}{N}\sum_{n=0,n\neq k}^{N-1} E\left[\frac{e^{j2\pi(f_m+\frac{n-k}{T_{mc}})T_{mc}}-1}{j2\pi(f_m+\frac{n-k}{T_{mc}})T_{mc}}\right] \\ &= \frac{1}{N}\sum_{n=0,n\neq k}^{N-1}\frac{Si\left\{2\pi(f_{\max}+\frac{n-k}{T_{mc}})T_{mc}\right\}}{2\pi f_{\max}T_{mc}}\end{aligned} \tag{4.46}$$

When there is frequency offset between the cooperating signals, the power of the desired signal is reduced and the lost signal power is spread over the other subcarriers as shown in Figure 4.2. The adjacent subcarriers are affected more severely from this interference. When the interfering signals from all other subcarriers are considered, the average interference on subcarrier k can be approximated as

$$ICI(k) \approx \frac{1}{2}\sum_{n=0,n\neq k}^{N-1}\frac{(1-D_{fo,n})}{N-1} = \frac{1}{2}(1-D_{fo}) \tag{4.47}$$

where D_{fo} is the amount of signal loss which is independent of subcarrier number as shown in (4.43) and the factor $1/2$ is added since only one side of spreading signal is interfering on subcarrier k. Using the approximation of ICI, the SINR of subcarrier k with frequency offset is given by

$$SINR(k) = \frac{ME[\sqrt{\alpha_m}]^2 E[||h_m||]^2 L_{fo,k}}{ME[\sqrt{\alpha_m}]^2 E[||h_m||]^2 (1 - D_{fo})^2/4 + \sigma_n^2}$$
$$= \frac{SNR_{perf} L_{fo,k}}{SNR_{perf}(1 - D_{fo})^2/4 + 1}. \tag{4.48}$$

As shown in (4.48), there is additional performance degradation due to ICI when frequency offset among the cooperating signals is not controlled properly.

Finally, distributed beamforming gain in OFDM systems with M cooperating nodes is given by

$$SINR(k) = \frac{ME[\sqrt{\alpha_m}]^2 E[||h_m||]^2 L_{so,k} L_{po,k} L_{fo,k}}{ME[\sqrt{\alpha_m}]^2 E[||h_m||]^2 L_{so,k} L_{po,k}(1 - D_{fo})^2/4 + \sigma_n^2}$$
$$= \frac{SNR_{perf} L_{so,k} L_{po,k} L_{fo,k}}{SNR_{perf} L_{so,k} L_{po,k}(1 - D_{fo})^2/4 + 1}. \tag{4.49}$$

When there is no offsets among the cooperating signals (*i.e.*, $\tau_m=0$, $\theta_m=0$, and $f_m=0$), $L_{so,k}$, $L_{po,k}$, $L_{fo,k}$, and D_{fo} are one from (4.35), (4.39), (4.43), and (4.44), and the achievable SINR of subcarrier k in (4.49) will be SNR_{perf}.

4.4 Performance Comparison

When the channel coefficient is assumed to be constant for the entire symbol duration in single-carrier and OFDM systems, the effect of phase offset between the cooperating signals is the same as shown in (4.19) and (4.39). Figure 4.3 shows the SNR loss due to phase offset for both systems when the number of cooperating signals is 5, *i.e.*, $M = 5$. The performance degradation due to phase offset is not large when the phase offset is moderate. However, the SNR loss increases rapidly if it is not controlled properly.

OFDM systems have an advantage of robustness to symbol timing error using a guard interval with a cyclic prefix. If symbol timing error is less than the guard interval in the
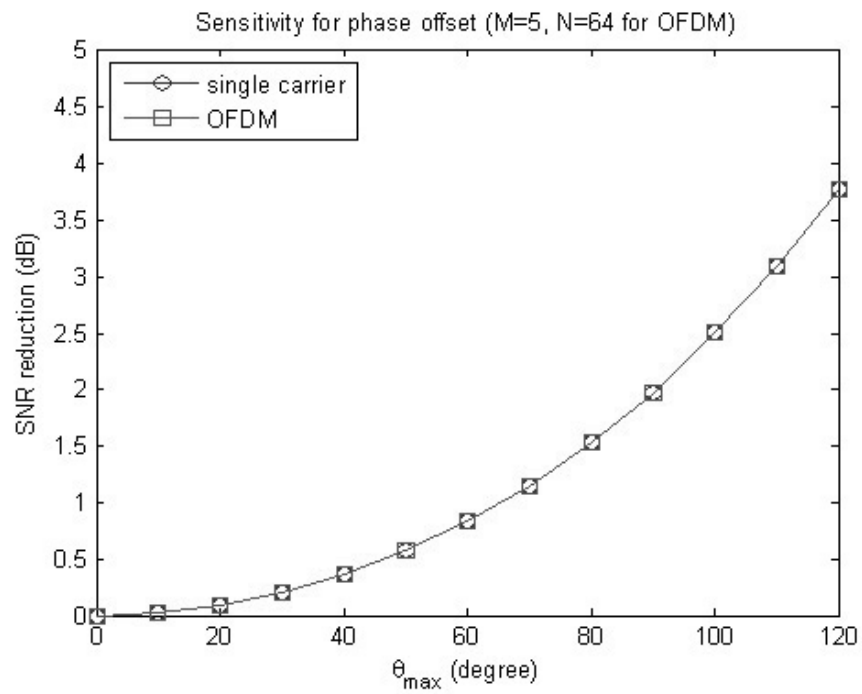
Figure 4.3: SNR reduction due to phase offset in distributed beamforming ($M = 5$, single carrier and OFDM systems)
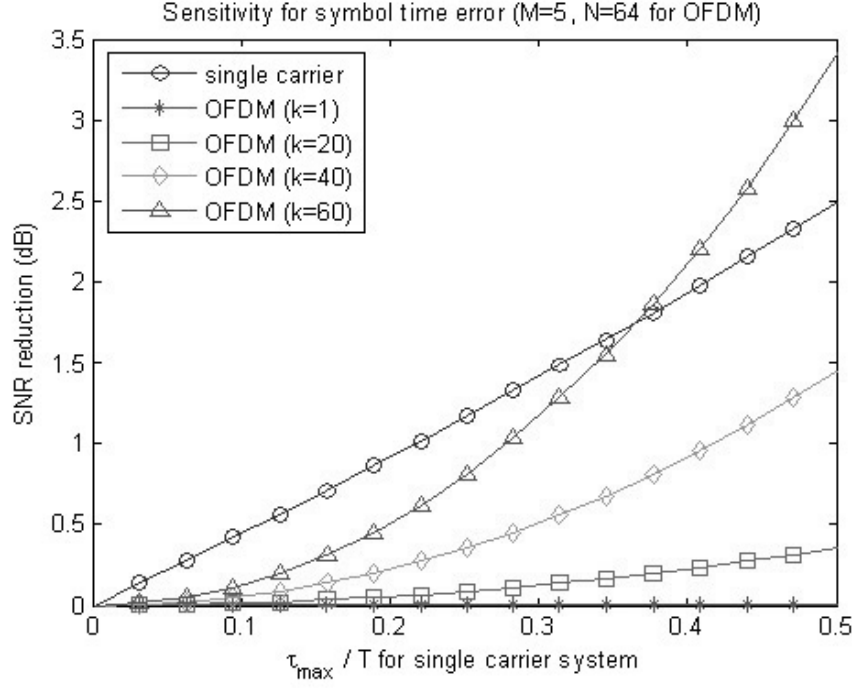
Figure 4.4: SNR reduction due to symbol time error in distributed beamforming ($M = 5$, single carrier system and OFDM system for k=1, 20, 40, and 60)

typical OFDM system, it is converted into a phase shift and can be compensated by a simple method. In distributed beamforming, however, phase offset due to symbol timing errors cannot be adjusted when cooperating signals arrived with different timing offsets. Figure 4.4 shows the SNR degradation due to symbol timing error for single-carrier and OFDM systems. High frequency subcarriers in OFDM systems are more susceptible to timing offset since they are affected relatively more by the same amount of phase shift.

   In distributed beamforming, OFDM systems are fairly robust to symbol timing error except high frequency subcarriers as compared to single-carrier systems. However, it is more sensitive to carrier frequency offset. The performance degradation due to frequency offset in OFDM systems results from not only power loss of the desired signal but also ICI from the other subcarriers. Figure 4.5 shows signal loss due to frequency offset in single-carrier and
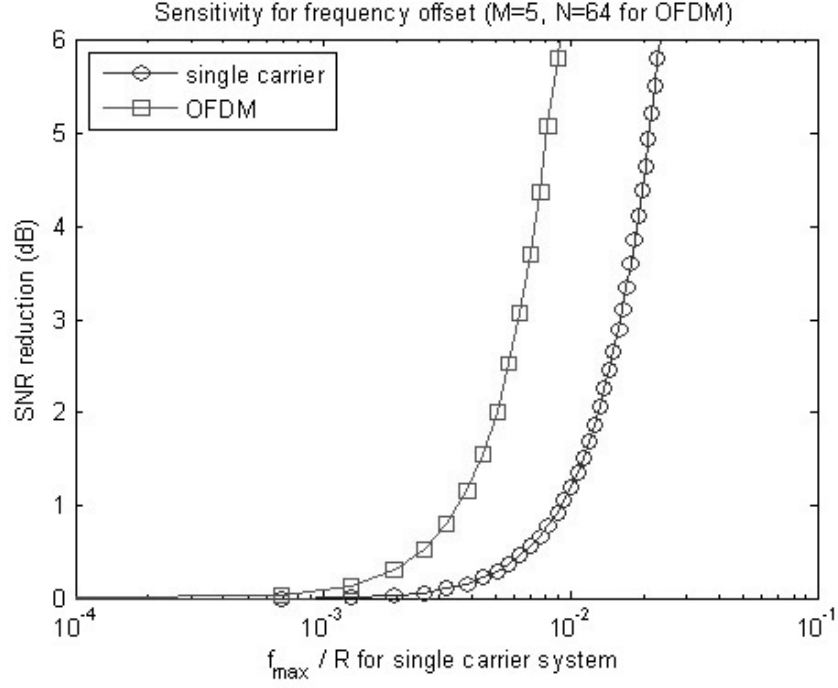
Figure 4.5: SNR reduction due to frequency offset in distributed beamforming ($M = 5$, single carrier system with $Ks = 64$ and OFDM system with $N = 64$)

OFDM systems where 64 symbols are used for single carrier systems, $K_s = 64$, to meet the same number of transmit symbols. OFDM systems show high sensitivity to frequency offset as compared to single-carrier systems. ICI caused by frequency offset is shown in Figure 4.6. The numerical and analytical results are well matched and the approximated ICI in (4.47) is also well matched.

Figure 4.7 shows the achievable SNR (SINR for OFDM systems) with M cooperating signals for various offset values, which are given for single-carrier systems. It is assumed that the average SNR of the cooperating signals is the same and is 5 dB. The analytical results are well-matched with the simulated results except when the number of cooperating nodes is small. The difference between the analytical and simulated results comes from the approximation in the analysis where the law of large numbers is used. When offset values are
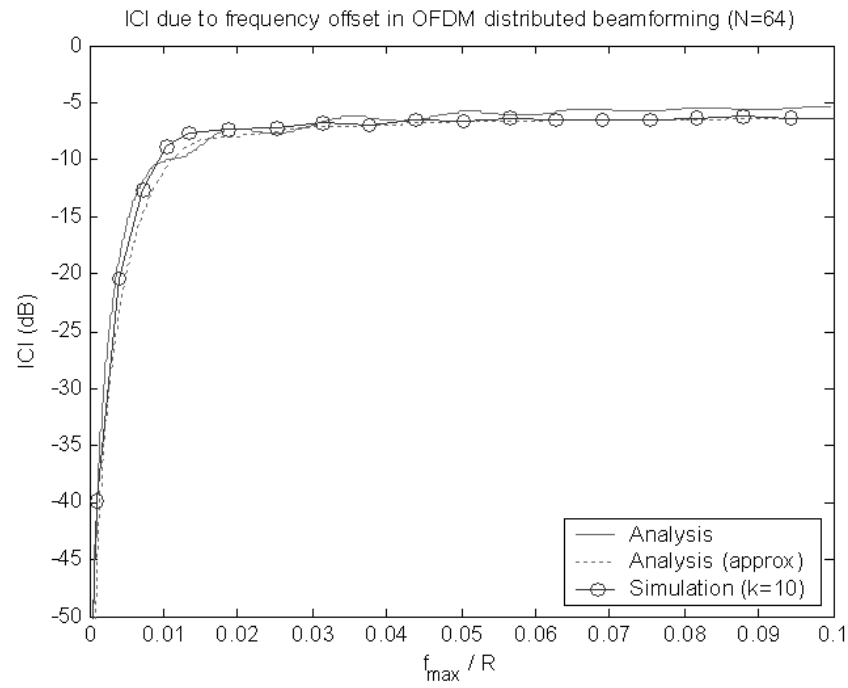
Figure 4.6: ICI in OFDM system due to frequency offset in distributed beamforming ($M = 5$, $k = 10$)
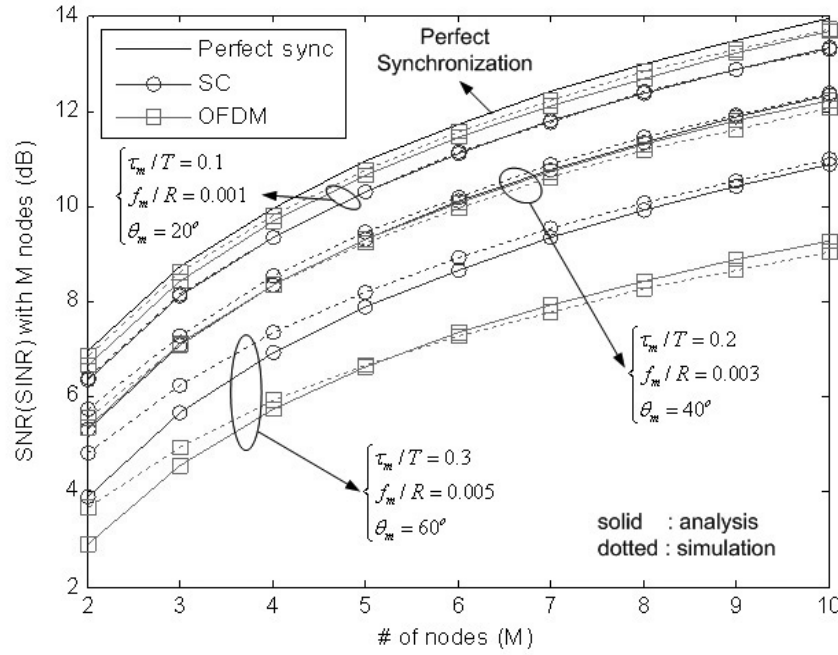
Figure 4.7: Achievable SNR (SINR) varying the number of nodes with various offset values($M = \{2, \cdots, 10\}$, single carrier and OFDM systems)

small, the difference is also small even with the small number of cooperating nodes since offset values are distributed over small ranges. Distributed beamforming in OFDM systems shows good performance when there is a small frequency offsets among the cooperating signals. However, its performance degrades very sharply when frequency offsets are not controlled properly and the benefit from a large number of cooperating nodes is diminished.

4.5 Chapter Summary

The effects of synchronization errors in distributed beamforming were investigated for single-carrier and OFDM systems. When the channel is constant over a symbol duration, the performance degradation due to phase offset is the same for both single-carrier and OFDM systems. For symbol timing offset in OFDM systems, high frequency subcarriers are more

susceptible as compared to low frequency ones. Frequency offset is critical in OFDM systems since it leads to interference from the other subcarriers as well as power loss in the desired signal.

When distributed beamforming is used for packet retransmission, the method of offset estimation and compensation will be examined in the next chapter. The effect of residual offsets will be also investigated.

Chapter 5

Cooperative ARQ Scheme in Mobile Environments

The effects of synchronization errors in distributed beamforming was examined in the previous chapter. In the proposed cooperative ARQ scheme in Chapter 3, perfect synchronization between cooperating signals was assumed by using a NACK message. In this chapter, we will investigate an offset estimation method and the effect of residual offset. A feedback approach with a small bandwidth will be also examined to adjust phase variation due to the residual offset after offset compensation.

5.1 Cooperative Retransmission with Offset Estimation

In the proposed retransmission scheme in Chapter 3, the NACK message is used to obtain carrier phase and frequency offsets between the cooperating node and the destination. Note that symbol timing offset is ignored in this research based on the assumption that the difference in propagation delay between cooperating nodes and the destination is small as

compared to the symbol duration. This assumption is reasonable in a small-range wireless ad hoc network. In [41], it was shown that 10% timing jitter does not have much effect on the BER performance of cooperative transmission. In the analysis of the previous chapter, the average SNR degradation is shown to be less than 1 dB when timing offset is around 20% of the symbol duration. For example, when a symbol rate of 1 Mbps is used for transmission, about 60m of distance difference between cooperating links, which is 20% of symbol rate, can be allowed with a negligible performance degradation. This amount of distance difference might be reasonable in a small wireless ad hoc network, especially with the proposed cooperative retransmission scheme where cooperating nodes might be located close to receive both data and NACK packets correctly.

The preamble part of the NACK message is used for offset estimation which is assumed to be divided into N_p subgroups with the length of L_p as shown in Figure 5.1, where $c_i, i = 1, 2, \cdots, L_p N_p$, is the preamble bit. The received preamble part of the NACK message at cooperating node l is given by

$$r_{p,l}(t) = \sqrt{\alpha_{rd,l}} h_{rd,l} e^{j2\pi f_l t} c(t) + n_l(t) \tag{5.1}$$

where $c(t)$ is the preamble signal given by $c(t) = [c_1(t), c_2(t), \cdots, c_{N_p L_p}(t)]$ and f_l is the carrier frequency offset between the destination and cooperating node l. When channel coefficient is assumed to be constant for the preamble duration, the discrete time expression of the first subgroup is given by

$$r_{p,l}(i) = \sqrt{\alpha_{rd,l}} |h_{rd,l}| e^{j\theta_l(i)} + n_l(i), \quad i = 1, \cdots, L_p \tag{5.2}$$

where $\theta_l(i)$ is phase value of sample i at cooperating node l which includes both phases due to channel and frequency offset, and $n_l(i)$ is the noise sample at cooperating node i. The average phase offset of the first subgroup is estimated from (5.2) and the same procedure is performed
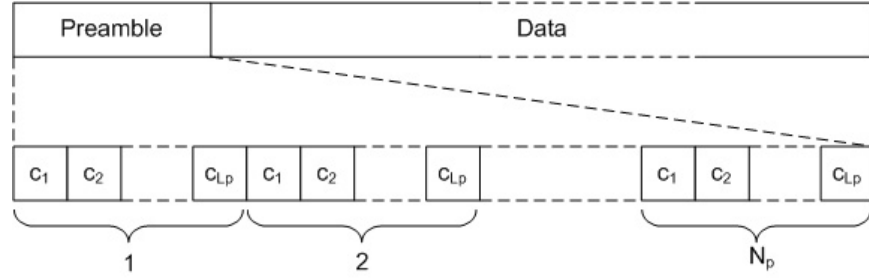
Figure 5.1: Example of packet format with preamble signal
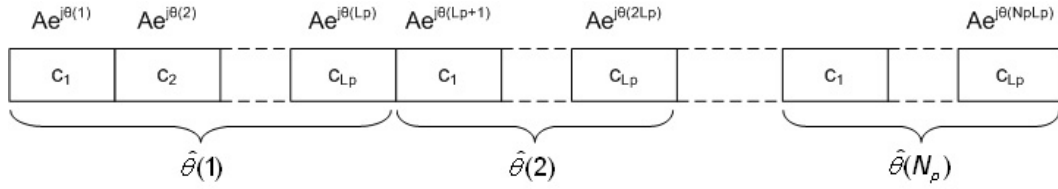
Figure 5.2: Example of phase estimation with preamble signal

for remaining preamble subgroups. Figure 5.2 shows an example of phase estimation with the preamble signal where the signal magnitude is simplified as $A = \sqrt{\alpha_{rd,l}}|h_{rd,l}|$. When the estimates of phase offset are given by $\hat{\theta}_l(i)$ for $i = 1, 2, \cdots, N_p$, frequency offset between the destination and cooperating node l can be estimated using two phase estimates as

$$\hat{f}_l = \frac{\hat{\theta}_l(k) - \hat{\theta}_l(j)}{2\pi(k-j)T_p} \tag{5.3}$$

where T_p is the time duration of a subgroup. The goal of phase and frequency offset estimation is to compensate these offsets on the retransmitting signal on cooperating node l. When the length of the NACK message is T_{NACK}, the initial phase offset of the cooperating signal (*i.e.*, the retransmit data packet) at node l is given by $\hat{\theta}_{l,co} = \hat{\theta}_l(1) + 2\pi\hat{f}_l(T_{NACK} - 0.5T_p)$. Cooperating node l will adjust its phase with the weight of $e^{-j\hat{\theta}_{l,co}}e^{-j2\pi\hat{f}_l t}$ for the retransmit packet, where t is time from the start of the retransmit packet.

When frequency offset is small, phase variation due to frequency offset during one

preamble subgroup can be ignored and (5.2) can be approximated as

$$
\begin{aligned}
r_{p,l}(i) &= \sqrt{\alpha_{rd,l}}|h_{rd,l}|e^{j\theta_l(i)} + n_l(i) \\
&\approx \sqrt{\alpha_{rd,l}}|h_{rd,l}|e^{j\theta_l} + n_l(i), \quad i = 1, \cdots, L_p.
\end{aligned}
\tag{5.4}
$$

By defining the estimation error as $\theta_e \triangleq \hat{\theta}_l - \theta_l$, where θ_l is assumed to be uniformly distributed over $[-\pi, \pi)$, the estimator searches an estimate to minimize the mean-square estimation error (MMSE estimate). The pdf of θ_e is given by [68]

$$
p_{\theta_e}(\theta, \eta_l) = \frac{1}{2\pi}e^{-\eta_l}\left[1 + \sqrt{4\pi\eta_l}\cos\theta e^{\eta_l \cos^2\theta}Q\left(-\sqrt{2\eta_l}\cos\theta\right)\right], \qquad -\pi \leq \theta < \pi \tag{5.5}
$$

where $\eta_l = \alpha_{rd,l}|h_{rd,l}|^2 L_p/\sigma_n^2$ and $Q(\cdot)$ is the Q-function defined as

$$
Q(z) = \frac{1}{\sqrt{2\pi}}\int_z^\infty e^{-\lambda^2/2}d\lambda. \tag{5.6}
$$

The average phase estimation error for a given channel is

$$
\bar{\theta}_e(\eta_l) = \int_{-\pi}^\pi |\theta| p_{\theta_e}(\theta, \eta_l)d\theta \tag{5.7}
$$

The frequency offset estimation is obtained by phase variation between two phase estimators as shown in (5.3). The amount of phase variation between two consecutive phase samples is defined as phase shift, $\phi = \theta_l(i+1) - \theta_l(i)$. Assuming that two $\hat{\theta}_l$ are used to estimate ϕ, the estimation error of ϕ (*i.e.*, ϕ_e), is the sum of two i.i.d. random variables of $\hat{\theta}_e$. The distribution of ϕ_e can be evaluated by convolution and given by

$$
\begin{aligned}
p_{\phi_e}(\phi, \eta_l) &= \int_{-\infty}^{\infty} p_{\theta_e}(\phi - \theta, \eta_l) p_{\theta_e}(\theta, \eta_l) d\theta \\
&= \frac{e^{-2\eta_l}}{4\pi^2} \int_{-\pi}^{\phi} \left[1 + \sqrt{4\pi\eta_l} \cos(\phi - \theta) e^{\eta_l \cos^2(\phi - \theta)} Q\left(-\sqrt{2\eta_l} \cos(\phi - \theta) \right) \right] \\
&\quad \cdot \left[1 + \sqrt{4\pi\eta_l} \cos\theta e^{\eta_l \cos^2\theta} Q\left(-\sqrt{2\eta_l} \cos\theta \right) \right] d\theta.
\end{aligned}
\tag{5.8}
$$

The average estimation error of phase variation for a given channel can be obtained by

$$
\bar{\phi}_e(\eta_l) = \int_{-\pi}^{\pi} |\phi| p_{\phi_e}(\phi, \eta_l) d\phi.
\tag{5.9}
$$

The average frequency estimation error is directly related to $\bar{\phi}_e(\eta_l)$ and given by

$$
\bar{f}_e(\eta_l) = \frac{\bar{\phi}_e(\eta_l)}{2\pi T_p}.
\tag{5.10}
$$

Figures 5.3 and 5.4 show the average estimation errors of phase and frequency offsets at five cooperating nodes which have the same average received SNR. For the preamble signal, $L_p = 32$ and $N_p = 6$ are assumed. It is shown that the analytical and numerical results are well matched.

As shown in (3.7), the received signal from L cooperating nodes with perfect synchronization is given by

$$
\mathbf{r}_2 = \frac{1}{\sqrt{L}} \sum_{l=1}^{L} \sqrt{\alpha_{rd,l}} |h_{rd,l}| \mathbf{s} + \mathbf{n}_2.
\tag{5.11}
$$

When cooperating nodes adjust their phase and frequency offsets with the estimated values as mentioned earlier, the received signal of the cooperatively retransmitted packet can be expressed by

$$
\mathbf{r}_2 = \frac{1}{\sqrt{L}} \sum_{l=1}^{L} w_l \sqrt{\alpha_{rd,l}} |h_{rd,l}| \mathbf{s} + \mathbf{n}_2
\tag{5.12}
$$
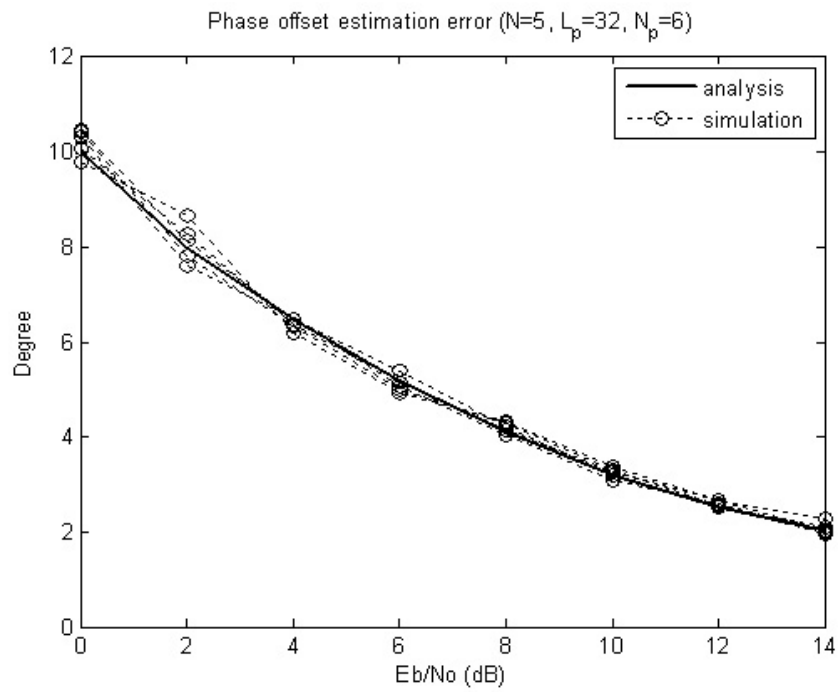
Figure 5.3: Phase offset estimation error with NACK message (5 cooperating nodes, $L_p = 32$, $N_p = 6$, Maximum frequency offset = 2 kHz)
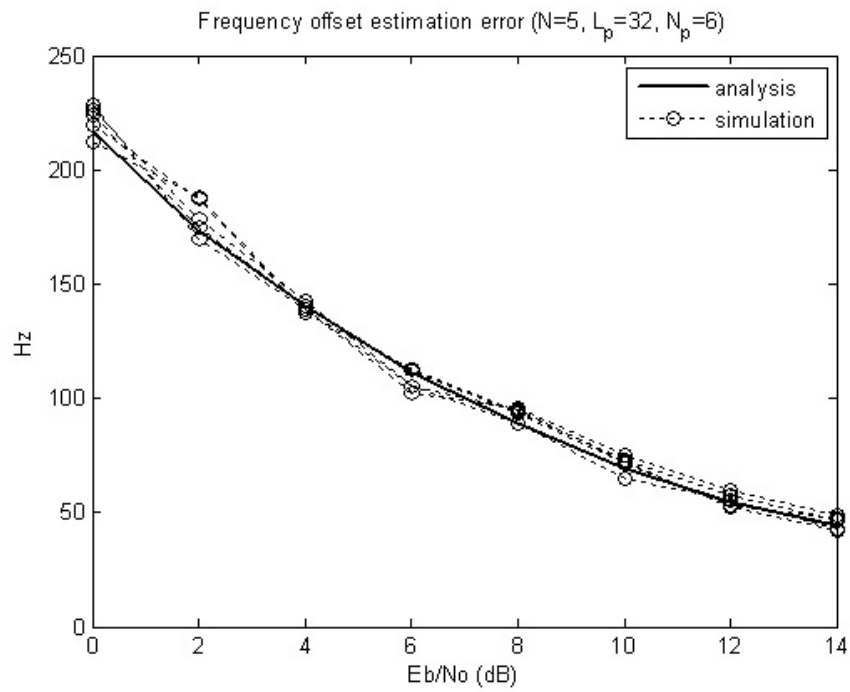
Figure 5.4: Frequency offset estimation error with NACK message (5 cooperating nodes, L_p = 32, N_p = 6, Maximum frequency offset = 2 kHz)

where w_l is the loss factor of the cooperating signal l due to the offset estimation errors which is given by $w_l = \bar{\theta}_e(\eta_l)\bar{f}_e(\eta_l)$. After combining it with the first received signal using MRC, the mutual information of the combined signal is given by

$$I_{co,est}^L = \frac{1}{2}\log_2\left(1 + \eta|h_{sd}|^2 + \frac{1}{L\sigma_n^2}|X_w|^2\right) \tag{5.13}$$

where X_w is the sum of cooperating signals with offset estimation which is given by

$$X_w = \sum_{l=1}^{L} w_l\sqrt{\alpha_{rd,l}}|h_{rd,l}|. \tag{5.14}$$

Then, the outage probability with the offset estimation scheme is given by

$$
\begin{aligned}
P_{o,L}^{est} &= \Pr\left\{I_{co,est}^L < R_{th}\right\} \\
&= \Pr\left\{\frac{1}{2}\log_2\left(1 + \eta|h_{sd}|^2 + \frac{|X_w|^2}{L\sigma_n^2}\right) < R_{th}\right\}.
\end{aligned}
\tag{5.15}
$$

As mentioned in Chapter 3, the outage probability of the proposed cooperative retransmission scheme depends on the probability of cooperation from neighboring nodes. When there are M neighboring nodes around the direct link and probability of cooperation is assumed to be independent between nodes, the outage probability of the proposed cooperative retransmission scheme with offset estimation is given by

$$P_{o,M}^{co} = (1 - p_{co})^M P_{o,2}^{sd} + \sum_{m=1}^{M}\binom{M}{m}p_{co}^m(1 - p_{co})^{M-m}P_{o,m}^{est} \tag{5.16}$$

where $P_{o,2}^{sd}$ is the outage probability when there are no cooperating nodes which is given in (3.6). p_{co} is the probability of cooperation of a neighboring node given in (3.15).

Figure 5.5 shows the outage probability of the cooperative retransmission scheme with

perfect synchronization and offset estimation. It is assumed that $\eta_{NACK}{}^1 = 5$ dB, the transmission bandwidth is 1 MHz, and the length of data packet is 2 ms. It is also assumed that all neighboring nodes are located at the same relative distance as $d_{sr} = 0.2d_{sd}$ and $d_{rd} = 0.8d_{sd}$. The analytical results are well matched with the numerical results even though there is some performance difference for the perfect synchronization case due to the approximation. The proposed cooperative retransmission scheme works well and its outage performance is close to the case of perfect synchronization. As the number of neighboring nodes increases, better outage performance is achieved as expected. The proposed cooperative retransmission scheme shows better performance than decode-and-forward cooperation by exploiting only good quality cooperating signals through distributed beamforming. Note again that the transmit power of the cooperatively retransmitted signal was normalized by the number of cooperating nodes.

5.2   Cooperative Retransmission for Long Data Packets

5.2.1   Effect of Residual Phase and Frequency Offsets

The cooperative retransmission scheme with offset estimation using the NACK message performs very well for short data packets as shown in Figure 5.5. When the length of the retransmitted packet increases, cooperating channel coefficients for the retransmitted packet can no longer be assumed to be constant. Furthermore, the latter part of the retransmitted packet will be more out of phase due to the residual frequency offset. Figure 5.6 shows the outage probability for long retransmitted packets. It is assumed that the packet length is 10 ms and the cooperating channels are also varying due to a Doppler spread of 20 Hz. As shown in Figure 5.6, the proposed cooperative retransmission scheme does not work well

---

[1]The required SNR to receive the NACK message correctly
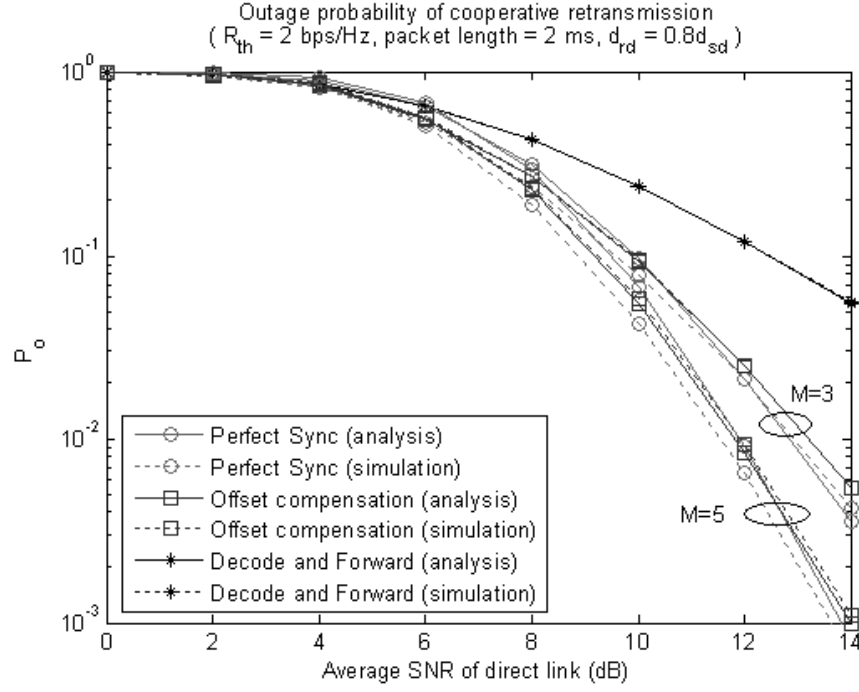
Figure 5.5: Outage performance with cooperative retransmission scheme using phase and frequency offset compensation ($M = \{3, 5\}$, packet length $= 2$ ms, Maximum frequency offset $= 2$ kHz, $d_{rd} = 0.8\ d_{sd}$)
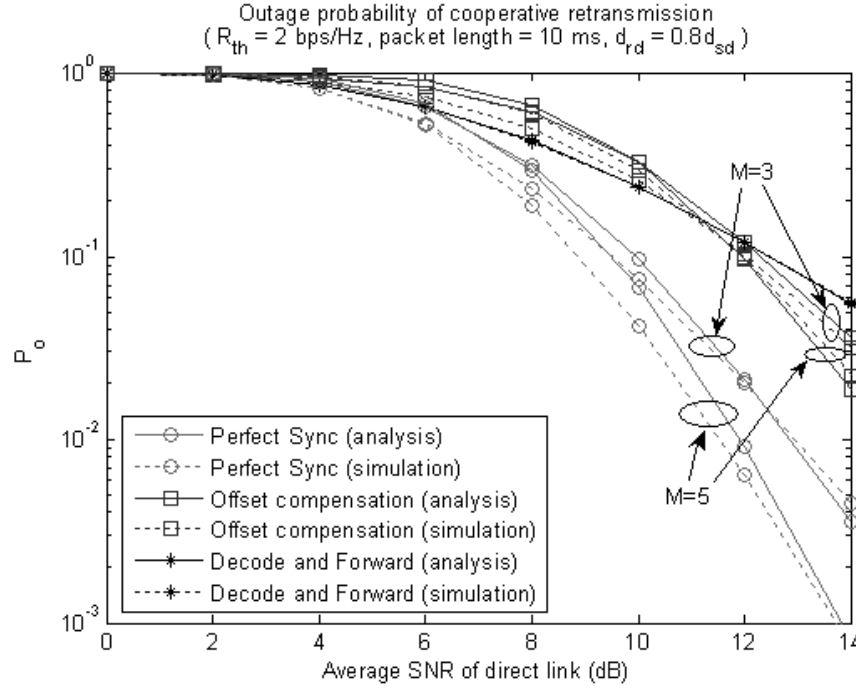
Figure 5.6: Outage performance with cooperative retransmission scheme using phase and frequency offset compensation ($M = \{3, 5\}$, packet length $= 10$ ms, Maximum frequency offset $= 2$ kHz, Doppler spread $= 20$ Hz, $d_{rd} = 0.8\ d_{sd}$)

anymore due to channel variation and phase rotation caused by the residual frequency offset. The effect of the residual offsets is clear from the fact that there is no performance gain even with a large number of neighboring nodes.

5.2.2　Phase Adjustment via Feedback Channel

A low-rate feedback channel will now be considered to adjust phase variation due to the time-varying channel and the residual frequency offset. To track the phase variation of each cooperating signal, a small phase offset will be induced intentionally at the retransmitted signals. Since no information concerning the other cooperating nodes is available, each cooperating node adds a randomly generated phase offset during a feedback interval and updates its phase offset according to feedback information.

Let $\Delta\theta$ be the amount of the intentional phase offset and $\mathbf{A}_l$ be a set of the randomly generated binary bits with length N_g at cooperating node l. Note that $\mathbf{A}_l$ will be generated independently at each cooperating node. Let $\boldsymbol{\Theta}_l$ be an induced phase set given by $\boldsymbol{\Theta}_l = \Delta\theta\mathbf{A}_l$ and it will be repeated N_s times to form a final set of induced phase offsets, $\mathbf{B}_l = (\boldsymbol{\Theta}_l, \boldsymbol{\Theta}_l, \cdots, \boldsymbol{\Theta}_l)$. Figure 5.7 shows an example of the feedback procedure with two cooperating nodes where $N_g = 4$ and $N_s = 3$ are used. During feedback group i, cooperating nodes randomly chose their induced phase sets as $\boldsymbol{\Theta}_1 = (\Delta\theta, \Delta\theta, -\Delta\theta, \Delta\theta)$ and $\boldsymbol{\Theta}_2 = (-\Delta\theta, -\Delta\theta, \Delta\theta, \Delta\theta)$, respectively. Those phase sets are repeated N_s times to generate the entire set of phase offset for feedback group i, given by $\mathbf{B}_1 = (\boldsymbol{\Theta}_1, \boldsymbol{\Theta}_1, \boldsymbol{\Theta}_1)$ and $\mathbf{B}_2 = (\boldsymbol{\Theta}_2, \boldsymbol{\Theta}_2, \boldsymbol{\Theta}_2)$, respectively. The current reference phase offsets, $\theta_{1,ref}$ and $\theta_{2,ref}$, are added to the generated phase sets to obtain the final induced phase offsets. The received signal of the cooperatively retransmitted packet during a feedback interval can be expressed by

$$\mathbf{r}_f(t) = \frac{1}{\sqrt{L}} \sum_{l=1}^{L} \sqrt{\alpha_{rd,l}} |h_{rd,l}| \mathbf{C}_l \mathbf{s}_f + \mathbf{n}_f \tag{5.17}$$

where $\mathbf{C}_l$ is a term representing the phase mismatch due to both offset estimation errors and the induced phase offset and is given by $\mathbf{C}_l = e^{j\theta_{e,l}} e^{j2\pi f_{e,l}t} e^{j\mathbf{B}_l}$. $\theta_{e,l}$ and $f_{e,l}$ are the residual phase and frequency offsets of cooperating signal l, respectively. $\mathbf{s}_f$ and $\mathbf{n}_f$ are the transmit signal and noise vectors during a feedback interval.

After receiving cooperating signals during a feedback interval, the destination averages the magnitude of N_s subsets of the received signal and searches the the index k in the induced phase set $\boldsymbol{\Theta}$ which has the maximum average magnitude. The index k is delivered to the cooperating nodes via a feedback channel. A low-rate feedback channel can be used since only the index of the phase set needs to be delivered to the cooperating nodes. After receiving the index of the induced phase set, each cooperating node updates its reference
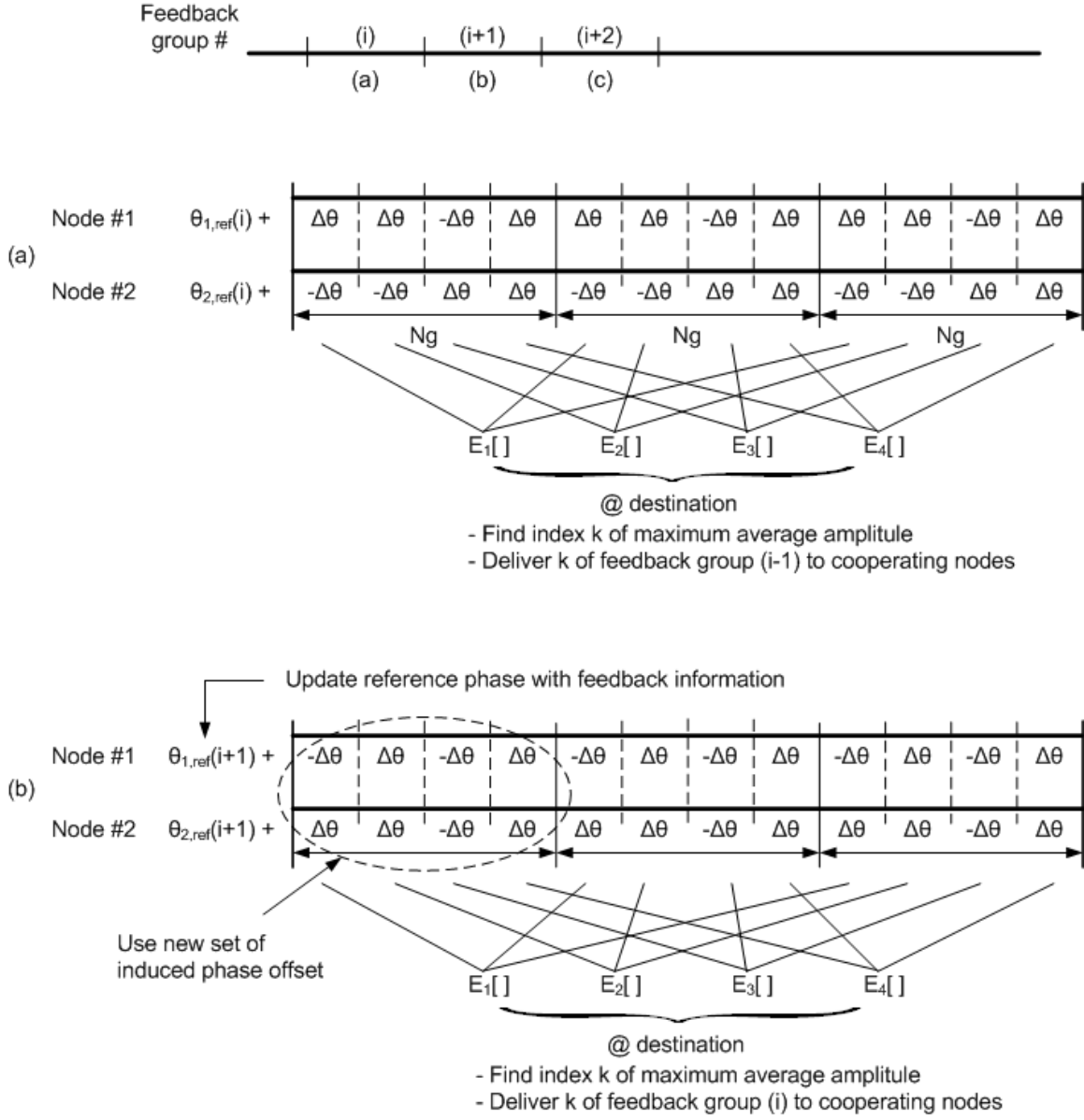
Figure 5.7: Example of feedback approach for phase adjustment ($M = 2$, $N_g = 4$, $N_s = 3$)

Table 5.1: Phase adjustment procedure with feedback channel

When NACK is received at the cooperating mode l
    Extract phase and frequency offsets from the preamble of NACK
    Compensate phase and frequency offsets of the cooperating data packet
        with the estimated values
    Set initial reference phase offset as zero, $\theta_{l,ref} = 0$
    Generate the induced phase offset, $\mathbf{B}_l(\boldsymbol{\Theta}_l)$
    for p = 1 to N_f
        Retransmit data packet after inducing phase offset $\mathbf{B}_l$
        At the destination
            Find the index k of $\boldsymbol{\Theta}$ which has maximum average received magnitude
            Deliver k to cooperating nodes via feedback channel
        At the cooperating node l
            Update reference phase offset as $\theta_{l,ref} = \theta_{l,ref} + \boldsymbol{\Theta}_l(k)$
            Generate the new induced phase offset, $\mathbf{B}_l$
            Add reference phase offset to $\mathbf{B}_l$, $\mathbf{B}_l = \mathbf{B}_l + \theta_{l,ref}$

phase offset as $\theta_{l,ref} = \theta_{l,ref} + \boldsymbol{\Theta}_l(k)$. A new generated phase offset will be added to the updated reference phase offset for the next group. The number of feedback message, N_f, is determined by $N_f = \lfloor T_d/T_f \rfloor$ where T_d is the retransmitted packet duration, T_f is the feedback interval, and $\lfloor z \rfloor$ is the nearest integer to z towards negative infinity. The updating of the phase offset for cooperating signals is continued until N_f is reached. Note that the modulated signal is assumed to be a constant envelope such as M-ary phase shift keying (M-PSK). The phase adjustment procedure using a feedback channel is summarized in Table 5.2.2.

Figures 5.8 and 5.9 show the outage probabilities of the cooperative retransmission scheme using a feedback channel with $M = 3$ and 5, respectively. The same parameters used for Figure 5.6 are assumed for the transmission channel. For the feedback channel, a 10 kHz bandwidth, $N_p = 16$, $N_s = 25$, and $\Delta\theta = 30^o$ are used. As shown in both Figures, the outage probability is substantially improved by using a small feedback channel. Note

Figure 5.8: Outage probability with cooperative retransmission scheme using phase and frequency offset compensation ($M = 3$, packet length $= 10$ ms, Doppler spread $= 20$ Hz, Maximum frequency offset $= 2$ kHz, $d_{rd} = 0.8\ d_{sd}$)

that the extra usage due to the feedback channel is included in the numerical results where total bandwidth is 1.01 MHz including the transmission bandwidth. As compared to the performance without a feedback channel, a performance gain is also achieved as the number of neighboring nodes increases.

The proposed cooperative retransmission scheme can also be easily used in an INR ARQ scheme, which is examined in Chapter 3, by transmitting the redundant code block via cooperating nodes when it is requested by the destination. An INR ARQ scheme is suitable for the proposed cooperative retransmission scheme since it will be less susceptible to residual phase and frequency offsets due to the shorter packet length. To examine the PER performance of INR ARQ with the cooperative retransmission scheme, a $R_c = 1/3$ convolutional code with $K = 4$ is considered. The polynomial generators are $g_1 = 15_{(8)}$,
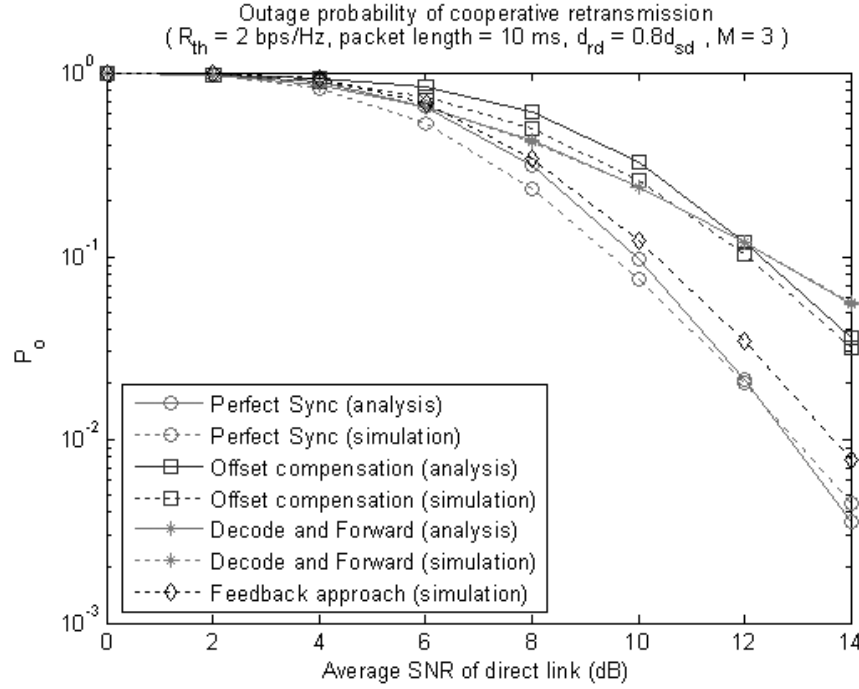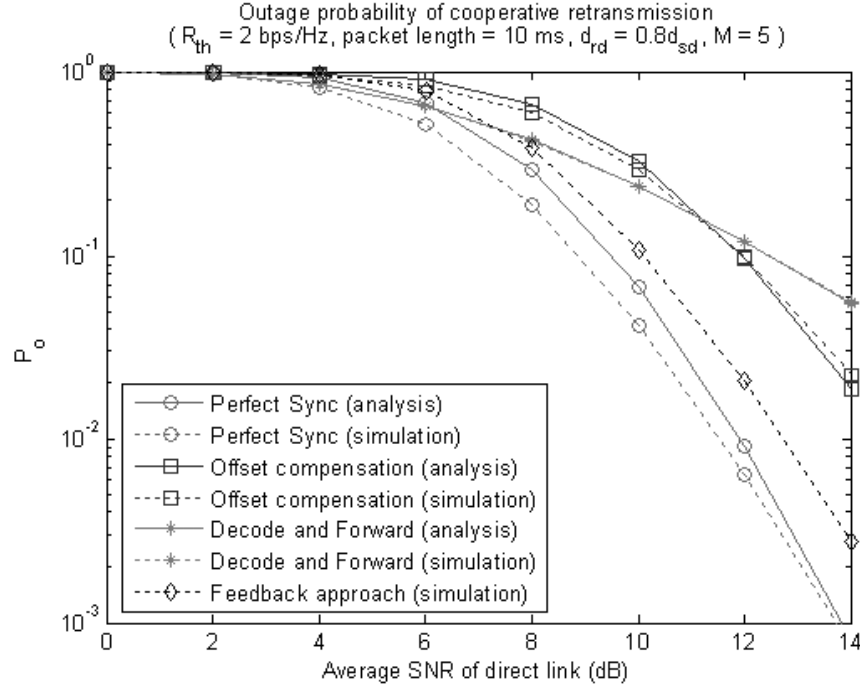
Figure 5.9: Outage probability with cooperative retransmission scheme using phase and frequency offset compensation ($M = 5$, packet length = 10 ms, Doppler spread = 20 Hz, Maximum frequency offset = 2 kHz, $d_{rd} = 0.8\ d_{sd}$)

$g_2 = 17_{(8)}$ and $g_3 = 13_{(8)}$. The first code block, $\mathbf{C}_1$, is a $R_c = 1/2$ convolutional code which is obtained by puncturing the whole code block. The punctured bits will be the redundant code block, $\mathbf{C}_2$, which will be delivered to the destination if necessary. BPSK modulation is used and the length of the information data is assumed to be 10 ms, which will be 1250 bytes of the retransmitted data packet.

High PER performance gain can be achieved even for long data packets with a low-rate feedback channel as shown in Figure 5.10. It is assumed that all neighboring nodes are located at the same relative distance as $d_{sr} = 0.2d_{sd}$ and $d_{rd} = d_{sd}$. When the feedback channel is not used, there is no benefit with a large number of neighboring nodes using the proposed method. By using a small feedback channel, however, the proposed cooperative retransmission scheme can efficiently utilize a large number of neighboring nodes and outperforms the retransmission scheme by the source.

5.2.3   Power Control with Limited Information

In the proposed cooperative retransmission scheme, proper power control for the retransmission packet is essential in wireless ad hoc networks to reduce power consumption and interference to other communication links. Total transmit power is assumed to be normalized for a fair comparison to the results in the previous section. In the proposed retransmission scheme, however, power normalization at each cooperating node is not possible since neighboring nodes are involved in cooperation independently, *i.e.*, without sharing information. If the required signal power of the next code block is included in the NACK message, cooperating nodes can adjust their transmit power using this information. We will examine such a power control method in this section.

We will use the same example systems considered in the previous section for PER performance evaluation where an INR ARQ is used with a convolutional code of $R_c = 1/3$.
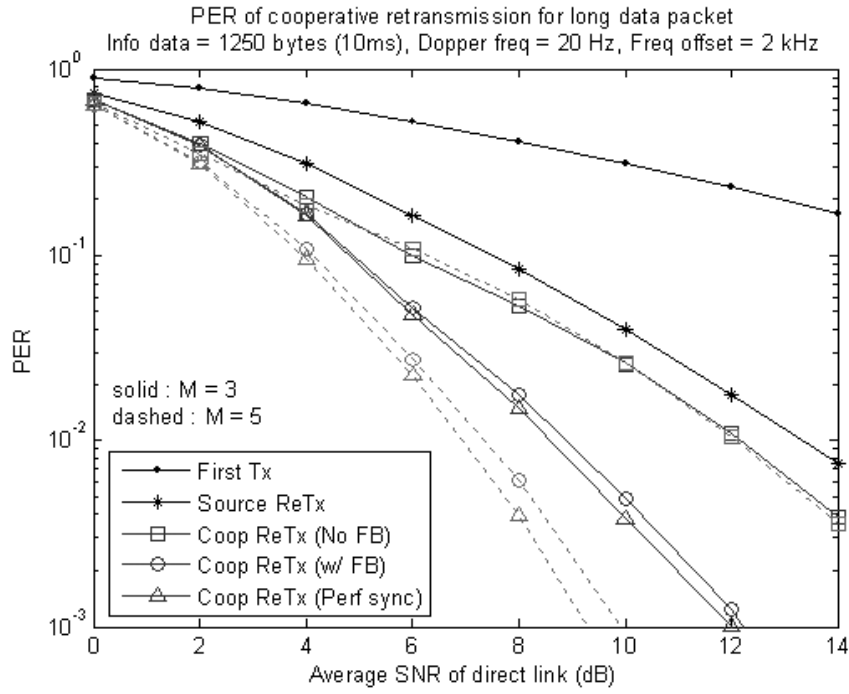
Figure 5.10: PER performance of INR ARQ scheme with cooperative retransmission ($M = \{3, 5\}$, retransmit packet length = 10 ms, Doppler spread = 20 Hz, Maximum frequency offset = 2 kHz, $d_{sr} = 0.2d_{sd}$, $d_{rd} = d_{sd}$)

When the first code block is erroneous, the destination calculates the required power for the next code block based on a predefined PER. When a convolutional code is used, the union bound of PER with B information bits is given by [69]

$$PER_{pkt} = \sum_{j=1}^{B} P_e(j) < BT(W) \tag{5.18}$$

where $P_e(j)$ is the probability of selection error at j^{th} symbol. $T(W)$ is the transfer function of the corresponding convolutional code and $W = e^{-E_s/N_o}$ where E_s is symbol energy and N_o is noise variance. For the given convolutional code, which is $K = 4$, $g_1 = 15_{(8)}$, $g_2 = 17_{(8)}$ and $g_3 = 13_{(8)}$, the transfer function is given by

$$
\begin{aligned}
T(W)|_{R=1/3} &= \frac{W^{10}(3 - 4W^2 + 5W^4 - 4W^6 + W^8)}{1 - 2W^2 - 2W^4 + 2W^6 - 4W^8 + 4W^{10} - W^{12}} \\
&\approx 3W^{10} + 2W^{12} + 15W^{14} + 24W^{16} + 87W^{18} + 188W^{20} + 577W^{22}.
\end{aligned} \tag{5.19}
$$

The union bound for PER is related to the symbol energy of whole code block. Since the received symbol energy for the first code block and next code block might be different in an INR ARQ scheme, the average symbol energy of the two code blocks will be used as the whole symbol energy, $E_s = (E_{s,1}T_{s,1} + E_{s,2}T_{s,2})/(T_{s,1} + T_{s,2})$. $E_{s,i}$ and $T_{s,i}$ represent the received symbol energy and time duration of the code block i. $E_{s,1}$ is already known at the destination from the first received signal. The required $E_{s,2}$ can be found using the union bound of PER given in (5.19) and the desired PER. The required E_s for the next code block, $E_{s,2}$, will be included in the NACK message which will be used for the next code block.

Figures 5.11 and 5.12 show PER performance and average transmit power for the next code block with the proposed cooperative INR scheme, respectively. It is assumed that the desired PER at the destination is 10^{-2} and the number of information bits is 250 bytes which corresponds to a 10 ms code block with BPSK modulation. PER performance with
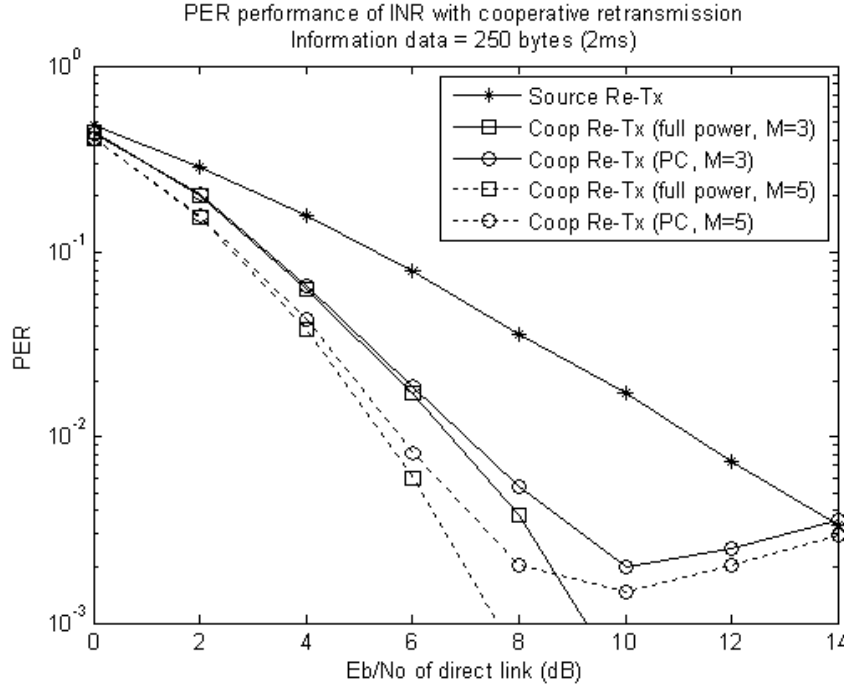
Figure 5.11: PER performance with the cooperative INR scheme (target PER $= 10^{-2}$, packet length $= 2$ ms, M $= \{3,5\}$)

power control is similar to the cases of full transmit power. The average transmit power for the second code block can be significantly reduced with power control while the PER is maintained near the desired performance at high SNR ranges.

Figures 5.13 and 5.14 show the PER performance and average transmit power for the next code block with 1250 bytes information bits. The same trend of PER and average retransmission power is shown for longer data packets even though the average transmit power with power control increases slightly to maintain the target PER. Note that the transmit power for retransmission can be reduced even more if there is additional information about the cooperating signals. Also, the feedback channel for phase adjustment can be used for power control. The transmit power with those approaches will be investigated with a target SNR in a multihop configuration in Chapter 6.
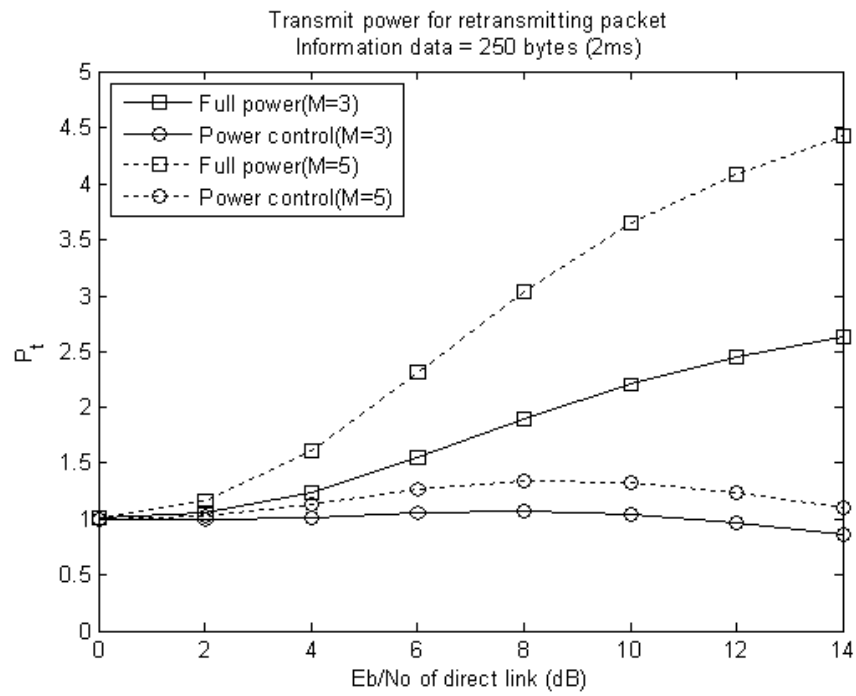
Figure 5.12: Average transmit power for retransmission (target PER $= 10^{-2}$, packet length $= 2$ ms, M $= \{3,5\}$)
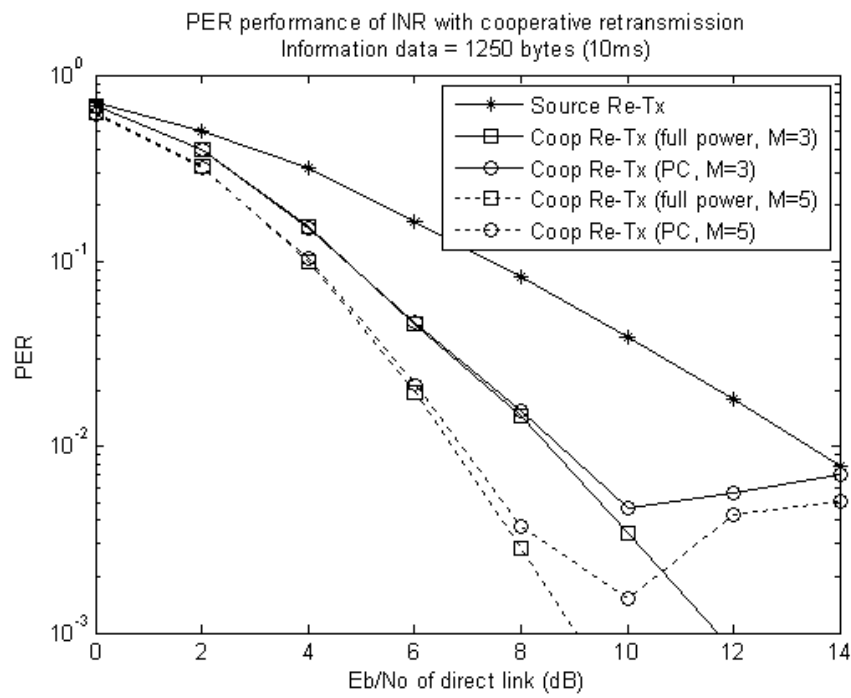
Figure 5.13: PER performance of the cooperative INR scheme (target PER $= 10^{-2}$, packet length = 2 ms, M = {3,5})
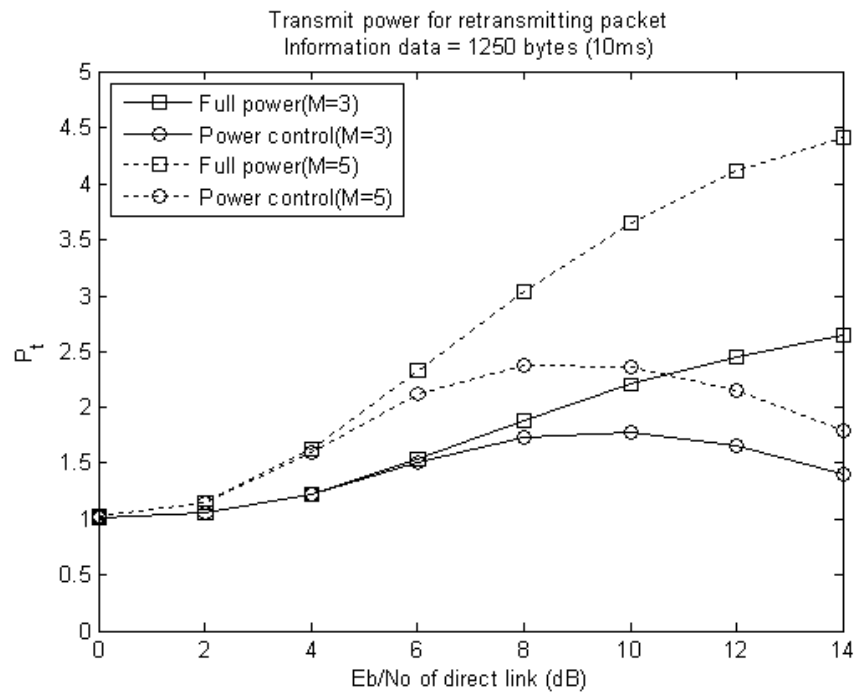
Figure 5.14: Average transmit power for retransmission (target PER $= 10^{-2}$, packet length $= 2$ ms, M $= \{3,5\}$)

5.3   Chapter Summary

An offset estimation method for the proposed cooperative retransmission scheme was investigated using the NACK message. The analytical and simulated results with offset estimation were well matched to each other. The performance with offset estimation was close to the perfect synchronization case for short data packets where the effect of residual offsets is relatively small. The residual frequency offset and channel variation can diminish the benefits of the cooperative retransmission scheme especially for long data packets. A low-rate feedback channel was proposed for adjusting phase shift and substantial gains were achieved, especially for long data packets. Power control with limited information was also examined for an INR ARQ scheme and the average transmit power for the second code block can be significantly reduced while PER is maintained under the desired performance.

Chapter 6

Cooperative Retransmission in Multihop Networks

In this chapter, a two-state Markov model is used in order to investigate the throughput efficiency and the average packet delay of the proposed cooperative retransmission scheme. The analytical results are first compared with the simulated results for a simple single-hop configuration. The performance of the cooperative retransmission scheme is then investigated in a multihop configuration where multiple packet transmission is simulated to verify the performance in the presence of concurrent transmissions. The average transmit power of the retransmitted packet is also examined with various power control approaches.

6.1 Throughput Efficiency and Average Delay in Single-Hop Networks

The network configuration shown in Figure 6.1 will be considered to analyze and simulate the throughput efficiency and average delay performance. There are M neighboring nodes around the direct link which are involved in the cooperation as described in Chapter 3.
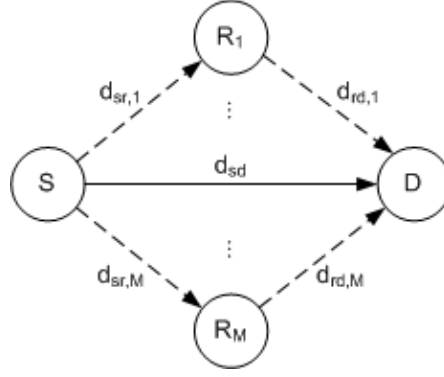
Figure 6.1: Network model for throughput and delay analysis

d_{sd} denotes the distance between the source and the destination. $d_{sr,m}$ and $d_{rd,m}$ denote the distance from the source and the destination to neighboring node m, respectively. The throughput efficiency and the average packet delay will be analyzed for both retransmission by the source and the proposed cooperative retransmission scheme.

A two-state Markov process as shown in Figure 6.2 can be used to describe the packet success/failure model for the cooperative retransmission scheme [70]. Let $O(k)$ denote the state of the cooperative stop-and-wait (SW) ARQ at packet k. $O(k)$ is either in the transmission (T) state or the retransmission (R) state. In state T, the source delivers a new packet to the destination. In state R, the erroneous packet is retransmitted by cooperating nodes which is only the source itself in the traditional ARQ scheme. The source can retransmit the erroneous packet in the cooperative ARQ scheme depending on the decoding result of the NACK message. If the source fails to decode the NACK message and there is no cooperative transmission until a waiting timer for the NACK message is expired, the source will retransmit the previous packet. Note that the waiting time for the NACK message is longer than the length of the NACK message. The transition probabilities of this Markov model are defined as
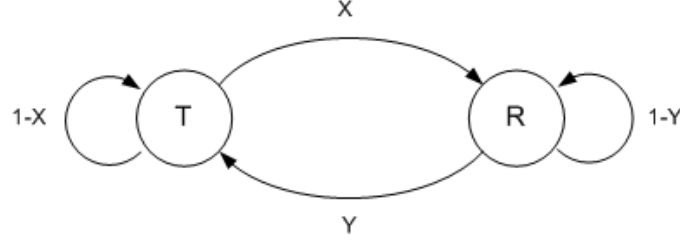
Figure 6.2: Markov model of SW ARQ scheme

$$X \triangleq \Pr\{O(k) = R | O(k-1) = T\}$$
$$Y \triangleq \Pr\{O(k) = T | O(k-1) = R\}.$$

(6.1)

For the go-back-N ARQ scheme with the number of blocks of N_B, the throughput efficiency is given by [71]

$$\bar{S} = \lim_{t \to \infty} \frac{\# \text{ of packets accepted by time } t}{\# \text{ of packets accepted by time } t + \# \text{ of packets retransmitted by time } t}$$
$$= \frac{Y[1 - (\zeta - 1)^{N_B}]}{Y[1 - (\zeta - 1)^{N_B}] + N_B(2 - \zeta)(2 - \zeta - Y)}$$

(6.2)

where $\zeta = 2 - (X + Y)$. By applying this Markov model in an SW ARQ scheme with $N_B=1$, the throughput efficiency of SW ARQ with the cooperative retransmission scheme can be simplified as [70]

$$\bar{S} = \frac{Y}{X + Y}.$$

(6.3)

The transition of $O(k)$ between the T and R states is related to the previous state, $O(k-1)$, the state of the direct link, $D(k)$, and the state of the retransmission link, $C(k)$, depending on the ARQ scheme. The whole transition logic between the T and R states is given in Table 6.1. $D(k)$ and $C(k)$ will be in the good state (G) or in the bad state (B).
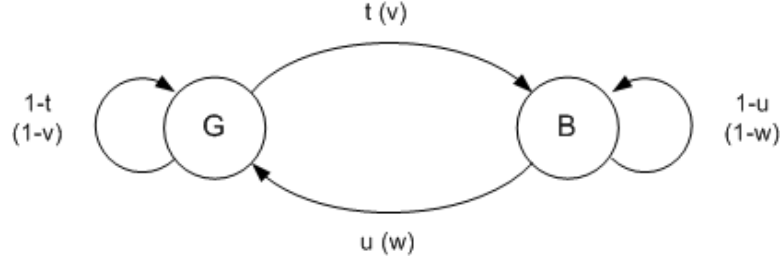
Figure 6.3: Markov model for the direct(retransmission) link

In state G, the channel condition of the link is good enough to receive the packet correctly. Otherwise, the link is in the B state. The state of the SW ARQ scheme depends on the states of the direct and the retransmission links which can will be another Markov model shown in Figure 6.3. The corresponding Markov parameters of $D(k)$ and $C(k)$ are defined as

$$
\begin{aligned}
t &= \Pr\{D(k) = B | D(k-1) = G\} \\
u &= \Pr\{D(k) = G | D(k-1) = B\}
\end{aligned}
\tag{6.4}
$$

and

$$
\begin{aligned}
v &= \Pr\{C(k) = B | C(k-1) = G\} \\
w &= \Pr\{C(k) = G | C(k-1) = B\}.
\end{aligned}
\tag{6.5}
$$

As shown in Table 6.1, the new state of the SW ARQ scheme for packet k, $O(k)$, depends on the previous state, the state of the direct link, and the state of the retransmission link. Therefore, there are eight possible steady-states which are denoted as S_i for $i = 0, \cdots, 7$. Let p_i be the steady-state probability of being in state S_i. Then, X and Y are given by

Table 6.1: State transition of the stop-and-wait ARQ scheme

state(S)	$\Pr\{S = S_i\}$	$O(k-1)$	$D(k-1)$	$C(k-1)$	$O(k)$
S_0	p_0	T	G	G	T
S_1	p_1	T	G	B	T
S_2	p_2	T	B	G	R
S_3	p_3	T	B	B	R
S_4	p_4	R	G	G	T
S_5	p_5	R	G	B	T
S_6	p_6	R	B	G	T
S_7	p_7	R	B	B	R

$$X = \Pr\{O(k) = R | O(k-1) = T\} = \frac{p_2 + p_3}{p_o + p_1 + p_2 + p_3}$$
$$Y = \Pr\{O(k) = T | O(k-1) = R\} = \frac{p_4 + p_5 + p_6}{p_4 + p_5 + p_6 + p_7}. \tag{6.6}$$

Figure 6.4 shows the state transition diagram based on the logic given in Table 6.1. In steady-state, the state diagram is satisfied with

$$P = BP$$
$$p_o + p_1 + \cdots + p_7 = 1 \tag{6.7}$$

where $P = [p_o \, p_1 \, \cdots \, p_7]^T$ and

$$
B = \begin{bmatrix}
\bar{t}\bar{v} & \bar{t}w & 0 & 0 & \bar{t}\bar{v} & \bar{t}w & u\bar{v} & 0 \\
\bar{t}v & \bar{t}\bar{w} & 0 & 0 & \bar{t}v & \bar{t}\bar{w} & uv & 0 \\
t\bar{v} & tw & 0 & 0 & t\bar{v} & tw & \bar{u}\bar{v} & 0 \\
tv & t\bar{w} & 0 & 0 & tv & t\bar{w} & \bar{u}v & 0 \\
0 & 0 & u\bar{v} & uw & 0 & 0 & 0 & uw \\
0 & 0 & uv & u\bar{w} & 0 & 0 & 0 & u\bar{w} \\
0 & 0 & \bar{u}\bar{v} & \bar{u}w & 0 & 0 & 0 & \bar{u}w \\
0 & 0 & \bar{u}v & \bar{u}\bar{w} & 0 & 0 & 0 & \bar{u}\bar{w}
\end{bmatrix}
\tag{6.8}
$$

where $\bar{(\cdot)} = 1 - (\cdot)$. The steady-state probability vector P can be found by solving (6.7) and the throughput efficiency of the SW ARQ scheme given in (6.3) can be expressed by the state transition probabilities of the direct and the retransmission links which will be analyzed for both the simple ARQ and the hybrid ARQ with MRC in the following sections.

Packet delay is defined as the time required to complete the packet delivery from the source to the destination. Since resource allocation is not considered in this paper, delay analysis does not include the queuing delay such as random backoff time. Then, the average packet delay depends on the packet length and the number of retransmissions. Let T_f be the length of a packet which is assumed to be fixed. When there is no packet error from the source to the destination, the total transmission delay will be T_f. However, the average packet delay is expected to be higher than this value due to possible packet errors. The average packet delay of the Markov model given in Figure 6.2 is given by [70]

$$
\bar{D} = \frac{X + Y}{Y} T_f.
\tag{6.9}
$$
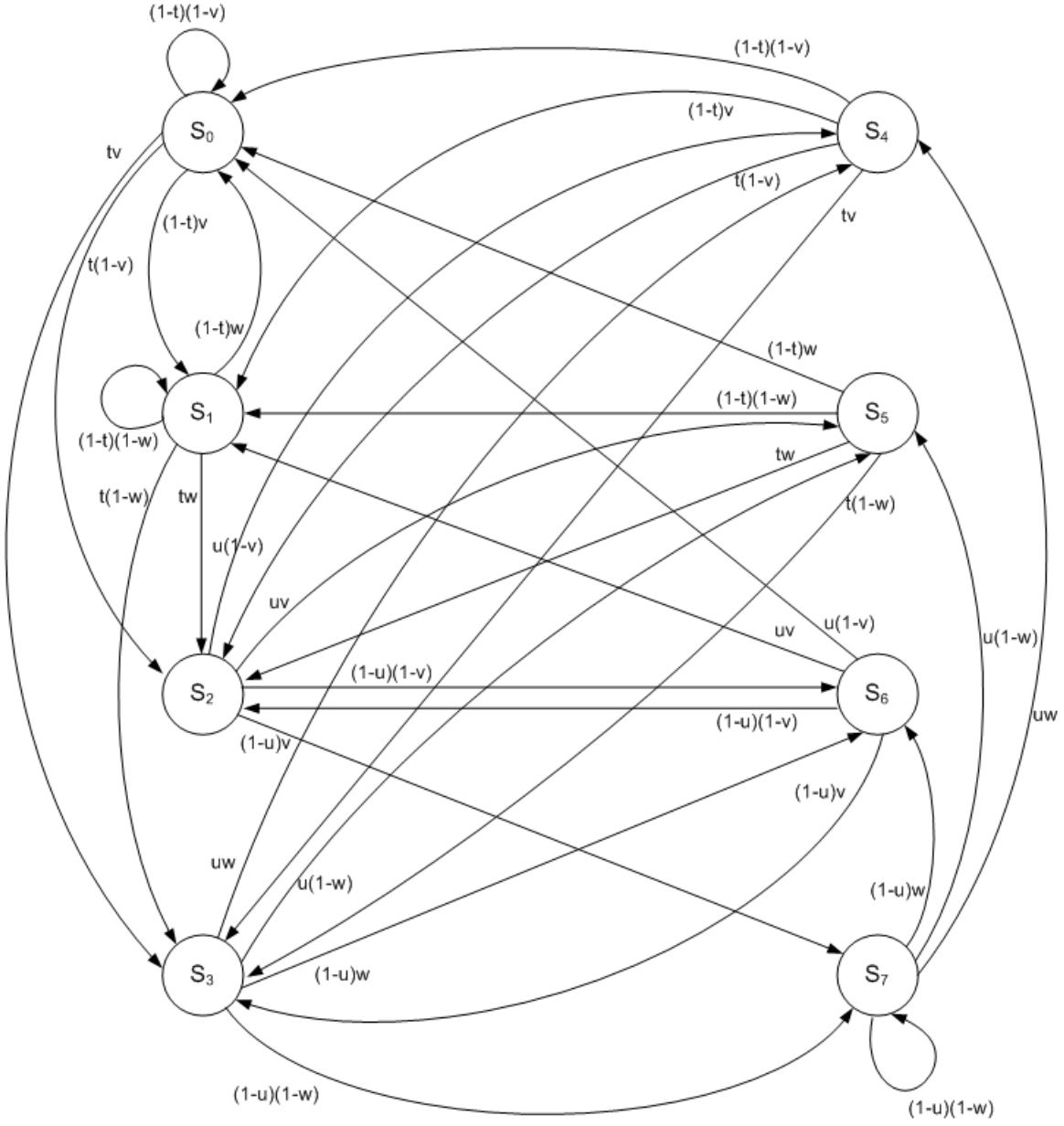
Figure 6.4: Markov model for $\{O(k-1), D(k), C(k)\}$

6.1.1   Simple ARQ

First, we will consider throughput efficiency without cooperation of neighboring nodes when simple ARQ is used at the destination. Since an erroneous packet is discarded in this ARQ scheme, the state can be modeled by only the state of the direct link, $D(k)$. When the channel condition is assumed to be independent for each transmission, the state transition probabilities are given by

$$
\begin{aligned}
X = t &= \Pr\{D(k) = B | D(k-1) = G\} = \Pr\{D(k) = B\} \\
Y = u &= \Pr\{D(k) = G | D(k-1) = B\} = \Pr\{D(k) = G\}.
\end{aligned}
\tag{6.10}
$$

The received signal of the direct link after matched filtering and sampling can be expressed by

$$
\mathbf{r}_{sd} = \sqrt{\alpha_{sd}} h_{sd} \mathbf{s} + \mathbf{n}_{sd}
\tag{6.11}
$$

where α_{sd} the large-scale power path loss of the direct link, and h_{sd} is the small-scale channel coefficient of the direct link which is a complex Gaussian random variable with zero mean and 0.5 variance per dimension. $\mathbf{s}$ is the transmit signal and $\mathbf{n}_{sd}$ is noise vector of the received signal of the direct link whose values are complex Gaussian random variables with zero mean and variance σ_n^2. It is assumed that the channel remains constant during a packet transmission time. When the source transmits packet k to the destination, it cannot be decoded correctly if the received SNR is below a certain threshold SNR, η_{th}, *i.e.*,

$$
D(k) =
\begin{cases}
B, & \text{if } \eta_{sd}|h_{sd}|^2 \leq \eta_{th} \\
G, & \text{if } \eta_{sd}|h_{sd}|^2 > \eta_{th}
\end{cases}
\tag{6.12}
$$

where $\eta_{sd} = \alpha_{sd}/\sigma_n^2$. $|h_{sd}|^2$ is an exponentially distributed random variable with pdf given

by

$$f_Y(y) = \frac{1}{2\sigma^2}e^{-y/2\sigma^2} = e^{-y}, \quad y \geq 0. \tag{6.13}$$

The final expression is obtained by substituting $\sigma^2 = 0.5$, which is channel variance per dimension as mentioned earlier. The probabilities of state transition for the direct link are given by

$$t = \int_0^{\beta_{sd}} f_Y(y)dy = F_Y(\beta_{sd}) = 1 - e^{\beta_{sd}} = \gamma(1, \beta_{sd})$$

$$u = 1 - \gamma(1, \beta_{sd}) \tag{6.14}$$

where $\beta_{sd} = \eta_{th}/\eta_{sd}$ and $F_Y(y)$ is the cdf of the received signal. $\gamma(a, x)$ is incomplete gamma function which is defined in (3.5). Note that the incomplete gamma function is used for consistency with the case of the hybrid ARQ in next section. Finally, when the source retransmits an erroneous packet to the destination, the throughput efficiency with the simple ARQ scheme is given by

$$\bar{S} = \frac{Y}{X + Y} = 1 - \gamma(1, \beta_{sd}). \tag{6.15}$$

The throughput efficiency in (6.15) can be rewritten as $\bar{S} = 1 - t$ which can be interpreted as the probability that the direct link is in the good state.

When neighboring nodes are involved in retransmission of the erroneous packet, the state transition of the retransmission link is different than that of the direct link and needs to be considered. In the proposed cooperative retransmission scheme, distributed beamforming is used for accommodating multiple cooperating nodes where the NACK message is used for synchronization of cooperating signals. Outage performance with offset estimation is slightly worse as compared to the perfect synchronization case. However, it might be good enough

to be assumed as perfect synchronization for a small number of cooperating nodes when residual offsets are adjusted by a feedback channel as shown in the previous chapter.

Assuming perfect synchronization, the received signal from cooperating nodes can be approximated as the sum of Rayleigh random variables. Note that the actual distribution of the cooperating signal is not a sum of Rayleigh random variables since the signal strength of each cooperating signal is greater than the threshold for successful NACK reception. In the high SNR regime of the $r \to d$ link, however, this approximation is well matched with the actual distribution. Again for simplicity of analysis, it is assumed that the large-scale path loss of the cooperating links is same, *i.e.*, $d_{sr,j} = d_{sr}$ and $d_{rd,j} = d_{rd}$ for $j = 1, \cdots, M$. Then, the received signal from L cooperating nodes can be expressed by

$$
\begin{aligned}
\mathbf{r}_{co} &\approx \frac{1}{\sqrt{L}} \sum_{l=1}^{L} \sqrt{\alpha_{rd,l}} |h_l| \mathbf{s} + \mathbf{n}_{co} \\
&= \sqrt{\frac{\alpha_{rd}}{L}} \sum_{l=1}^{L} |h_l| \mathbf{s} + \mathbf{n}_{co}
\end{aligned}
\tag{6.16}
$$

where $\mathbf{n}_{co}$ is noise vector of the received signal of the cooperating link. The received SNR of the cooperating signal is given by

$$
y_{co} = \frac{\alpha_{rd}}{L\sigma_n^2} \left(\sum_{l=1}^{L} |h_l| \right)^2 = \frac{\delta \eta_{sd}}{L} X_L
\tag{6.17}
$$

where η_{sd} is average SNR of the direct link and

$$
X_L = \left(\sum_{l=1}^{L} |h_l| \right)^2.
\tag{6.18}
$$

The pdf of X_L is given in (3.11) and its cdf is given by

$$
F_{X_L}(x) = \frac{1}{(L-1)!} \gamma \left(L, \frac{x}{2b(L)} \right).
\tag{6.19}
$$

The outage of the cooperating link with L nodes occurs when the received SNR is less than the threshold SNR given by

$$
\begin{aligned}
\Pr\{&C(k) = B, L \text{ cooperating nodes}\} \\
&= \Pr\{y_{co} \leq \eta_{th}\} = \Pr\left\{X_L \leq \frac{L}{\delta}\frac{\eta_{th}}{\eta_{sd}}\right\} = F_{X_L}\left(\frac{L\beta_{sd}}{\delta}\right).
\end{aligned}
\tag{6.20}
$$

The state of the retransmission link with the cooperative retransmission scheme depends on the number of cooperating nodes and their channel conditions. To be involved in the cooperation, the neighboring node must receive the data packet and the NACK message correctly. Therefore, the probability of cooperation for the neighboring node is given by

$$
\begin{aligned}
p_{co} &= \Pr\{\eta_{sr}|h_{sr}|^2 > \eta_{th}\}\Pr\{\eta_{rd}|h_{rd}|^2 > \eta_{NACK}\} \\
&= e^{-\beta_{sr}}e^{-\beta_{rd}}
\end{aligned}
\tag{6.21}
$$

where $\beta_{sr} = \eta_{th}/\eta_{sr}$, $\beta_{rd} = \eta_{NACK}/\eta_{rd}$, and η_{NACK} is the required SNR for the successful reception of the NACK message. When there are M cooperating nodes around the direct link, the transition probabilities of the retransmission link are given by

$$
\begin{aligned}
v &= \Pr\{C(k) = B\} \\
&= \Pr\{D(k) = B, \text{No cooperation}\} + \sum_{m=1}^{M}\Pr\{C(k) = B, m \text{ cooperating nodes}\} \\
&= (1 - p_{co})^M\gamma(1, \beta_{sd}) + \sum_{m=1}^{M}p_{co}^m(1 - p_{co})^{M-m}F_{X_m}(m\beta_{sd}/\delta) \\
&= (1 - p_{co})^M\gamma(1, \beta_{sd}) + \sum_{m=1}^{M}p_{co}^m(1 - p_{co})^{M-m}\frac{1}{(m-1)!}\gamma\left(m, \frac{\beta_{sd}}{\xi(m)}\right) \\
w &= \Pr\{C(k) = G\} = 1 - v
\end{aligned}
\tag{6.22}
$$

where $\xi(m) = 2\delta b(m)/m$ which is defined in (3.12). The first term in v represents the
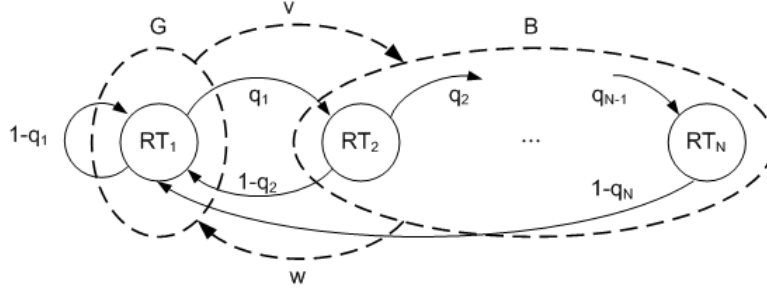
Figure 6.5: Markov model for the retransmission link

source retransmission when there are no cooperating nodes and the second term represents cooperative retransmission with M neighboring nodes. The throughput efficiency with the proposed cooperative ARQ can be obtained by solving (6.7) and (6.8) using (6.14) and (6.22).

6.1.2 Hybrid ARQ with MRC

When the previously received signals are combined with the currently received signal, the state of the retransmission link depends on the number of retransmissions. Figure 6.5 shows the Markov model of the retransmission link in detail where RT_n represents the state of nth retransmission and q_n represents the probability of state transition from state n to state $n + 1$. It is assumed that all packets are successful after N retransmissions, *i.e.*, $q_N = 0$.

Let p_n^c be the probability that the state of retransmission is in state n. Then, the relation between state probabilities is given by

$$\begin{cases} q_1 p_1^c = (1 - q_1)p_1^c + (1 - q_2)p_2^c + \cdots + (1 - q_N)p_N^c \\ q_n p_n^c = p_{n+1}^c, \qquad n = 1, 2, \cdots, N - 1 \\ p_1^c + p_2^c + \cdots + p_N^c = 1. \end{cases} \qquad (6.23)$$

After solving (6.23), the probabilities of state transition for the retransmission link are given by

$$v = 1 - \frac{1}{g}(1 - q_1)$$

$$w = \frac{1}{g}\sum_{n=1}^{N-2}\left(\prod_{j=1}^{n}q_j\right)(1 - q_{n+1}) \tag{6.24}$$

where g is given by

$$g = 1 + \sum_{n=1}^{N-1}\prod_{j=1}^{n}q_j. \tag{6.25}$$

Let's first consider the case when the source retransmits the erroneous packet to the destination. When the channel of each retransmission is assumed to be independent, the received SNR after n retransmissions is the sum of $n + 1$ exponential random variables including the first transmission and its pdf and cdf are given by

$$f_{U_n}(u) = \frac{1}{n!}u^n e^{-u}$$

$$F_{U_n}(u) = \frac{1}{n!}\gamma(n + 1, u). \tag{6.26}$$

The probability of state transition from state n to state $n + 1$ is given by $q_n = F_{U_n}(\beta_{sd})$. Finally, the probabilities of state transition for the retransmission link are given by

$$v = 1 - \frac{1 - \gamma(2, \beta_{sd})}{g}$$

$$w = \frac{1}{g}\sum_{n=1}^{N-2}\left(1 - \frac{\gamma(n + 2, \beta_{sd})}{(n + 1)!}\right)\prod_{j=1}^{n}\frac{\gamma(j + 1, \beta_{sd})}{j!} \tag{6.27}$$

where

$$g = 1 + \sum_{n=1}^{N-1}\prod_{j=1}^{n}\frac{\gamma(j + 1, \beta_{sd})}{j!}. \tag{6.28}$$

The state transition diagram in Figure 6.5 can also be used for the proposed cooperative retransmission scheme and the state transition probabilities are given by (6.24). The

difference between the source retransmission and the cooperative retransmission is the distribution of the received signal at the destination. When there are L cooperating signals, the received SNR of the combined signal at state n can be approximated by

$$
\begin{aligned}
z_{n,L} &\approx \eta_{sd} \sum_{i=1}^{n_f+1} |h_i|^2 + \eta_{sd} \frac{\delta}{L} \left(\sum_{l=1}^{L} |h_l| \right)^2 \\
&= \eta_{sd} \left[\sum_{i=1}^{n_f+1} |h_i|^2 + \frac{\delta}{L} \left(\sum_{l=1}^{L} |h_l| \right)^2 \right]
\end{aligned}
\tag{6.29}
$$

where the first term represents the received signals from the source and the second term represents the received signals from L cooperating nodes. $n_f = \lfloor n/2 \rfloor$ where $\lfloor z \rfloor$ is the nearest integer to z towards negative infinity. Let $Z_{n,L} = U_{n_f+1} + (\delta/L)X_L$ where the distribution of U_n and X_L is given in (6.26) and (6.19), respectively. The pdf of $Z_{n,L}$ can be evaluated by multiple convolution and its integration which is given by

$$
f_{Z_{n,L}}(z) = \frac{z^{n_f+L}e^{-z}}{\xi(L)^L(n_f+L)!} {}_1F_1 \left(L; L+n_f+1; \left(1 - \frac{1}{\xi(L)}\right) z \right)
\tag{6.30}
$$

where ${}_1F_1(a;b;c)$ is the confluent hypergeometric function of the first kind. The cdf of $Z_{n,L}$, $F_{Z_{n,L}}(z)$, cannot be found as the closed form and will be obtained by computer calculation using $f_{Z_{n,L}}(z)$.

When there are M neighboring nodes around the direct link and hybrid ARQ is used with MRC, the transition probability from state n to state $n + 1$ with the cooperative retransmission scheme is given by

$$
q_n = (1 - p_{co})^M F_{U_{n_f}}(\beta_{sd}) + \sum_{m=1}^{n_c M} p_{co}^m (1 - p_{co})^{n_c M - m} F_{Z_{n,m}}(\beta_{sd}).
\tag{6.31}
$$

$n_c = \lceil n/2 \rceil$ where $\lceil z \rceil$ is the nearest integer to z towards positive infinity. Note that $n_c M$ is the total number of cooperating signals during n retransmission. Probabilities of state transition using the cooperative retransmission scheme can be obtained by substituting (6.31) into (6.24) and (6.25).

6.2   Numerical Results

Throughput efficiency and average packet delay will be compared for the traditional and the cooperative ARQ schemes to observe the benefit of the proposed retransmission scheme. The configuration shown in Figure 6.1 will be considered where two neighboring nodes are located around the direct link, $M = 2$, with $d_{sr,j} = 0.7d_{sd}$, and $d_{rd,j} = 0.7d_{sd}$ for $j = 1, 2$. It is assumed that the path loss coefficient is four, and the required SNR for the successful reception of data and NACK packets are 5 dB and 3 dB, respectively. It is also assumed that the packet length is fixed with a 10 ms.

Figures 6.6 and 6.7 show the throughput efficiency and the average packet delay with both the traditional ARQ and the cooperative ARQ schemes, respectively, when the erroneous packet is discarded at the destination. The analytical results are well matched with the simulated results for both schemes. Significant throughput and delay performance gain can be achieved by using the cooperative retransmission scheme especially when average SNR of the direct link is poor.

Figures 6.8 and 6.9 show the throughput efficiency and average packet delay of both ARQ schemes when the hybrid ARQ with MRC is used. Again, the analytical and the simulated results are well matched with each other. When MRC is used for the retransmitted packets, both schemes show relatively good performance even for low SNR ranges. The cooperative ARQ scheme outperforms the traditional ARQ scheme especially when the direct link has low SNR. In Figure 6.9, it is shown that the average packet delay is reduced by
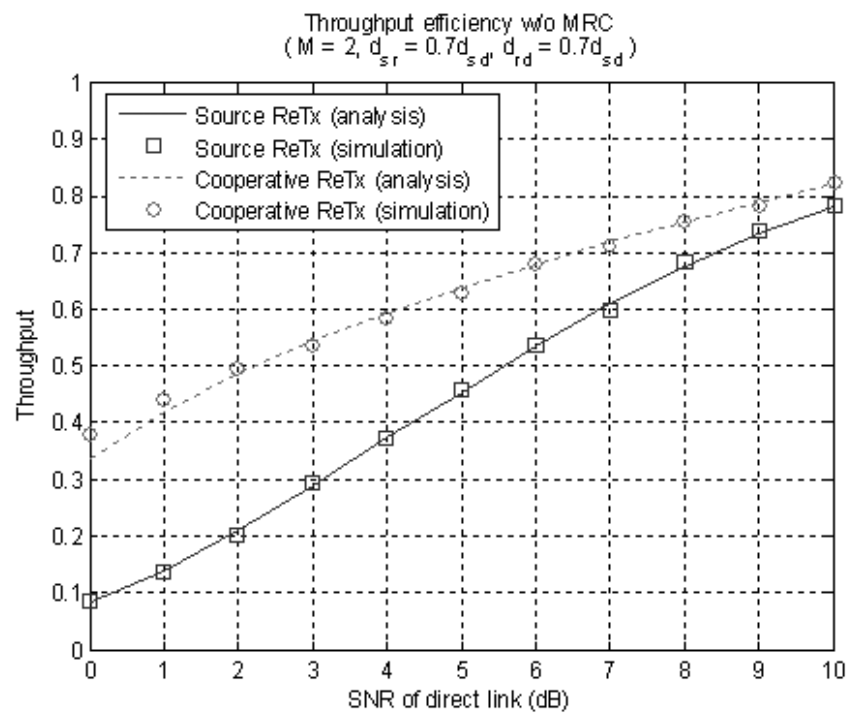
Figure 6.6: Throughput efficiency with a simple ARQ in single-hop networks ($M = 2$, $d_{sr} = 0.7d_{sd}$, $d_{rd} = 0.7d_{sd}$)

Figure 6.7: Average packet delay with a simple ARQ in single-hop networks ($M = 2$, $T_f = 10$ms, $d_{sr} = 0.7d_{sd}$, $d_{rd} = 0.7d_{sd}$)
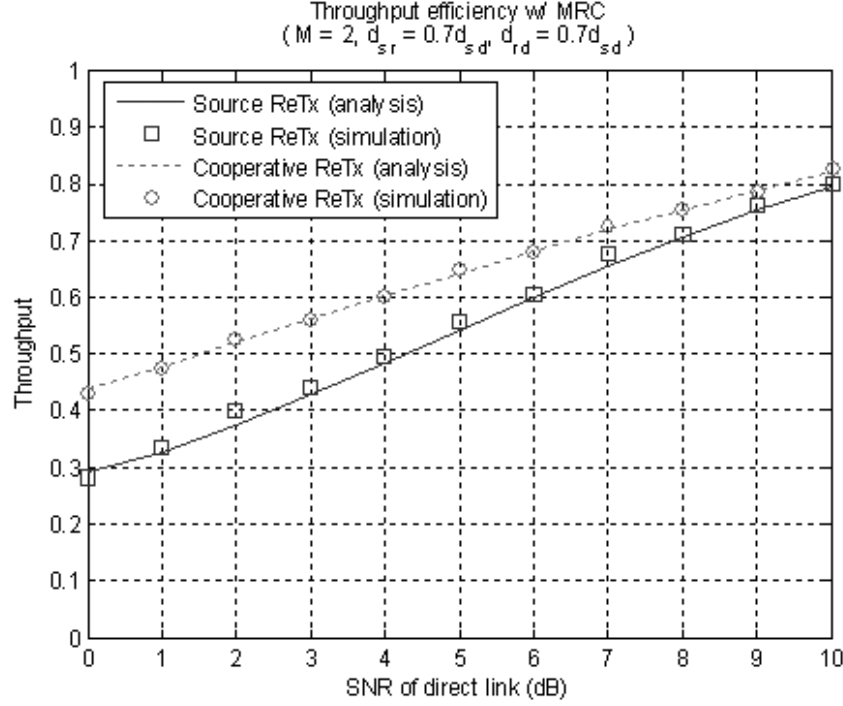
Figure 6.8: Throughput efficiency with a hybrid ARQ using MRC in single-hop networks ($M = 2$, $d_{sr} = 0.7d_{sd}$, $d_{rd} = 0.7d_{sd}$)

about 30% at low SNR ranges where channel condition of the direct link is poor. The benefits of the cooperative retransmission scheme decrease at high SNR ranges since retransmission through the source is enough to recover the erroneous packet.

6.3   Multi-Hop Configuration

A single-hop configuration with the same distance of cooperating links was considered in the previous section to verify the analysis of the proposed cooperative retransmission scheme. The performance of the cooperative retransmission scheme will be investigated with the randomly distributed network configuration as shown in Figure 6.10. It is assumed that 100 nodes are randomly distributed in 100 square meters and there are two transmission links
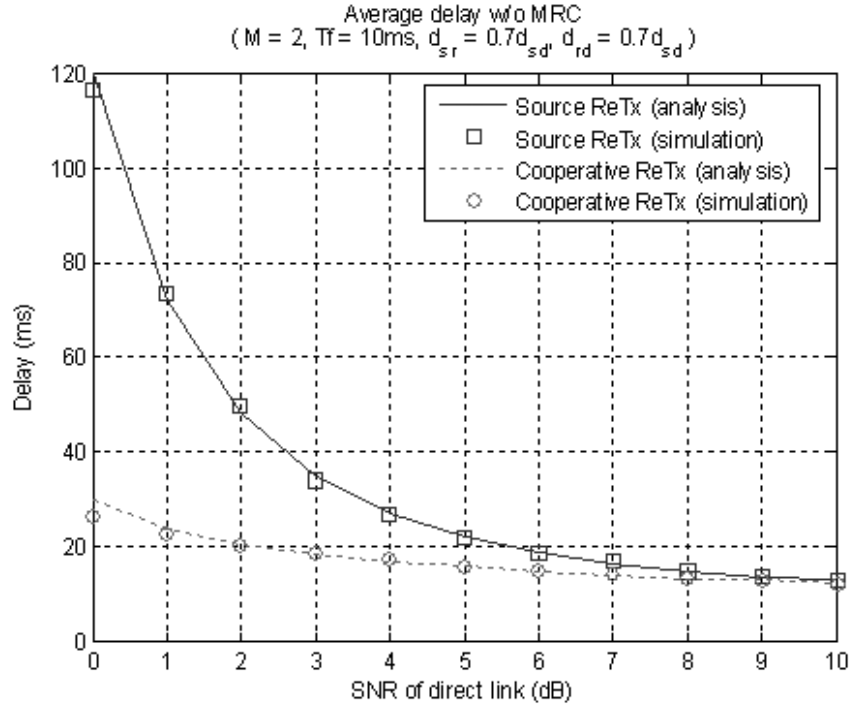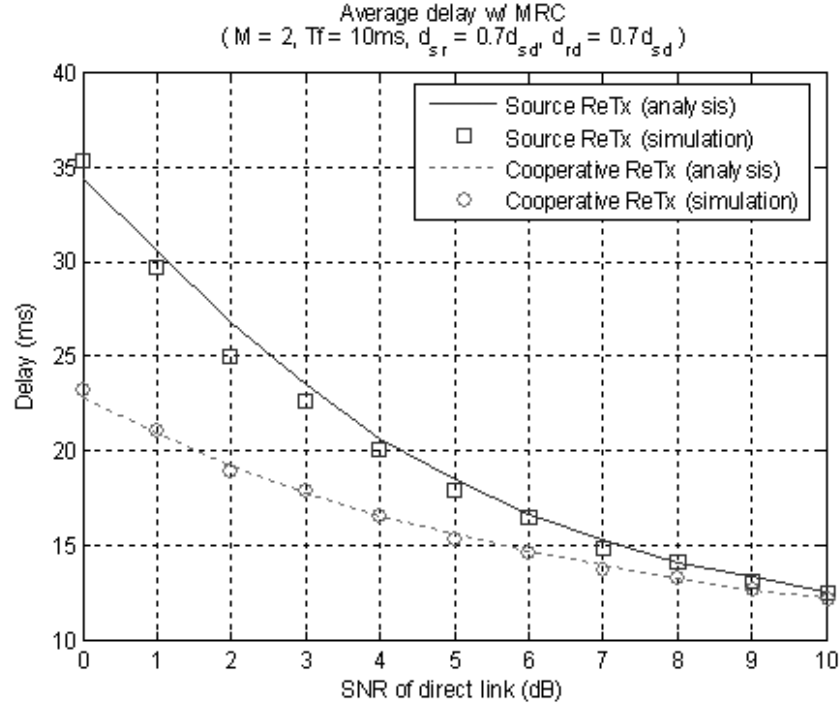
Figure 6.9: Average packet delay with a hybrid ARQ using MRC in single-hop networks (M = 2, T_f = 10ms, $d_{sr} = 0.7d_{sd}$, $d_{rd} = 0.7d_{sd}$)
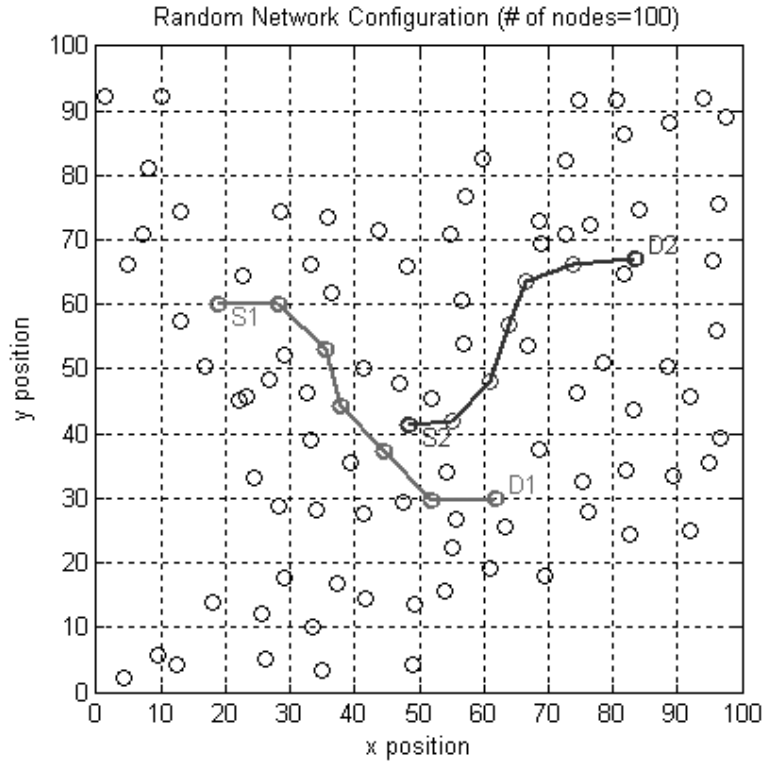
Figure 6.10: Random network configuration (# of nodes = 100, two transmission links with six hops)

with six hops from the source to the final destination. It is also assumed that each initial source node has ten packets to be delivered at the final destination and the length of each packet is a 10 ms. The dual busy tone multiple access (DBTMA) is assumed to be used with ACK at the end of message delivery [66]. When channel is busy or packet reception is unsuccessful, random backoff procedure will be initiated at the transmitter based on IEEE 802.11 standard [72].

Transmit power for the retransmitting packet is also an important issue in terms of battery lifetime and interference to other nodes. In the analysis of the previous section, the transmit power of cooperating signals is assumed to be normalized with the number of cooperating nodes for fair comparison with the retransmission by the source. As mentioned

in the previous chapter, however, the cooperative retransmission is decided independently at each neighboring nodes and there is no information exchange among them. When channel is assumed to be constant during the consecutive data packet transmission, each cooperating node can adjust its own transmit power of the retransmitting packet based on the channel condition of the NACK message. It will be referred as power control with *local* information. Due to the limited information, the received signal power for the retransmitted signal might be greater than the required one when there are multiple cooperating nodes. More efficient power control can be achieved if cooperating nodes share their information which will be referred as power control with *global* information. However, it requires the additional over-head for information exchange and the proper coordination among cooperating nodes. In the previous chapter, a small feedback channel is used for phase adjustment in the cooperative retransmission scheme, which can be also used for power control of the retransmitting signal. At the start of the retransmitting data packet, power control with *local* information is performed at each cooperating node. After receiving the cooperatively retransmitted packet, the destination observes the received signal power and reassigns the proper transmit power for the cooperating signal through the feedback channel. Note that outage probability with channel estimation was compared with the perfect synchronization case in Chapter 5 where performance difference is less than 1 dB with three neighboring nodes between the direct link. The single-hop and multi-hop configurations considered in this chapter are well covered by that configuration and perfect synchronization can be assumed with a small performance difference.

Figures 6.11 and 6.12 show the throughput efficiency and the average packet delay in the traditional and the cooperative ARQ when the erroneous packet is discarded at the destination. Unit distance for average SNR is assumed to be 10 m. In both transmission links, the cooperative ARQ outperforms the retransmission by the source in terms of throughput efficiency and average packet delay. Especially at low SNR ranges of the direct link, a
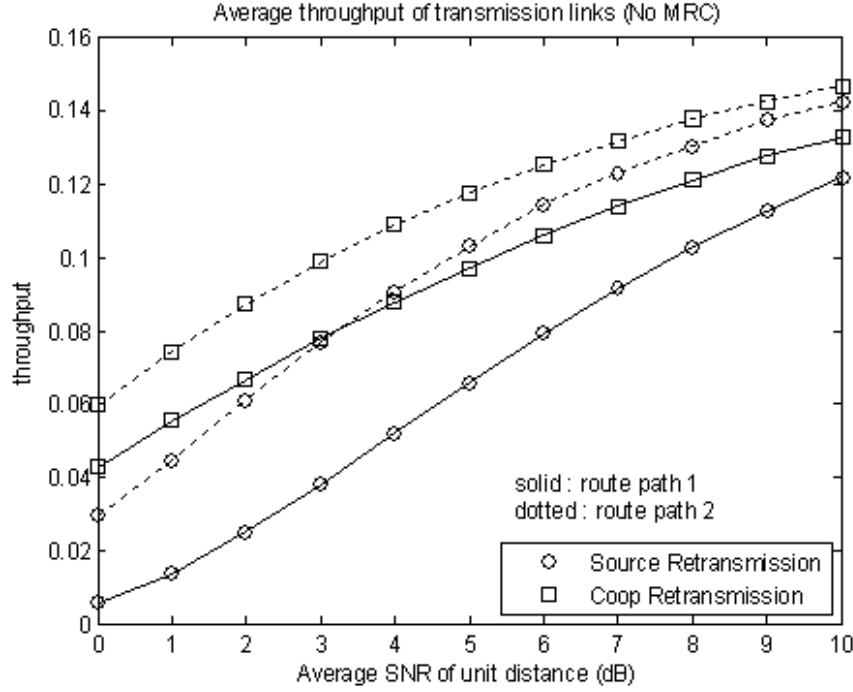
Figure 6.11: Throughput efficiency for both transmission links with a simple ARQ (six hops)

significant delay performance gain can be achieved with the proposed retransmission scheme.

Figure 6.13 shows throughput efficiency of two paths considered in network configuration. Four power control schemes are considered for the cooperative ARQ. For the normalized transmit power and the power control with *global* information, it is assumed that additional information such as the number of cooperating nodes and CSIs of cooperating links is provided at cooperating nodes. Power control methods with *local* information and feedback channel can be performed with the proposed cooperative retransmission scheme. The cooperative ARQ with any power control approach shows better performance than the typical source retransmission. All power control methods considered show almost same performance, which means that the signal quality of cooperating links is good enough to recover the transmitted packet as regardless of power control methods.

Figure 6.14 shows the average packet delay from the source to the final destination.
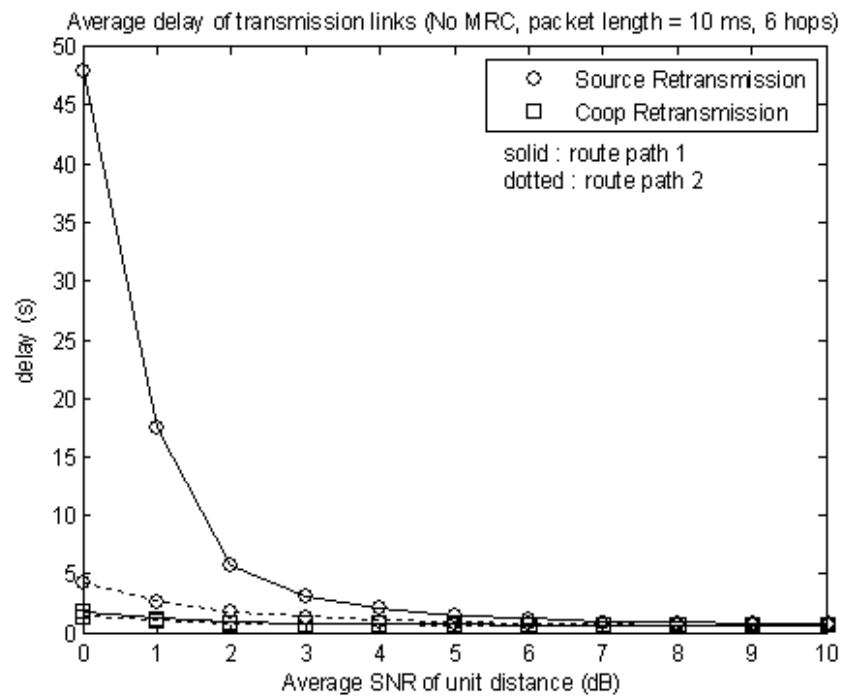
Figure 6.12: Average packet delay for both transmission links with a simple ARQ (six hops, packet length = 10 ms)
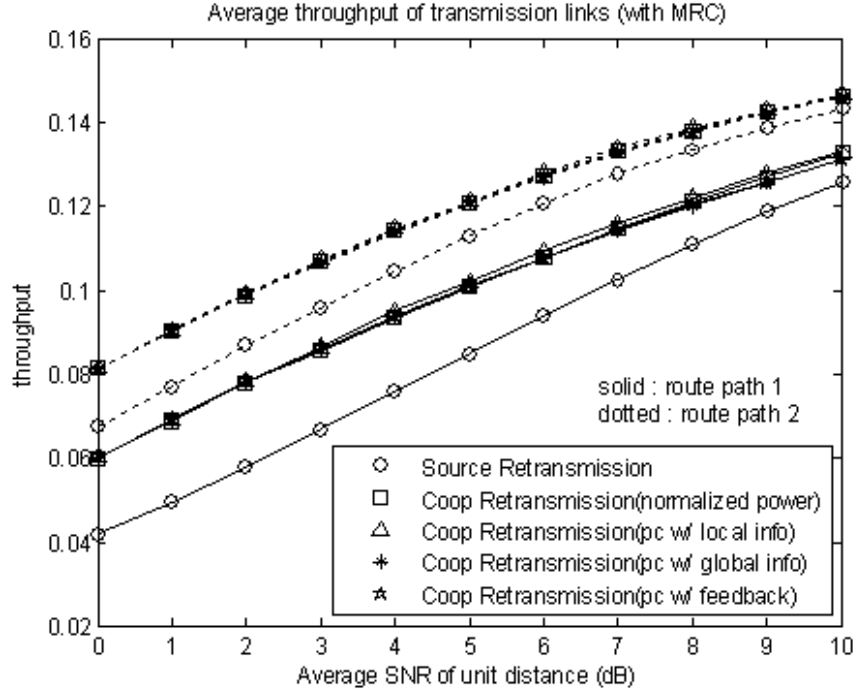
Figure 6.13: Throughput efficiency for both transmission links with a hybrid ARQ using MRC (six hops, normalized transmit power, power control with local/global information and feedback channel)

There is significant delay performance gain with the cooperative retransmission scheme. For example, about 40% packet delay can be reduced for the first path with the proposed cooperative ARQ when the average SNR of each hop is poor.

The advantage of the cooperative retransmission scheme is diminished in terms of throughput efficiency and packet delay as the average SNR of each hop increases. However, transmit power for retransmission can be reduced with the proper power control method. Figure 6.15 shows the average transmit power of the retransmitted signal. As indicated in the figure, the cooperative retransmission scheme with the normalized power uses the same transmit power as the source retransmission scheme. The transmit power of the retransmitting packet can be significantly reduced when all information are shared among cooperating nodes. When each cooperating node knows its own channel information only and adjusts its
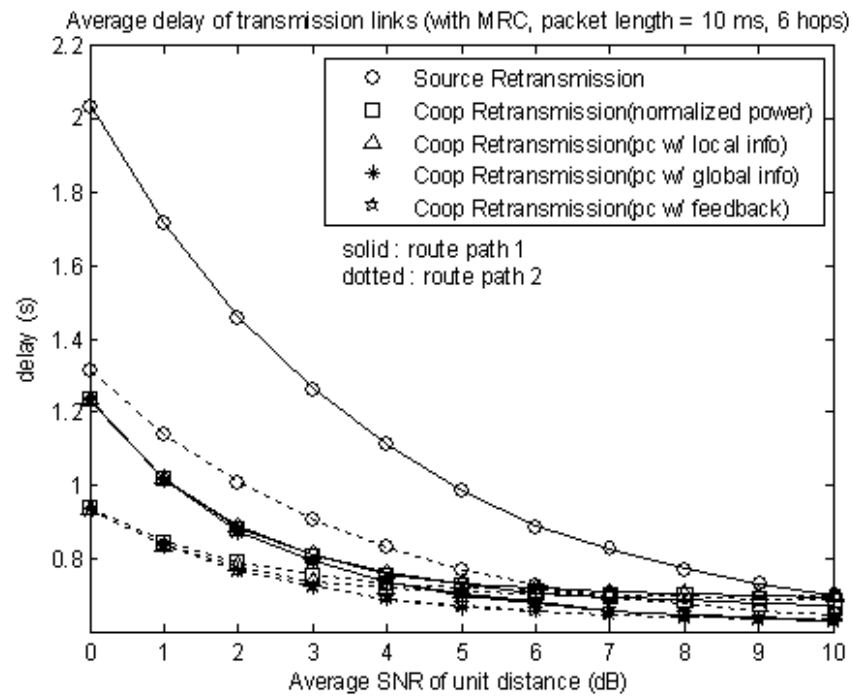
Figure 6.14: Average packet delay for both transmission links with a hybrid ARQ using MRC (six hops, packet length = 10 ms, normalized transmit power, power control with local/global information and feedback channel)
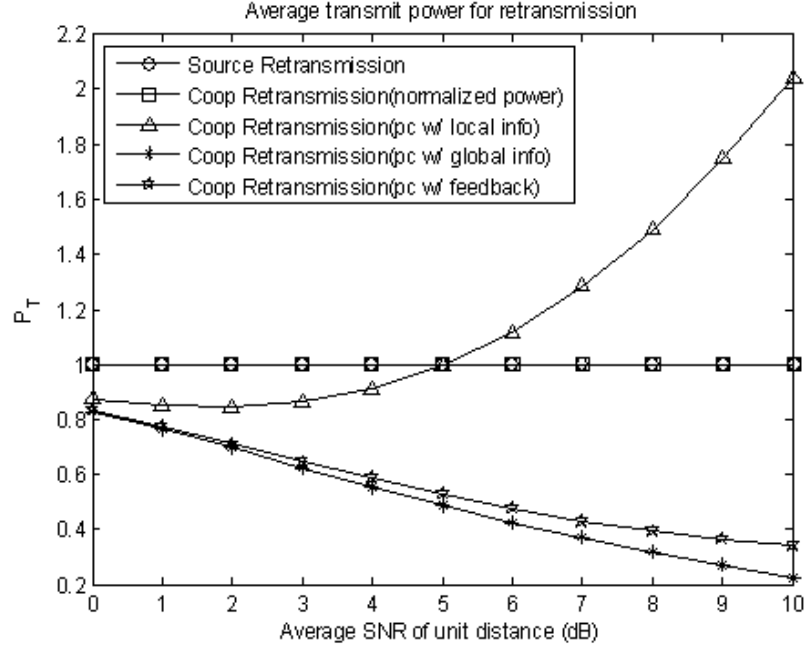
Figure 6.15: Average transmit power for retransmission (normalized transmit power, power control with local/global information and feedback channel)

transmit power based on it, redundant power will be received at high SNR ranges where a large number of neighboring nodes are involved in cooperation. The transmit power with the proposed cooperative retransmission scheme can be reduced significantly by using a small feedback channel without sharing channel information of other cooperating nodes.

6.4   Chapter Summary

The throughput efficiency and average packet delay of the proposed cooperative retransmission scheme were analyzed using a two-state Markov model for a simple ARQ and a hybrid ARQ with MRC. The analytical results were found to be in good agreement with the simulated results. Even with a small number of neighboring nodes, improved throughput efficiency and delay performance can be achieved by using the cooperative retransmission

scheme in wireless ad hoc networks. When the hybrid ARQ with MRC is used for the erroneous packets, for example, about 30% performance gain in throughput efficiency and average packet delay can be achieved at low SNR ranges with only two neighboring nodes in the vicinity of the direct link. It is shown that the benefits of the cooperative retransmission scheme increases especially when channel conditions of the direct link are poor.

The benefits of the cooperative ARQ were also verified in a multihop network with random configurations when there is concurrent packet transmissions. When each cooperating node adjusts its retransmitting signal power based on the NACK message, the total transmit power of the cooperating signal increases as the number of cooperating nodes increases. However, total transmit power for the cooperatively retransmitted packet can be significantly reduced by using a small feedback channel without sharing any information between cooperating nodes.

Chapter 7

Power Allocation Strategies in Cooperative MIMO Networks

One of challenges in this research is to develop efficient cooperative communication techniques with multiple antennas at each node. In cooperative MIMO networks, we focus on power allocation methods to achieve a good overall capacity without global information. An efficient power allocation method will be introduced which requires no channel information of the direct link and can be used for an arbitrary number of antennas.

Cooperative MIMO networks will be considered in this chapter where all nodes in the network have multiple antennas to transmit and receive the signal. It is assumed that the cooperating node forwards the received signal to the destination only when the signal is decoded properly, that is, a decode-and-forward method is used at the cooperating node. The outage probability of the channel capacity will be examined specifically based on the power assignment strategies at the nodes.

7.1 System Model

Figure 7.1 shows the assumed cooperative MIMO network model. It is assumed that all nodes have the same number of transmit and receive antennas, $N_T = N_R = N$. For the cooperative protocol, it is assumed that a time division orthogonal protocol is used. During the first time interval the source transmits a data packet to the destination and the cooperating node. The cooperating node decodes the received signal during the first time slot and retransmits the decoded data to the destination in the second time interval. The received signal at the destination during two time slots can be expressed by

$$
\mathbf{y} = \begin{pmatrix} \sqrt{\alpha_{sd}}\mathbf{H}_{sd} & 0 \\ 0 & \sqrt{\alpha_{rd}}\mathbf{H}_{rd} \end{pmatrix} \begin{pmatrix} \mathbf{s}_1 \\ \mathbf{s}_2 \end{pmatrix} + \begin{pmatrix} \mathbf{n}_1 \\ \mathbf{n}_2 \end{pmatrix} \tag{7.1}
$$

where $\mathbf{s_1}$ and $\mathbf{s_2}$ are the $N \times 1$ transmitted signal vectors from the source and the cooperating node, respectively. $\mathbf{H}_{ij}$ is the $N \times N$ channel matrix from node i to node j, where $i, j \in \{s, r, d\}$ and s, r, d stand for source, relay (cooperating node), and destination, respectively. The entries of the channel matrix are i.i.d. complex Gaussian random variables with zero mean and variance $1/2$ in each dimension. $\mathbf{n}_1$ and $\mathbf{n}_2$ are the noise vectors during the two time slots at the destination which are the complex Gaussian noise with $\mathcal{CN}(0, I_N)$. Note that $\mathbf{y}$ is a $2N \times 1$ vector, where the first N components represent the signal received on N antennas in the first time slot and the second N components represent the signal received during the second time slot.

As mentioned earlier, a decode-and-forward method is considered at the cooperating node. Therefore, if the instantaneous achievable rate at the cooperating node is above the given threshold data rate, the cooperating node works cooperatively. Otherwise, the cooperating node does not transmit the received signal to the destination. The threshold data rate will be the transmit data rate at the source. Since two time slots are used for
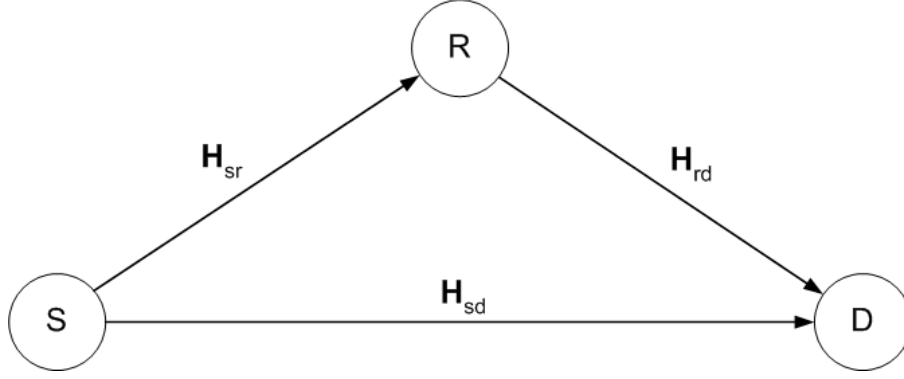
Figure 7.1: MIMO relay systems

cooperation, the ergodic cooperative channel capacity in the MIMO system is given by

$$
C_{mimo}^{co} = \begin{cases} E_H\left[\dfrac{1}{2}\log_2\det\left(1+\eta_{sd}\mathbf{H}_{sd}\mathbf{H}_{sd}^H\right)\right], & \text{relay can't cooperate} \\[2ex] E_H\left[\dfrac{1}{2}\log_2\det\left(1+\eta_{sd}\mathbf{H}_{sd}\mathbf{H}_{sd}^H+\eta_{rd}\mathbf{H}_{rd}\mathbf{H}_{rd}^H\right)\right], & \text{relay cooperates} \end{cases} \tag{7.2}
$$

where $E_H\{x\}$ is the expectation of x over the variable $\mathbf{H}$, and η_{ij} is the average received SNR at node j for the signal transmitted from node i. $\mathbf{A}^H$ is Hermitian transpose of $\mathbf{A}$. The first term in (7.2) represents the channel capacity when the cooperating node cannot decode the received data, while the second term represents the channel capacity when the cooperating node decodes the received data correctly and is working cooperatively.

7.2   Cooperative MIMO Channel Capacity

7.2.1   Outage Probability at the Cooperating Node

As shown in (7.2), the channel capacity of cooperative transmission with a decode-and-forward method highly depends on the outage probability at the cooperating node since the cooperating node forwards the received signal only when it is decoded successfully. For this reason, the error probability at the cooperating node needs to be investigated. With

multiple antennas at the nodes, spatial multiplexing will be considered for data transmission. In spatial multiplexing, a different data stream is transmitted over each spatial channel. Therefore, the outage for each stream has to be considered at the cooperating node to decide whether the received signal can be forwarded or not.

To simplify the analysis, it is assumed that the number of antennas at each node is two, $N = 2$. The main focus here is on power allocation across data streams. In equal power allocation which is usually used when the channel information is not available at the transmitter, the source assigns equal transmit power for each stream, $P_{sd,1} = P_{sd,2} = P_t/2$. P_t is the total transmit power, and $P_{sd,i}$ is the allocated transmit power for i^{th} channel between the source and the destination. When singular value decomposition (SVD) is used for the $s \rightarrow d$ link in the spatial multiplexing case, the $s \rightarrow r$ link cannot be separated with the same method. It is assumed that a zero forcing (ZF) method is used at the cooperating node for channel separation. Then, the instantaneous achievable rate of each channel at the cooperating node is given by

$$I_1^r = \log_2 \left(1 + \eta_{sr}\gamma_{sr,1}P_{sd,1}\right)$$
$$I_2^r = \log_2 \left(1 + \eta_{sr}\gamma_{sr,2}P_{sd,2}\right)$$

$$(7.3)$$

where $\gamma_{sr,i} = 1/[(\mathbf{H}_{sr}^H\mathbf{H}_{sr})^{-1}]_{i,i}$ for the uncorrelated channel [73]. $[\mathbf{X}]_{m,n}$ stands for the $(m,n)^{th}$ element of $\mathbf{X}$. Then, the outage probability for each channel is given by

$$p_{o1} = \Pr[I_1^r < R_1] = \Pr[\log_2 \left(1 + \eta_{sr}\gamma_{sr,1}P_{sd,1}\right) < R_1]$$
$$p_{o2} = \Pr[I_2^r < R_2] = \Pr[\log_2 \left(1 + \eta_{sr}\gamma_{sr,2}P_{sd,2}\right) < R_2]$$

$$(7.4)$$

where R_1 and R_2 are the threshold data rates for each channel. It is assumed that the total transmit data rate, R_t, is equally distributed over all spatial channels in equal power allocation. Therefore, the threshold date rate for each channel is $R_1 = R_2 = R_t/2$ in equal

power allocation. Finally, the outage probability at the cooperating is given by

$$P_o^r = 1 - (1 - p_{o1})(1 - p_{o2}). \tag{7.5}$$

With waterfilling power allocation, the threshold data rate for each channel at the cooperating node is not fixed since the transmit data rate at the source varies based on channel conditions between the source and the destination. The instantaneous achievable rate for each channel of the direct link is given by

$$I_1^d = \log_2(1 + \eta_{sd}\lambda_{sd,1}P_{sd,1})$$
$$I_2^d = \log_2(1 + \eta_{sd}\lambda_{sd,2}P_{sd,2}) \tag{7.6}$$

where $\lambda_{sd,i}$ is the ith eigenvalue of $\mathbf{H}_{sd}\mathbf{H}_{sd}^H$, and the transmit power of ith channel, $P_{sd,i}$, is assigned based on waterfilling. To find the outage probability at the cooperating node with waterfilling, the instantaneous achievable rate for each channel at the cooperating node has to be compared with the corresponding one of the direct link. For the first channel, for example, if the instantaneous achievable rate of the $s \rightarrow r$ link is less than that of the $s \rightarrow d$ link, an outage of this channel will occur at the cooperating node. Therefore, the outage probability for each channel is given by

$$p_{o1} = Pr[I_1^r < I_1^d] = Pr[\eta_{sr}\gamma_{sr,1} < \eta_{sd}\lambda_{sd,1}]$$
$$p_{o2} = Pr[I_2^r < I_2^d] = Pr[\eta_{sr}\gamma_{sr,2} < \eta_{sd}\lambda_{sd,2}]. \tag{7.7}$$

Then, outage probability at the cooperating node for waterfilling power allocation can be obtained from (7.5). In the following sections, the cooperative capacity for different power allocation methods will be examined when the cooperating node can forward the received signal.

7.2.2   Waterfilling Power Allocation

In waterfilling, the transmitter has knowledge of the channel information for SVD and adequate power allocation for each channel. It is assumed that waterfilling at the source and waterfilling at the cooperating node are performed independently based on their channel conditions. That is, the total transmit power from the source to the destination and from the cooperating node to the destination will be optimized according to $\mathbf{H}_{sd}$ and $\mathbf{H}_{rd}$, respectively. Note that the total transmit power at the source will not be optimized for the channel between the source and the cooperating node since it is optimized for $\mathbf{H}_{sd}$. When the cooperating node is involved in cooperation, the channel capacity of the cooperative MIMO network can be expressed by

$$C_{mimo\_co}^{wf} = E_H \left[\frac{1}{2} \sum_{i=1}^{2} \log_2 \left(1 + \rho_i^d + \rho_i^r \right) \right] \tag{7.8}$$

where ρ_i^d and ρ_i^r are the instantaneous SNRs for i^{th} channel by the direct and the cooperating links, respectively, and are given by

$$\begin{aligned} \rho_i^d &= \eta_{sd} \lambda_{sd,i} P_{sd,i} \\ \rho_i^r &= \eta_{rd} \lambda_{rd,i} P_{rd,i} \end{aligned} \tag{7.9}$$

where $\lambda_{rd,i}$ is the ith eigenvalue of $\mathbf{H}_{rd}\mathbf{H}_{rd}^H$, and $P_{rd,i}$ is the allocated power for i^{th} channel between the cooperating node and the destination using a waterfilling power allocation.

7.2.3   Optimal Power Allocation at Cooperating Node

If the cooperating node has additional knowledge of the direct path, $\mathbf{H}_{sd}$, a better cooperative capacity can be achieved by proper power allocation at the cooperating node. When waterfilling is used at the source, the capacity expression in (7.8) can be rewritten as

$$C_{mimo\_co}^{opt} = E_H \left[\frac{1}{2} \log_2 \left(\prod_{i=1}^{2} \left(1 + \rho_i^d + \eta_{rd} \lambda_{rd,i} P_{rd,i} \right) \right) \right]. \tag{7.10}$$

Note that $\rho_1^d \geq \rho_2^d$ from the characteristic of the waterfilling method and the values can be obtained at the cooperating node with knowledge of $\mathbf{H}_{sd}$. With the given constraints that $\rho_1^d \geq \rho_2^d$ and $P_{rd,1} + P_{rd,2} = P_t$, the maximum capacity can be achieved when $\lambda_{rd,2} \geq \lambda_{rd,1}$ with the following power allocations:

$$\begin{aligned} P_{rd,1} &= P_t/2 + k \\ P_{rd,2} &= P_t/2 - k \end{aligned} \tag{7.11}$$

where

$$k = \frac{\lambda_{rd,1} - \lambda_{rd,2} - \rho_1^d \lambda_{rd,2} + \rho_2^d \lambda_{rd,1}}{2\eta_{rd} \lambda_{rd,1} \lambda_{rd,2}}. \tag{7.12}$$

This power allocation method at the cooperating node will be referred to *optimal with waterfilling*. However, this power allocation at the cooperating node is optimal on the condition that the source uses a waterfilling method for the direct link. Therefore, this might not be optimal from the overall system capacity perspective.

7.2.4   Inverse-Waterfilling Power Allocation

When N is greater than two, a search is required to find the optimal weights for each channel at the cooperating node. From the *optimal with waterfilling* power allocation for $N = 2$, a higher overall cooperative capacity was achieved by combining large eigenvalues of $\mathbf{H}_{sd}\mathbf{H}_{sd}^H$ with small eigenvalues of $\mathbf{H}_{rd}\mathbf{H}_{rd}^H$. If the source used the waterfilling power allocation, this combination can be easily obtained by an inverse-waterfilling power allocation approach at the cooperating node. An improved overall cooperative capacity can be achieved by inverse-waterfilling power allocation as opposed to standard waterfilling power allocation at the cooperating node. The inverse-waterfilling power allocation may not be the optimal
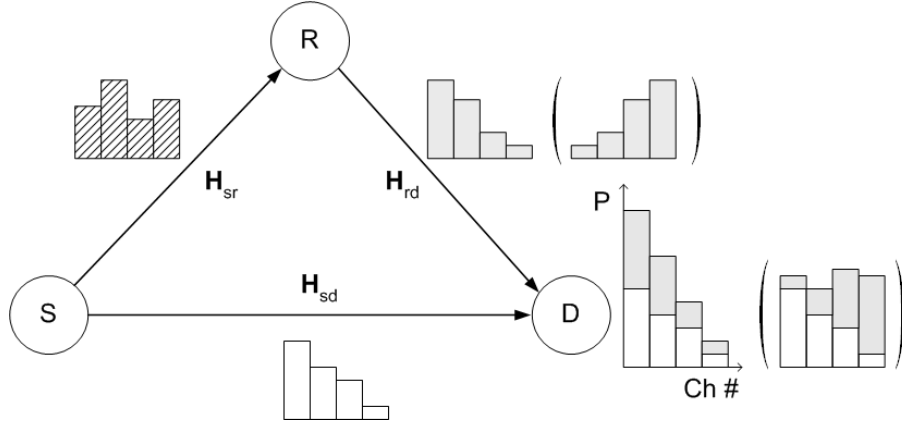
Figure 7.2: Waterfilling (Inverse-Waterfilling) power allocation at the source and the cooperating node (# of antennas at nodes = 4)

power allocation at the cooperating node since the assigned power for each channel cannot be guaranteed to be the same as (7.11). However, this method is very simple and does not require channel information of the direct link. Figure 7.2 illustrates an example of waterfilling and inverse-waterfilling power allocation at the cooperating node for $N = 4$ when waterfilling is used at the source. Inverse-waterfilling power allocation can be easily realized by using the same waterfilling power allocation method in the cooperating node. The cooperating node performs waterfilling power allocation with $\mathbf{H}_{rd}$ and assigns data streams with reverse-order at each stream. For example, if the source assigned data streams on four channels as $\{s_1, s_2, s_3, s_4\}$, the cooperating node assigned data streams as $\{s_4, s_3, s_2, s_1\}$ after performing waterfilling with the corresponding channel. At the destination, the same data stream will be combined after stream separation of the cooperating signal. When the allocated transmit power is decided for each channel, inverse-waterfilling power allocation shows the best overall cooperative capacity. The proof of this statement is shown in Appendix 8.

7.2.5   Waterfilling for the Cooperating Channel

The performance of cooperative MIMO networks depends largely on the error probability at the cooperating node. To maximize the probability that the cooperating node is involved in cooperation, waterfilling power allocation can be used between the source and the cooperating node instead of the destination. This configuration can be considered as a multihop transmission where the destination can also detect and use the first-hop signal. Using this power allocation, the instantaneous achievable rate at the cooperating node is given by

$$I^r = \log_2\left(1 + \eta_{sr}\lambda_{sr,1}P_{sr,1} + \eta_{sr}\lambda_{sr,2}P_{sr,2}\right) \tag{7.13}$$

where $P_{sr,i}$ will be assigned by waterfilling for the channel $\mathbf{H}_{sr}$. In this method, the cooperating node can be treated as the first destination and the source uses best effort to deliver the data properly to the cooperating node with waterfilling. Therefore, the instantaneous achievable rate at the cooperating node given in (7.13) is used to decide whether the received signal at the cooperating node can be decoded correctly or not. In other words, the cooperating node forwards the received data to the destination when $I^r \geq R_t$. After assuming a simple equal power allocation is used at the cooperating node, the cooperative MIMO capacity at the destination is given by

$$C_{mimo\_co}^{wf4r} = E_H\left[\frac{1}{2}\sum_{i=1}^{2}\log_2\left(1 + \eta_{sd}\gamma_{sd,i}P_{sr,i} + \eta_{rd}\lambda_{rd,i}P_{rd,i}\right)\right] \tag{7.14}$$

where $\gamma_{sd,i} = 1/[(\mathbf{H}_{sd}^H\mathbf{H}_{sd})^{-1}]_{i,i}$ when a ZF method is used for channel separation, and equal power allocation is used for the $r \rightarrow d$ link, $P_{rd,1} = P_{rd,2} = P_t/2$. If the cooperating node has information concerning $\mathbf{H}_{sd}$, optimal power allocation can be used at the cooperating node to increase the overall capacity at the destination.

7.3   Performance Results

The outage probability of cooperative MIMO networks with different power allocation techniques will be examined through computer simulation. The number of transmit and receive antennas is assumed to be two, $N = 2$. It is assumed the path loss coefficient is four, $n = 4$. The average received SNR at each node is normalized by the average SNR of the direct link using the pass loss coefficient and the relative distances. For simplicity, the distance of $s \rightarrow d$ link is set to be one, $d_{sd} = 1$.

Figure 7.3 shows the outage probability at the cooperating node for three different relay locations when waterfilling and equal power allocation are used for the channel between the source and the destination. As SNR increases, the outage probability decays exponentially for a fixed threshold data rate such as equal power allocation. In waterfilling, however, the threshold data rate is not fixed at the cooperating node. From (7.7), the outage probability at the cooperating node depends on the ratio of the average SNRs at the cooperating node and the destination which is constant at a fixed location of the cooperating node. As the distance from the source increases the outage probability at the cooperating node also increases since the average received SNR is decreasing.

Figure 7.4 shows the outage probability of the channel capacity when the data rate is fixed, $R = 2$ bps/Hz, and the cooperating node is close to the source, $d_{sr} = 0.2$ and d_{rd} =0.8. The performance between direct transmission and cooperation is compared. Also, the figure shows the performance of the five different power assignment schemes. For direct transmission, the performance of waterfilling is better than that of an equal power allocation as expected. For cooperative MIMO transmission, the outage probability at the cooperating node is relatively low since it is close to the source, $d_{sr} = 0.2$. In this case, the performance of cooperative transmission highly depends on the power allocation methods at the cooperating node. Inverse-waterfilling and *optimal with waterfilling* methods at the cooperating node
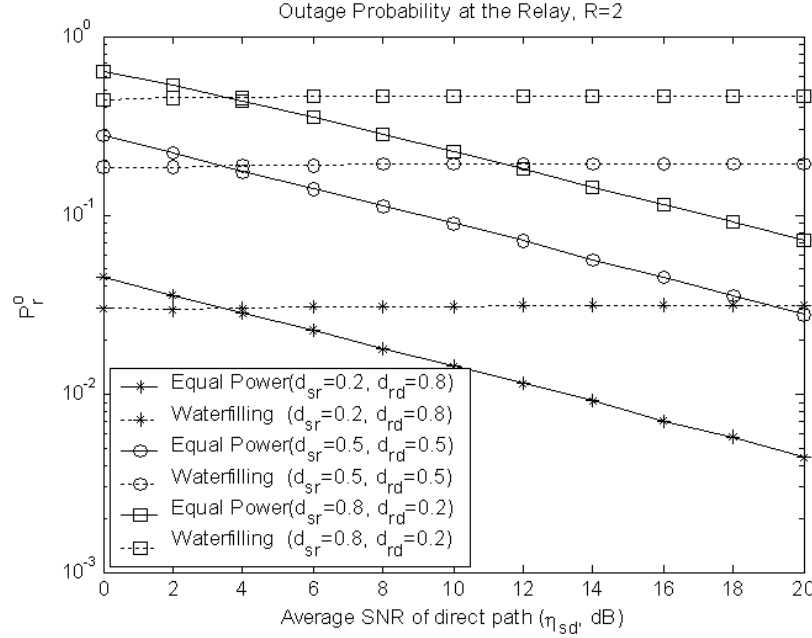
Figure 7.3: Outage probability at the cooperating node with different locations

efficiently use spatial diversity from two signal paths since a bad channel of the direct path is combined with a good one of the cooperating path and vice versa. For this reason, the two power allocation methods at the cooperating node provide good performance at low SNRs. Note that inverse-waterfilling achieve the almost same performance as *optimal with water-filling* using a simple method without channel information of the direct link. As the average received SNR increases, three waterfilling methods to the destination (standard waterfilling, inverse-waterfilling, and *optimal with waterfilling*) converge to the same performance since the difference due to power allocation is small at high SNR. Waterfilling to the cooperating node shows the best performance at high SNR due to the high probability of cooperation.

Figure 7.5 shows the outage probability for a fixed average SNR of the direct link when $d_{sr} = 0.2$ and $d_{rd} = 0.8$. Waterfilling at the source and the cooperating node shows the worst performance since this method poorly uses spatial diversity by combining good channels from both paths and bad ones from both paths. On the contrary, inverse-waterfilling

Figure 7.4: Outage probability with different power allocations ($R = 2$ bps/Hz, $d_{sr} = 0.2$, $d_{rd} = 0.8$)

and *optimal with waterfilling* at the cooperating node fully use spatial diversity and provide good performance.

Figure 7.6 shows the outage probability of the cooperative MIMO transmission for R = 2 bps/Hz when the cooperating node is located in the middle between the source and the destination. First, equal power allocation and waterfilling to the destination will be considered. Due to the tradeoff between outage probability at the cooperating node and proper power allocation on the channel, the outage probability of both methods shows the similar performance. For the three waterfilling methods to the destination, the only difference is the power allocated at the cooperating node. However, the difference is small as compared to the average received SNR from the shorter path. This results in the same performance for the three methods in this case. Waterfilling for the $s \rightarrow r$ link can reduce the effect of the high outage probability at the cooperating node. This method shows much better performance than the others due to the low outage probability at the cooperating node and

Figure 7.5: Outage probability with different power allocations (average $\text{SNR}_{sd} = 10$ dB, d_{sr} $= 0.2$, $d_{rd} = 0.8$)

the shorter path gain of the $r \to d$ link.

Figure 7.7 shows the outage probability for the same position of the cooperating node as the transmit data rate varies. Waterfilling to the cooperating node outperforms the other methods for all considered data rate due to the low outage probability at the cooperating node. The three methods using waterfilling to the destination show almost the same performance for the reason mentioned above. Equal power allocation shows better performance than these power allocation methods for the considered data rates due to the low outage probability at the cooperating node. Direct transmission shows better performance than all cooperative methods except waterfilling to the cooperating node for moderate date rates. However, the outage probability of direct transmission increases exponentially as the transmit data rate increases and results in the worst performance at high data rates.

Figures 7.8 and 7.9 show the outage probability of cooperative MIMO transmission when the cooperating node is close to the destination, $d_{sr} = 0.8$ and $d_{rd} = 0.2$. Comparing
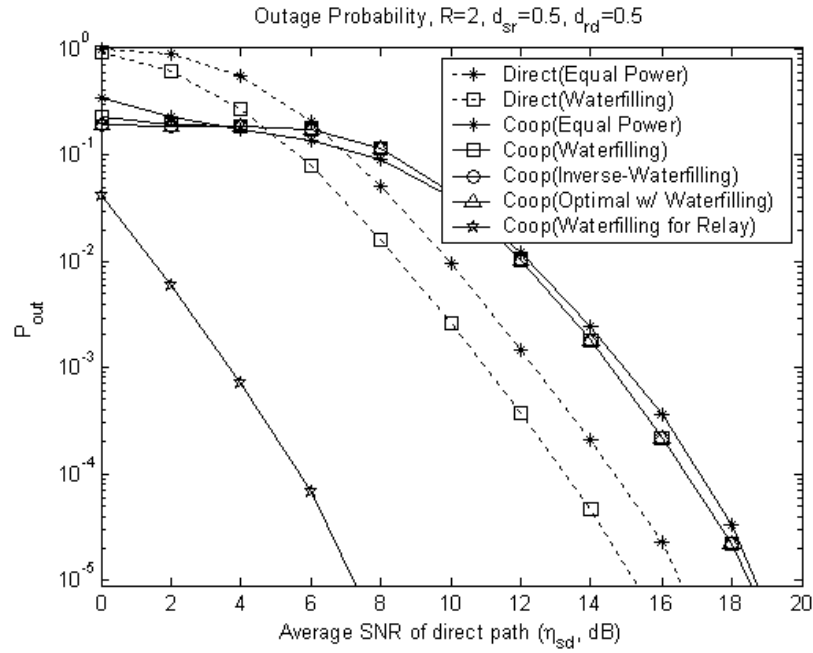
Figure 7.6: Outage probability with different power allocations ($R = 2$ bps/Hz, $d_{sr}= 0.5$, $d_{rd} = 0.5$)

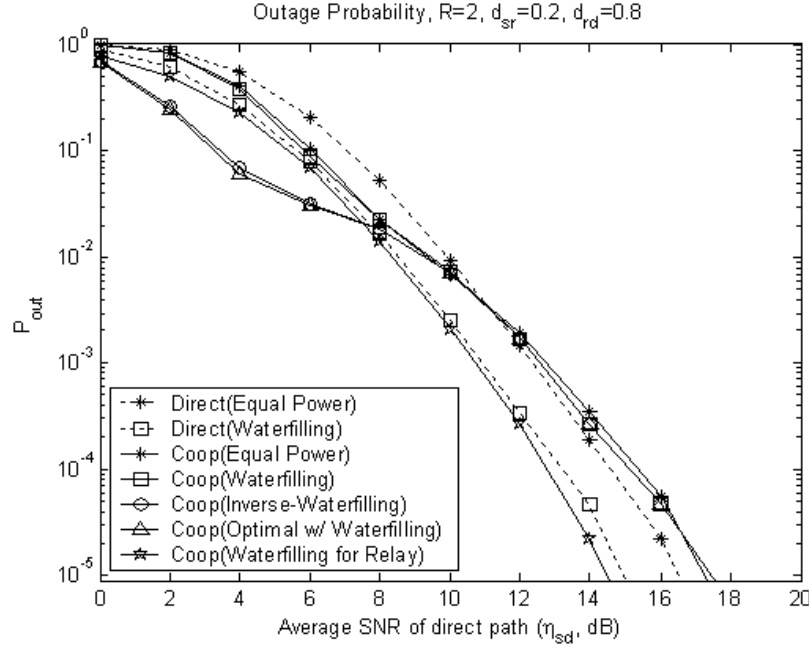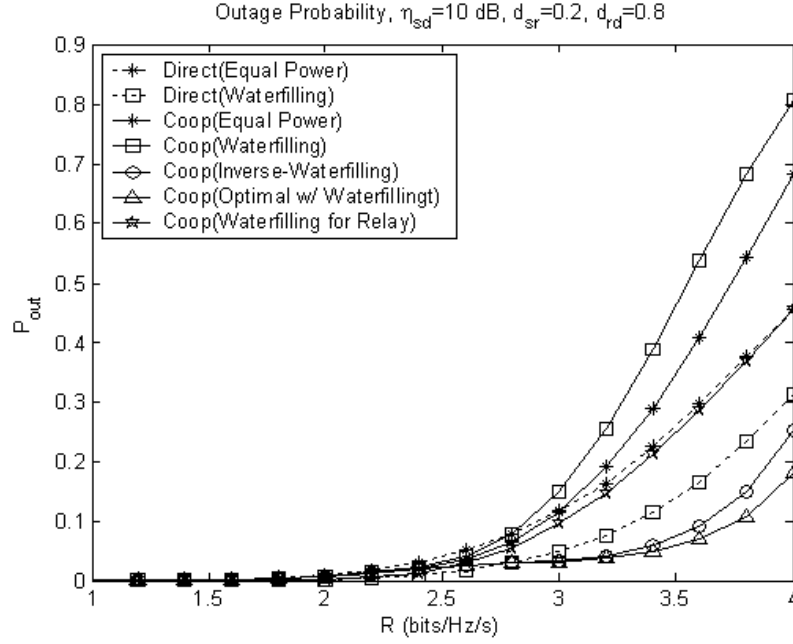Figure 7.7: Outage probability with different power allocations (average $\text{SNR}_{sd} = 10$ dB, $d_{sr} = 0.5$, $d_{rd} = 0.5$)
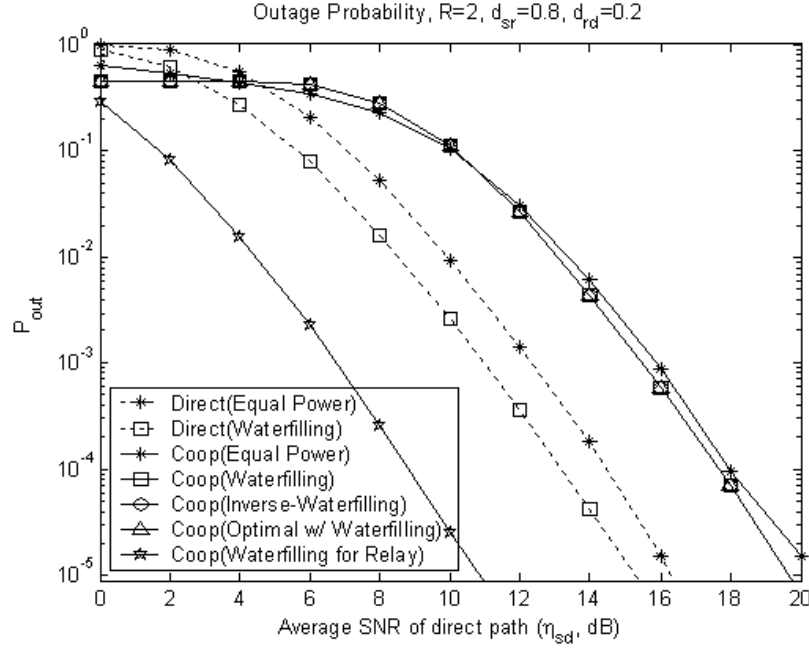
Figure 7.8: Outage probability with different power allocations ($R = 2$ bps/Hz, $d_{sr} = 0.8$, $d_{rd} = 0.2$)

this case with a center-located case, the performance of the former is worse than that of the latter for all cooperation methods due to the high outage probability at the cooperating node. The cooperative transmission (except waterfilling for the cooperating node) show significantly worse performance than direct transmission due to the waste of an additional time slot when the received signal at the cooperating node cannot be decoded correctly.

For the three waterfilling methods to the destination, the outage probability is almost constant at high data rates as shown in Figures 7.7 and 7.9. This is due to the shorter path gain between the cooperating node and the destination when the cooperating node decodes the received data successfully. The outage probability of these methods will increase again at higher data rates which was not considered in our simulation.
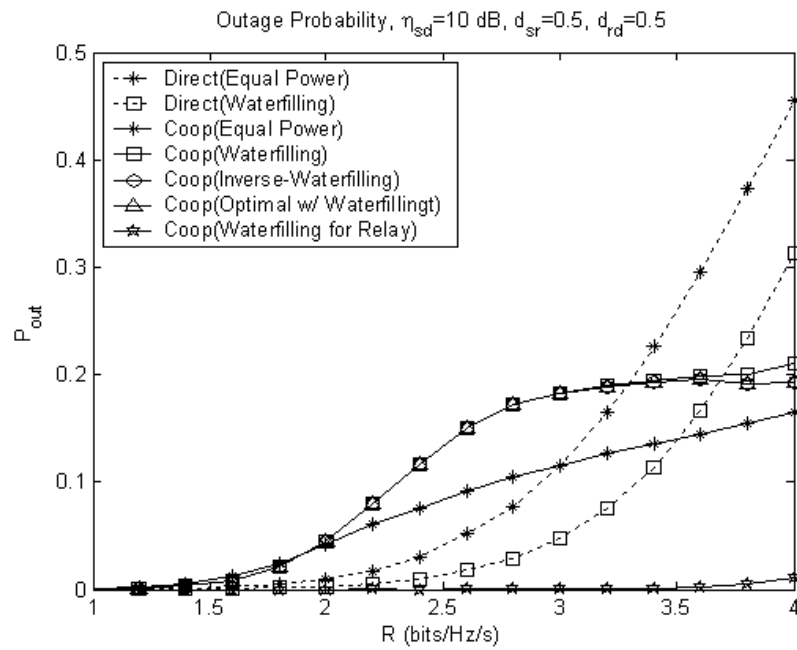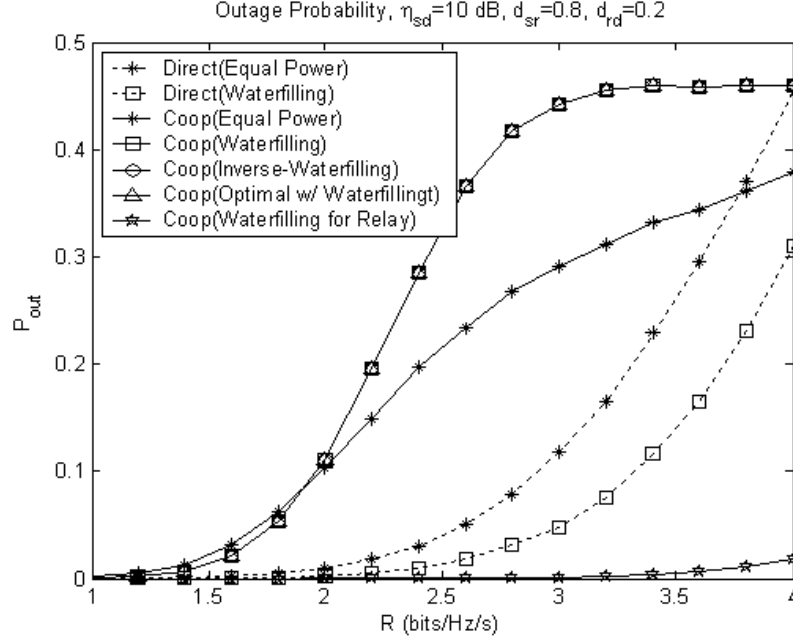
Figure 7.9: Outage probability with different power allocations (average $\text{SNR}_{sd} = 10$ dB, d_{sr} = 0.8, $d_{rd} = 0.2$)

7.4   Chapter Summary

Power allocation strategies for cooperative MIMO networks were examined in this chapter. It was found that waterfilling at the source and the cooperating node does not achieve maximum capacity in cooperative MIMO networks. For the two antenna case, the optimal power allocation method at the cooperating node was presented when waterfilling was used at the source. An inverse-waterfilling power allocation at the cooperating node was proposed to increase the overall channel capacity which was found to be close to the performance of optimal power allocation at the cooperating node. Also, this method can be easily used for a large number of antennas without channel information of the direct path. To increase the probability that the cooperating node can work cooperatively, waterfilling to the cooperating node was also examined.

When the cooperating node is close to the source, the performance of cooperative

MIMO networks depends largely on the proper power allocation at the cooperating node. As the distance between the source and the relay increases, the outage probability at the cooperating node plays an important role in cooperative MIMO transmission. A waterfilling method to the cooperating node instead of the destination can be used to reduce the outage probability at the cooperating node and substantially reduced outage probability is achieved in cooperative MIMO networks.

Chapter 8

Conclusions

Cooperative communications has received increased interest as a means to emulate a *virtual* multiple antenna system with multiple single-antenna devices. Cooperative communications provides several benefits in terms of link reliability, power consumption, and coverage in wireless ad hoc networks at the cost of other system resources.

In most of the cooperative communication methods proposed to date, there are wasteful cooperating signals when the received signal from the source is of sufficient quality to decode the transmit data or when the cooperating signal is of poor quality. The current research was motivated by this drawback. This dissertation proposed an efficient cooperative communication method in wireless ad hoc networks to increase bandwidth efficiency where cooperative transmission was initiated for packet retransmission *only when necessary* to avoid transmitting unneeded or unuseful cooperating signals. In the proposed cooperative transmission scheme, cooperative nodes were self-selected from neighboring nodes around the direct link by overhearing the message exchange between the source and the destination. This selection procedure required no *a priori* knowledge of the neighboring nodes and insured good quality cooperating signals. It was shown that the proposed cooperative retransmission scheme outperformed traditional retransmission by the source and proposed

cooperative schemes such as decode-and-forward cooperation.

In the proposed cooperative retransmission scheme, distributed beamforming was used as a means to accommodate multiple cooperating nodes, providing better bandwidth efficiency as compared to cooperative diversity using distributed STC. The retransmission request message from the destination (*i.e.*, NACK message) was used for achieving synchronization between the cooperating signals. The effects of synchronization errors in distributed beamforming were investigated for single-carrier and OFDM systems and the achievable gain was examined with a varying number of cooperating nodes and offset values. The outage probabilities of the received signals were derived for both the perfect synchronization case and when offset estimation was used for distributed beamforming. The performance with offset estimation was close to the perfect synchronization case, especially for short data packets. A low-rate feedback channel was used for adjusting the phase shift due to the residual offsets and it was found that a substantial gain can be achieved, even for long data packets.

The throughput efficiency and average packet delay of the proposed cooperative retransmission scheme were analyzed using a two-state Markov model for both a simple ARQ and a hybrid ARQ with maximum ratio combining. The analytical results were found to be in good agreement with the simulated results. Even with a small number of neighboring nodes, improved throughput efficiency and delay performance were achieved by using the cooperative retransmission scheme. The benefits of the cooperative ARQ were also verified in a multihop network with random configurations and in the presence of concurrent packet transmissions.

The average transmit power for the cooperating signals was also investigated in the proposed cooperative transmission scheme. When each cooperating node adjusted its retransmitting signal power based on the NACK message, the total transmit power of the cooperating signal increased as the number of cooperating nodes increased. However, total transmit power for the cooperatively retransmitted packet was significantly reduced by using

a small feedback channel without sharing any information between cooperating nodes.

Cooperative MIMO systems were examined mainly focusing on power allocation methods to increase overall channel capacity. It was found that waterfilling at the source and the cooperating node could not achieve maximum capacity in cooperative MIMO transmission. An inverse-waterfilling power allocation at the cooperating node was proposed to increase the overall channel capacity which was found to be close to the performance of optimal power allocation at the cooperating node. Also, this method can be easily used for a large number of antennas without channel information of the direct link. To increase the probability that the cooperating node was involved in the cooperation, waterfilling at the source to the cooperating node was also examined.

This research mainly focused on a cooperative transmission method to increase spectral and power efficiency. There are still many research issues in cooperative communications. One of them is the security issue in cooperative communications in decode-and-forward cooperation, where the cooperating node tries to corrupt the communications by sending the perverse signal. Cooperative communications can provide increased link coverage and connectivity. To use those benefits more efficiently in a multihop network, cross-layer design with upper layers such as routing protocol also needs to be further investigated.

Appendix A

Proof of Inverse-Waterfilling Power Allocation

When there are N channels for data streams for both the direct and the cooperating links, the instantaneous mutual information of cooperative MIMO transmission is given by

$$
\begin{aligned}
I_{mimo}^{co} &= \frac{1}{2} \log_2 \det \left(1 + \eta_{sd} \mathbf{H}_{sd} \mathbf{H}_{sd}^H + \eta_{rd} \mathbf{H}_{rd} \mathbf{H}_{rd}^H\right) \\
&= \frac{1}{2} \log_2 \prod_{n=1}^{N} \left(1 + \eta_{sd} \lambda_{sd,n} P_{sd,n} + \eta_{rd} \lambda_{rd,n} P_{rd,n}\right) \\
&= \frac{1}{2} \log_2 \prod_{n=1}^{N} \left(1 + x_n + y_n\right)
\end{aligned}
\tag{1}
$$

where $x_n = \eta_{sd} \lambda_{sd,n} P_{sd,n}$ and $y_n = \eta_{rd} \lambda_{rd,n} P_{rd,n}$ for $n = 1, 2, \cdots, N$. The objective is to find maximum I_{mimo}^{co} with given x_n and y_n.

$$
\begin{aligned}
\max_{x_n, y_n} I_{mimo}^{co} &= \max_{x_n, y_n} \frac{1}{2} \log_2 \prod_{n=1}^{N} \left(1 + x_n + y_n\right) \\
&= \max_{x_n, y_n} \prod_{n=1}^{N} \left(x_n + y_n\right)
\end{aligned}
\tag{2}
$$

138

If $P_{sd,n}$ and $P_{rd,n}$ are assigned by using waterfilling based on their corresponding channels, $x_1 \geq x_2 \geq \cdots \geq x_N$ and $y_1 \geq y_2 \geq \cdots \geq y_N$ are satisfied. For the case $N = 2$, $(x_1 - x_2)(y_1 - y_2) \geq 0$ and therefore $x_1 y_1 + x_2 y_2 \geq x_1 y_2 + x_2 y_1$. After adding $x_1 x_2 + y_1 y_2$ at the both side and summarizing them, then

$$(x_1 + y_2)(x_2 + y_1) \geq (x_1 + y_1)(x_2 + y_2) \tag{3}$$

For the general case, suppose that $\{z_1, z_2, \ldots, z_N\}$ is a rearrangement of $\{y_1, y_2, \ldots, y_N\}$ such that the product

$$P = (x_1 + z_1)(x_2 + z_2) \cdots (x_N + z_N) \tag{4}$$

is maximized. If there exists a pair $i < j$ with $z_i \geq z_j$, then $(x_i + z_i)(x_j + z_j) \leq (x_i + z_j)(x_j + z_i)$ from the $N = 2$ case. We can consecutively interchange these pairs, $i < j$ with $z_i \geq z_j$, until $z_1 \leq z_2 \leq \cdots \leq z_N$. Therefore,

$$(x_1 + z_1)(x_2 + z_2) \cdots (x_N + z_N) \tag{5}$$

is maximized if $z_1 \leq z_2 \leq \cdots \leq z_N$.

Bibliography

[1] D. G. Brennan, "Linear diversity combining techniques," *IEEE Proceedings*, vol. 91, pp. 331–356, Feb. 2003.

[2] H. Krim and M. Viberg, "Two decades of array signal processing research: The parametric approach," *IEEE Signal Processing Magazine*, vol. 13, pp. 67–94, July 1996.

[3] B. D. V. Veen and K. M. Buckley, "Beamforming: A versatile approach to spatial filtering," *IEEE Acoustics, Speech, and Signal Processing (ASSP) Magazine*, vol. 5, pp. 4–24, Apr. 1988.

[4] G. J. Foschini and M. J. Gans, "On limits of wireless communications in a fading environment when using multiple antennas," *IEEE Wireless Personal Communications*, vol. 6, pp. 311–335, Mar. 1998.

[5] G. E. Moore, "Cramming more components onto integrated circuits," *IEEE Proceedings*, vol. 86, pp. 82–85, Jan. 1998.

[6] J. N. Laneman, D. N. C. Tse, and G. W. Wornell, "Cooperative diversity in wireless networks: Efficient protocols and outage behavior," *IEEE Transactions on Infomation Theory*, vol. 50, no. 12, pp. 3062–3080, 2004.

[7] J. N. Laneman and G. W. Wornell, "Distributed space-time-coded protocols for ex-

ploiting cooperative diversity in wireless networks," *IEEE Transactions on Infomation Theory*, vol. 49, no. 10, pp. 2415–2425, 2003.

[8] T. E. Hunter and A. Nosratinia, "Diversity through coded cooperation," *IEEE Transactions on Wireless Communications*, vol. 5, Feb. 2006.

[9] T. E. Hunter, S. Sanayei, and A. Nosratinia, "Outage analysis of coded cooperation," *IEEE Transactions on Information Theory*, vol. 52, pp. 375–391, Feb. 2006.

[10] G. Barriac, R. Mudumbai, and U. Madhow, "Distributed beamforming for information transfer in sensor networks," *Third International Symposium on Information Processing in Sensor Networks (IPSN)*, pp. 81–88, Apr. 2004.

[11] R. Mudumbai, J. Hespanha, U. Madhow, and G. Barriac, "Scalable feedback control for distributed beamforming in sensor networks," *IEEE International Symposium on Information Theory*, pp. 137–141, Sep. 2005.

[12] T. M. Cover and A. A. E. Gamal, "Capacity theorems for the relay channel," *IEEE Transactions on Infomation Theory*, vol. 25, no. 5, pp. 572–584, 1979.

[13] A. Nosratinia, T. E. Hunter, and A. Hedayet, "Cooperative communicaiton in wireless networks," *IEEE Communications Magazine*, vol. 42, pp. 74–80, Oct. 2004.

[14] P. A. Anghel and M. Kaveh, "Exact symbol error probability of a cooperative network in a rayleigh-fading environment," *IEEE Transactions on Wireless Communications*, vol. 3, pp. 1416–1421, Sep. 2004.

[15] X. Deng and A. M. Haimovich, "Power allocation for cooperative relaying in wireless networks," *IEEE Communications Letters*, vol. 9, pp. 994–996, Nov. 2005.

[16] A. Agustin and J. Vidal, "Amplify-and-forward cooperation under interference-limited spatial reuse of the relay slot," *IEEE Transactions on Wireless Communications*, vol. 7, pp. 1952–1962, May 2008.

[17] M. Kaneko, K. Hayashi, P. Popovski, H. Ikeda, K. abd Sakai, and R. Prasad, "Amplify-and-forward cooperative diversity schemes for multi-carrier systems," *IEEE Transactions on Wireless Communications*, vol. 7, pp. 1845–1850, May 2008.

[18] A. Sendonaris, E. Erkip, and B. Aazhang, "User cooperation diversity part i and part ii," *IEEE Transactions on Communications*, vol. 51, pp. 1927–1948, Nov. 2003.

[19] H. Li and Q. Zhao, "Distributed modulation for cooperative wireless communications," *IEEE Signal Processing Magazine*, pp. 30–36, Sep. 2006.

[20] X. Liu and W. Su, "Ber performance analysis of the optimum ml receiver for decode-and-forward cooperative protocol," *IEEE International Conference on Acoustics, Speech and Signal Processing (ICASSP)*, vol. 3, pp. 485–488, Apr. 2007.

[21] T. Wang, A. Cano, G. B. Giannakis, and J. Laneman, "High-performance cooperative demodulation with decode-and-forward relays," *IEEE Transactions on Communications*, vol. 55, pp. 1427–1438, July 2007.

[22] T. Wang, A. Cano, and G. B. Giannakis, "Link-adaptive cooperative communications without channel state information," *IEEE Military Communications Conference (MILCOM)*, pp. 1–7, Oct. 2006.

[23] Z. Yi and I. Kim, "Diversity order analysis of the decode-and-forward cooperative networks with relay selection," *IEEE Transactions on Wireless Communications*, vol. 7, pp. 1792–1799, May 2008.

[24] Y. Zhao, R. Adve, and T. J. Lim, "Symbol error rate of selection amplify-and-forward relay systems," *IEEE Communication Letters*, vol. 10, pp. 757–759, Nov. 2006.

[25] E. Beres and R. S. Adve, "On selection cooperation in distributed networks," *40th Annual Conference on Information Sciences and Systems (CISS)*, pp. 1056–1061, Mar. 2006.

[26] A. Stefanov and E. Erkip, "Cooperative coding for wireless networks," *IEEE Transactions on Communications*, vol. 52, pp. 1470–1476, Sep. 2004.

[27] A. Stefanov and E. Erkip, "Cooperative space-time coding for wireless networks," *IEEE Transactions on Communications*, vol. 53, pp. 1804–1809, Nov. 2005.

[28] R. Liu, P. Spasojević, and E. Soljanin, "Cooperative diversity with incremental redundancy turbo coding for quasi-static wireless networks," *IEEE 6th Workshop Signal Processing Advances in Wireless Communications*, pp. 791–795, 2005.

[29] R. Liu, P. Spasojević, and E. Soljanin, "Incremental multi-hop based on "good" punctured codes and its reliable hop rate," *IEEE Wireless Communications and Networking Conference (WCNC)*, pp. 249–254, 2005.

[30] C. F. Leanderson and G. Caire, "The performance of incremental redundancy schemes based on convolutional codes in the block-fading gaussian collision channel," *IEEE Transactions on Wireless Communications*, vol. 3, pp. 843–854, May 2004.

[31] R. Knopp and P. A. Humblet, "On coding for block fading channels," *IEEE Transactions on Information Theory*, vol. 46, pp. 189–205, Jan. 2000.

[32] G. Caire and D. Tuninetti, "The throughput of hybrid-arq protocols for the gaussian collision channel," *IEEE Transactions on Information Theory*, vol. 47, pp. 1971–1988, July 2001.

[33] G. Scutari and S. Barbarossa, "Distributed space-time coding for regenerative relay networks," *IEEE Transactions on Wireless Communications*, vol. 4, pp. 2387–2399, Sep. 2005.

[34] P. A. Anghel and M. Kaveh, "On the performance of distributed space-time coding systems with one and two non-regenerative relays," *IEEE Transactions on Wireless Communications*, vol. 5, pp. 682–692, Mar. 2006.

[35] S. Yiu, R. Schober, and L. Lampe, "Distributed space-time block coding," *IEEE Transactions on Communications*, vol. 54, pp. 1195–1206, July 2006.

[36] J. He and P. Y. Kam, "On the performance of distributed space-time block coding over nonidentical ricean channels and the optimum power allocation," *IEEE International Conference on Communications (ICC)*, pp. 5592–5597, June 2007.

[37] S. Cui, A. J. Goldsmith, and A. Bahai, "Energy-efficiency of mimo and cooperative mimo techniques in sensor networks," *IEEE Journal on Selected Areas in Communications*, vol. 22, pp. 1089–1098, Aug. 2004.

[38] Z. Ding, W. H. Chin, and K. K. Leung, "Distributed beamforming and power allocation for cooperative networks," *IEEE Transactions on Wireless Communications*, vol. 7, pp. 1817–1822, May 2008.

[39] H. Ochiai, P. Mitran, H. V. Poor, and V. Tarokh, "Collaborative beamforming for distributed wireless ad hoc sensor networks," *IEEE Transactions on Signal Processing*, vol. 53, pp. 4110–4124, Nov. 2005.

[40] Y. Mei, Y. Hua, A. Swami, and B. Daneshrad, "Combating synchronization errors in cooperative relays," *IEEE International Conference on Acoustics, Speech, and Signal Processing*, pp. 369–372, 2005.

[41] S. Jagannathan, H. Aghajan, and A. J. Goldsmith, "The effect of time synchronization errors on the performance of cooperative miso systems," *IEEE Global Telecommunications Conference (GLOBECOM)*, pp. 102–107, 2004.

[42] F. Sivrikaya and B. Yener, "Time synchronization in sensor networks: A survey," *IEEE Network*, pp. 45–50, July/Aug. 2004.

[43] J. Y. Lee, A. Verma, H. S. Lee, and J. S. Ma, "A distributed time synchronization algorithm robust to traffic load for manets," *IEEE Vehicular Technology Conference (VTC)*, pp. 329–333, Sep. 2005.

[44] M. Oh, X. Ma, G. B. Giannakis, and D. Park, "Cooperative synchronization and channel estimation in wireless sensor networks," *IEEE Asilomar Conference on Signals, Systems and Computers*, vol. 1, pp. 238–242, Nov. 2003.

[45] M. L. Sichitiu and C. Veerarittiphan, "Simple, accurate time synchronization for wireless sensor networks," *IEEE Wireless Communications and Networking Conference (WCNC)*, vol. 2, pp. 1266–1273, Mar. 2003.

[46] J. Mietzner, J. Eick, and P. A. Hoeher, "On distributed space-time coding techniques for cooperative wireless networks and their sensitivity to frequency offsets," *IEEE ITG Workshop on Smart Antennas*, pp. 114–121, 2004.

[47] J. Zhang and T. M. Lok, "Performance comparison of conventional and cooperative multihop transmission," *IEEE Wireless Communications and Networking Conference (WCNC)*, pp. 897–901, 2006.

[48] J. Boyer, D. D. Falconer, and H. Yanikomeroglu, "Multihop diversity in wireless relaying channels," *IEEE Transactions on Communications*, vol. 52, pp. 1820–1830, Oct. 2004.

[49] S. Cui and A. J. Goldsmith, "Energy efficient routing based on cooperative mimo techniques," *IEEE International Conference on Acoustics, Speech and Signal Processing*, pp. 805–808, 2005.

[50] T. Miyano, H. Murata, and K. Araki, "Cooperative relaying scheme with space time code for multihop communications among single antenna terminals," *IEEE Global Telecommunications Conference (GLOBECOM)*, pp. 3763–3767, 2004.

[51] A. Azgin, Y. Altunbasak, and G. AlRegib, "Cooperative mac and routing protocols for wireless ad hoc networks," *IEEE Global Telecommunications Conference (GLOBECOM)*, pp. 2854–2859, 2005.

[52] Z. Yang, J. Liu, and A. Hø st Madsen, "Cooperative routing and power allocation in ad-hoc networks," *IEEE Global Telecommunications Conference (GLOBECOM)*, pp. 2730–2734, 2005.

[53] A. Scaglione, D. L. Goeckel, and J. N. Laneman, "Cooperative communications in mobile ad hoc networks," *IEEE Signal Processing Magazine*, pp. 18–29, Sep. 2006.

[54] A. Bletsas, A. Khisti, D. P. Reed, and A. Lippman, "A simple cooperative diversity method based on network path selection," *IEEE Journal on Selected Areas in Communications*, vol. 24, pp. 659–672, Mar. 2006.

[55] S. Biswas and R. Morris, "Exor: Opportunistic multi-hop routing for wireless networs," *ACM SIGCOMM*, vol. 35, pp. 133–144, Oct. 2005.

[56] M. Zorzi and R. Rao, "Geographic random forwarding (geraf) for ad hoc and sensor networks: Multihop performance," *IEEE Transactions on Mobile Computing*, vol. 2, no. 4, pp. 337–348, 2003.

[57] B. Wang, J. Zhang, and A. HøstMadsen, "On the capacity of mimo relay channels," *IEEE Transactions on Information Theory*, vol. 51, pp. 29–43, Jan. 2005.

[58] B. Rankov and A. Wittneben, "On the capacity of relay-assisted wireless mimo channels," *Fifth IEEE Workshop on Signal Processing Advances in Wireless Communications*, July 2004.

[59] O. Muñoz, J. Vidal, and A. Agustin, "Non-regenerative mimo relaying with channel state information," *IEEE International Conference on Acoustics, Speech and Signal Processing*, pp. 361–364, 2005.

[60] Z. Jingmei, S. Chunju, W. Ying, and Z. Ping, "Optimal power allocation for multiple-input multiple-output relaying system," *IEEE Vehicular Technology Conference (VTC)*, pp. 1405–1409, Sep. 2004.

[61] H. Shi, T. Abe, T. Asai, and H. Yoshino, "Relay techniques in mimo wireless networks," *IEEE Vehicular Technology Conference (VTC)*, vol. 4, pp. 2438–2443, Sep. 2005.

[62] H. Bölcskei, R. U. Nabar, O. Oyman, and A. J. Paulraj, "Capacity scaling laws in mimo relay networks," *IEEE Transactions on Wireless Communications*, vol. 5, pp. 1433–1444, June 2006.

[63] S. Kallel, "Sequential decoding with an efficient incremental redundancy arq scheme," *IEEE Transactions on Communications*, vol. 40, pp. 1588–1593, Oct. 1992.

[64] *3GPP Technical Specification 25.855 High Speed Downlink Packet Access (HSDPA) Overall UTRAN description.*

[65] *3GPP Technical Specification 25.856 High Speed Downlink Packet Access (HSDPA) Layer 2 and 3 aspects.*

[66] Z. J. Haas and J. Deng, "Dual busy tone multiple access (dbtma) - a multiple access control scheme for ad hoc networks," *IEEE Transactions on Communications*, vol. 50, pp. 975–985, June 2002.

[67] N. C. Beaulieu, "An infinite series for the computation of the complementary probability distribution function of a sum of independent random variables and its application to the sum of rayleigh random variables," *IEEE Transactions on Communications*, vol. 38, pp. 1463–1474, Sep. 1990.

[68] R. Reggiannini, "A fundamental lower bound to the performance of phase estimators over rician-fading channels," *IEEE Transactions on Communications*, vol. 45, pp. 775–778, July 1997.

[69] A. J. Viterbi, *CDMA Principles of Spread Spectrum Communication*. Addison-Wesley, 1995.

[70] M. Dianati, X. Ling, K. Naol, and X. Shen, "A node-cooperative arq scheme for wireless ad hoc networks," *IEEE Transactions on Vehicular Technology*, vol. 55, pp. 1032–1044, May 2006.

[71] C. H. C. Leung, Y. Kikumoto, and S. A. Sorensen, "The throughput efficiency of the go-back-n arq scheme under markov and related error structure," *IEEE Transactions on Communications*, vol. 3, pp. 231–233, Feb. 1988.

[72] *IEEE 802.11-2007 Part 11: Wireless LAN Medium Access Control (MAC) and Physical Layer (PHY) Specifications*. IEEE Standard for Information technology, June 2007.

[73] D. Gore, R. W. Heath Jr., and A. Paulraj, "On performance of the zero forcing receiver in presence of transmit correlation," *Proc. IEEE International Symposium on Information Theory*, p. 159, 2002.